

THE ROLE OF TISSUE TRANSGLUTAMINASE ACTIVE SITE MUTANTS IN  
RENAL CELL CARCINOMA AND EPITHELIAL TO MESENCHYMAL  
TRANSITION

by  
Bürge Ulukan



Submitted to Graduate School of Natural and Applied Sciences  
in Partial Fulfillment of the Requirements  
for the Degree of Master of Science in  
Biotechnology


Yeditepe University

2017

THE ROLE OF TISSUE TRANSGLUTAMINASE ACTIVE SITE MUTANTS IN  
RENAL CELL CARCINOMA AND EPITHELIAL TO MESENCHYMAL  
TRANSITION

APPROVED BY:

Assoc. Prof. Dr. Dilek Telci  
(Thesis Supervisor)



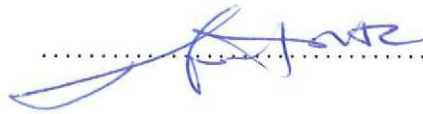
.....

Assoc. Prof. Dr. Elif Damla Arısan



.....

Assist. Prof. Dr. Hüseyin Çimen



.....

DATE OF APPROVAL: ..../..../2017

## ACKNOWLEDGEMENTS

I would like to specially thank to my thesis supervisor, Assoc. Prof. Dr. DILEK TELCI who always supported me to perform experiments in our laboratory. I am also very grateful for her guidance. Working with Assoc. Prof. Dr. DILEK TELCI has provided a great contribution to my academic perspective.

Furthermore, I am so thankful to my lab partners Inci KURT, Hande NAYMAN, Halime ILHAN, Ece NEZIR, Polen KOCAK and Zeynep BOLAT for helping and supporting me whenever I needed.

Special thank goes to my friends Merve OKTEM and Ceren NEMUTLU for their friendship and moral support during my study.

Lastly but most importantly, my deepest heart-felt gratitude is to my family, Muge ULUKAN and Kani ULUKAN, who has been always with me supporting with their love and concern. Without their emboldening and discernment it would have been impossible for me to complete this work.

## ABSTRACT

### **THE ROLE OF TISSUE TRANSGLUTAMINASE ACTIVE SITE MUTANTS IN RENAL CELL CARCINOMA AND EPITHELIAL TO MESENCHYMAL TRANSITION**

Multifunctionality of tissue transglutaminase 2 (TG2) allowed protein to act as a crosslinking enzyme, GTPase/ATPase, protein disulfide isomerase and as a protein kinase. TG2 is involved in several cellular processes such as adhesion, migration, invasion, cell growth, and epithelial mesenchymal transition (EMT). Evidence suggests that EMT might be crucial in the cellular processes including metastasis and drug resistance in many different tumor types. Renal cell carcinoma (RCC) is known as the subtype of kidney cancer and it accounts three per cent of the malignancies in adults. Our previous findings suggested that the upregulation in the expression level of TG2 in RCC was associated with tumor metastasis and with a significant decrease in disease- and cancer-specific survival outcome. Given the importance of the pro-metastatic function of TG2 in RCC, we aimed to investigate the possible allosteric contribution of TG2 enzyme in cell migration, invasion, EMT, and cancer stemness for RCC with a special emphasis on the TG2- NF $\kappa$ B axis. For that purpose, RenCa TG2 variants were generated by transducing mouse RCC cell line RenCa using wt-TG2, GTP-binding deficient form TG2-R580A, transaminase-deficient form with a low GTP-binding affinity TG2-C277S and transaminase-inactive form TG2-W241A. Results from CD marker analysis and spheroid assay suggested that GTP-binding function was important in the maintenance of mesenchymal phenotype and cancer stemness profile. The expression level analysis of EMT transcriptional factors and matrix metalloproteinases (MMPs) together with scattering and Matrigel invasion assays in RenCa TG2 variants suggested that GTPase activity of TG2 was indispensable for the cell migration and invasion of RCC. In addition, EMSA experiments performed on control and TG2-expressing mutant RenCa cells indicated that GTP-binding function of TG2 was essential for the activation of NF $\kappa$ B through the canonical pathway. Taken together, these findings supported that pro-metastatic role of TG2 in RCC was mainly dependent on the GTP-binding function of the enzyme. This project was funded by FP-7 TRANSPATH 289964 grant.

## ÖZET

### **DOKU TRANZGLÜTAMİNAZİ AKTİF BÖLGE MUTANTLARININ BÖBREK KANSERİ VE EPİTELYAL MEZENKİMAL GEÇİŞİNDEKİ ROLÜ**

Çok işlevsel doku transglütaminaz 2 (TG2) enzimi, proteinlerin çapraz bağlanmasında görev aldığı gibi, adrenerjik yolak GTPaz/ATPazı, protein kinazı ve protein disülfid isomerazı olarak da görev yapmaktadır. TG2 adezyon, hücre göçü, invazyon, hücre büyümesi ve epitelyaldan mezankimale geçiş (EMG) gibi bir çok hücre işlevine katkıda bulunmaktadır. Kanıtlar, birçok değişik tümör tiplerinde metastaz ve ilaç direnci dahil olmak üzere bir çok hücre işlevinde EMG'nin önemli bir yere sahip olduğunu ileri sürmektedir. Böbrek hücre kanseri, yetişkinlerde en sık rastlanan böbrek kanser türüdür ve yetişkinlerde yaklaşık yüzde üç oranındaki habis tümörüyle sonuçlanır. Önceden elde edilen sonuçlar doğrultusunda, böbrek kanserinde TG2 seviyesinin artışı tümör metastazı ve kansere özgü hayatta kalış profiliyle ilişkilendirilmiştir. TG2'nin böbrek kanserindeki metastaz artırıcı fonksiyonu göz önüne alındığında, TG2'nin böbrek kanserinde ki olası rolünün araştırılması, TG2 enziminin özellikle NFκB ile olan ilişkisi temel alınarak hedeflenmiştir. Bu bağlamda TG2 güdümlü hücre göçü, invazyon, EMG ve kanser kök hücre işlev kazanımı araştırılmıştır. Bu amaçla, fare böbrek hattı olan RenCa hücre hattı çeşitli TG2 varyasyonları ile; doğal fenotip, GTP bağlanma yoksunu TG2-R580A, transaminaz yoksunu ama düşük GTP bağlayabilen TG2-C277S ve sadece transaminaz yoksunu TG2-W241A transdükte edilmiştir. Hücre yüzey markörü analizleri ve kürecik tahlili sonuçları TG2'nin GTP-bağlama fonksiyonunun mezenkimal fenotipi ve kanser kök hücre profilinin devamlılığı için önemli olduğunu göstermiştir. Ayrıca EMG transkripsiyon faktörlerinin ve matris metaloproteinazlarının seviyeleri ile hücre saçılma ve matrijel invazyon tahlilleri doğrultusunda, TG2'nin GTPaz aktivitesinin böbrek kanseri hücre göçünde ve invazyonunda vazgeçilmez olduğu ortaya çıkmıştır. Bunlara ek olarak, EMSA deneyi sonuçları GTPaz fonksiyonunun NFκB aktivitesinde gerekli olduğunu göstermiştir. Ortaya çıkan tüm sonuçlar göz önüne alındığında, TG2'nin böbrek kanseri gelişiminin ve metastazının desteklenmesinde temel olarak GTP bağlama fonksiyonuna muhtaç olduğu anlaşılmıştır. Bu proje FP-7 TRANSPATH 289964 tarafından finanse edilmiştir.

## TABLE OF CONTENTS

ACKNOWLEDGEMENTS.....	iii
ABSTRACT.....	iv
ÖZET .....	v
LIST OF FIGURES .....	x
LIST OF TABLES.....	xiv
LIST OF SYMBOLS/ABBREVIATIONS.....	xv
1. INTRODUCTION .....	1
1.1. ANATOMY, PHYSIOLOGY, AND BASIC FUNCTIONS OF THE KIDNEY	
1	
1.2. KIDNEY CANCER.....	3
1.3. TYPES OF KIDNEY CANCER.....	4
1.3.1. Transitional Cell Carcinoma.....	4
1.3.2. Wilms Tumor.....	4
1.3.3. Renal Sarcomas.....	4
1.3.4. Benign (Non-Cancerous) Kidney Tumors.....	5
1.3.5. Renal Cell Carcinoma.....	6
1.3.5.1. Pathological and Molecular Assortment of RCC Subtypes.....	6
1.3.5.2. Clear Cell Renal Cell Carcinoma.....	7
1.3.5.3. Papillary Renal Cell Carcinoma .....	9
1.3.5.4. Rare Renal Cell Carcinomas Subtypes .....	9
1.3.6. Recent Renal Tumor Oncogenes .....	10
1.4. GRADING OF RENAL TUMORS.....	13
1.5. MOLECULARLY TARGETED THERAPIES OF RCC .....	14
1.6. TRANSGLUTAMINASES .....	15
1.7. TISSUE TRANSGLUTAMINASES TYPE II (TG2).....	16
1.7.1. TG2 in Tumor Progression .....	19
1.7.2. TG2 in Cell Adhesion, Migration and Invasion .....	20
1.7.3. Epithelial to Mesenchymal Transition and TG2.....	21

1.7.3.1. Interplay Between NF- $\kappa$ B and TG2	22
1.7.3.2. Drug Resistance and TG2	24
1.7.4. TG2 in RCC	26
1.8. AIM OF THE STUDY	27
2. MATERIALS	28
2.1. INSTRUMENTS	28
2.2. EQUIPMENTS	28
2.3. CHEMICALS	29
3. METHODS	32
3.1. CELL CULTURE METHODS	32
3.1.1. Cell Lines and Culturing Conditions	32
3.1.2. Cell Subculturing	32
3.1.3. Calculation of Cell Number	32
3.1.4. Cryopreservation of Cell Lines	33
3.1.5. Cell Thawing	33
3.2. ISOLATION OF TG2 CONSTRUCTS PLASMID DNA	33
3.2.1. Plasmid Isolation	33
3.3. LENTIVIRAL PARTICLE PRODUCTION OF TG2 CONSTRUCTS AND TRANSDUCTION	34
3.3.1. Transfection of HEK293FT with DNA of Interest	34
3.3.2. Transduction of RenCa Cells with Obtained Lentiviral Particles	35
3.4..... IDENTIFICATION OF CANCER STEM CELL PROFILE OF TG2 IN RENCA CELL LINE TRANSDUCED WITH LENTIVIRAL PARTICLES	35
3.4.1. Detection of Cell Surface CD Markers Using Flow Cytometer	35
3.4.2. Spheroid and Sub-spheroid Formation Assay	36
3.5. DETECTION OF PROTEIN LEVELS IN RENCA MUTANT CELLS	37
3.5.1. Preparation of the Cell Lysate	37
3.5.2. Measurement of Protein Concentration by Lowry Assay	37
3.5.3. SDS-PAGE	38

3.5.4. Immunoblotting .....	39
3.6. DETECTION OF TG2 ACTIVITY IN RENCA CELLS EXPRESSING TG2 MUTANT CONSTRUCTS .....	40
3.6.1. TG2 Activity Assay .....	40
3.7. DETECTION OF GENE EXPRESSION LEVELS IN RENCA CELLS EXPRESSING TG2 MUTANT CONSTRUCTS.....	40
3.7.1. Total RNA Isolation.....	40
3.7.2. Reverse Transcriptase Polymerase Chain Reaction.....	41
3.7.3. Quantitative Polymerase Chain Reaction .....	42
3.8. DETECTION OF ACTIVE NUCLEAR PROTEIN NF- $\kappa$ B VIA ELECTROPHORETIC MOBILITY SHIFT ASSAY (EMSA) .....	43
3.8.1. Protein Extraction for EMSA .....	43
3.8.2. Preparation and Pre-Run of the EMSA Gels .....	45
3.8.3. Binding Reaction .....	45
3.8.4. Electrophoresis of Binding Reaction and Electrophoretic Transfer to Nylon Membrane .....	46
3.8.5. Detection of Biotin-Labeled DNA by Chemiluminescence and Development of the Membrane .....	47
3.9. CELL MIGRATION – SCATTERING ASSAY .....	48
3.10. TRANSWELL MATRIGEL INVASION ASSAY .....	48
3.11. THE DRUG RESISTANCY OF TG2-EXPRESSING RENCA CELLS .....	48
3.12. STATISTICAL ANALYSIS .....	49
4. RESULTS .....	50
4.1. DNA SEQUENCE ANALYSIS OF TG2 CONSTRUCTS.....	50
4.2. CONTROL OF TRANSFECTION EFFICACY IN HEK 293FT .....	55
4.3. DETERMINATION OF TG2 EXPRESSION LEVELS IN RENCA CELLS EXPRESSING TG2 MUTANT CONSTRUCTS.....	56
4.4. ACTIVATION OF NF- $\kappa$ B SIGNALLING TOGETHER WITH EMT IS DEPENDENT ON A FUNCTIONAL GFP-BINDING DOMAIN OF TG2 .....	59



4.5. CANCER STEM CELL PROFILE OF RENCA CELLS EXPRESSING TG2 MUTANT CONSTRUCTS .....	65
4.5.1. Characterization of Stemness Profile.....	65
4.5.2. GTP-binding Function of TG2 is Crucial in the RCC Sphere Formation	71
4.6. ROLE OF GTP-BINDING ACTIVITY OF TG2 IN RCC CELL MIGRATION	75
4.7. ROLE OF GTP-BINDING ACTIVITY OF TG2 IN THE UPREGULATION OF MMP AND INVASIVENESS.....	79
4.8. GTP-BINDING ACTIVITY OF TG2 IS IMPORTANT IN ACQUIRED RESISTANCE FOR THE TYROSINE KINASE INHIBITORS SORAFENIB AND EVEROLIMUS.....	84
5. DISCUSSION.....	91
6. CONCLUSION AND FUTURE PERSPECTIVE .....	97
REFERENCES .....	98

## LIST OF FIGURES

Figure 1.1. Position and basic anatomy of the kidney .....	1
Figure 1.2. Histological representation of the RCC subtypes.....	7
Figure 1.3. The basic illustration of renal tumor grading system stages. ....	13
Figure 1.4. Biological pathways of the therapeutically targeted agents used in RCC.....	15
Figure 1.5. Simple illustration of the TG2 structure.....	17
Figure 1.6. 3D structures of compact ‘closed’ and the extended ‘open’ form of TG2.....	19
Figure 1.7. Intra- and extracellular regulation of TG2-mediated EMT .....	22
Figure 1.8. Canonical and non-canonical signaling pathway of NFκB system.....	23
Figure 1.9. Illustration of TG2-dependent NF-κB activation pathway through which constitutive activation of NF-κB .....	25
Figure 1.10. The possible activating mechanism of TG2-enhanced cell survival in c-Src mediated PI3K manner .....	26
Figure 4.1. Chromatogram result of wt-TG2 cDNA .....	51
Figure 4.2. Chromatogram result of TG2-C277S cDNA cloned in Plenti BLAST plasmid under CMV promoter.....	52
Figure 4.3. Chromatogram result of TG2-W241A cDNA cloned in Plenti BLAST plasmid under CMV promoter.....	53

Figure 4.4. Chromatogram result of TG2-R580A cDNA cloned in Plenti BLAST plasmid under CMV promoter.....	54
Figure 4.5. Images of transfected HEK 293FT with eGFP were taken under a fluorescent microscope with a 10x objective at 24 and 48 hours after transfection.....	55
Figure 4.6. The relative <i>hTGM2</i> mRNA levels in RenCa cells transduced with wt and mutant <i>hTGM2</i> constructs was evaluated using RT-PCR. ....	56
Figure 4.7. Analysis of TG2 protein levels in membrane and whole cell lysates for RenCa cells expressing TG2 mutant constructs .....	57
Figure 4.8. The analysis of TG2 transamidating activity in TG2 mutant transduced RenCa cells using the specific TG2-CovTest colorimetric microassay kit. ....	58
Figure 4.9. Western Blots showing the protein levels of ITGβ1 and SDC4 in RenCa cells transduced with TG2-variants.....	59
Figure 4.10. Nuclear extract prepared from mutant expressing RenCa cells were subjected to EMSA .....	60
Figure 4.11. Immunoblots showing membranes probed with IκB-α and p- IκB-α in RenCa cells expressing TG2 mutant constructs for the evaluation of the protein levels .....	61
Figure 4.12. Real time (RT-PCR) expression levels of EMT markers <i>Zeb1/Zeb2</i> in non-transduced and mock control RenCa cells and RenCa cells transduced with TG2 constructs .....	62
Figure 4.13. Real time (RT-PCR) expression levels of EMT markers <i>Twist1/Twist2</i> in non-transduced and mock control RenCa cells and RenCa cells transduced with TG2 constructs .....	63

Figure 4.14. Real time (RT-PCR) expression levels of EMT markers Snail1/Snail2 in non-transduced and mock control RenCa cells and RenCa cells transduced with TG2 constructs .....	64
Figure 4.15. Flow cytometry analysis of mouse IgG isotype control and, mouse CD44 marker in TG2- expressing RenCa cells. ....	66
Figure 4.16. Flow cytometry analysis of CD73, CD106 cell surface mesenchymal markers in TG2- expressing RenCa cells. ....	68
Figure 4.17. Flow cytometry analysis of mouse CD11b, mouse Sca-1 mouse CD45 cell surface mesenchymal markers in TG2- expressing RenCa cells. ....	70
Figure 4.18. Representative images of the formed spheres by non-transduced parental and mock control and TG2-expressing mutant RenCa cells from the day 1-11. ....	72
Figure 4.19. Representative images of the formed sub-spheres by non-transduced parental and mock control and TG2-expressing mutant RenCa cells from the day 1-11. ....	74
Figure 4.20. Cell motility potential of TG2-expressing transduced RenCa cells .....	76
Figure 4.21. Cell motility potential of TG2-expressing transduced RenCa cells were monitored using scattering assay .....	77
Figure 4.22. The mRNA level expression of cell to cell adhesion switching involving E-cadherin and N-cadherin by RT-PCR analysis. ....	78
Figure 4.23. RT-PCR analysis of vimentin expression of transduced RenCa cells with TG2 constructs. ....	79
Figure 4.24. Real Time (RT-PCR) analysis indicating the changes in the mRNA expression levels of MMP in TG2-expressing RenCa cells. ....	81

Figure 4.25. Invasion potential was evaluated in parental and TG2-expressing mutant cells .....	83
Figure 4.26. The role of TG2 functional domains on the drug resistance of non-transduced parental RenCa cells .....	85
Figure 4.27. The role of TG2 functional domains on the drug resistance of of wild type TG2 (wt-TG2).....	86
Figure 4.28. The role of TG2 functional domains on the drug resistance of transamidating inactive form of TG2 (TG2-C277S) cells.....	87
Figure 4.29. The role of TG2 functional domains on the drug resistance of transaminase inactive TG2-W241A RenCa cells.....	88
Figure 4.30. The role of TG2 functional domains on the drug resistance of GTP-binding null TG2-R580A cells.....	90

**LIST OF TABLES**

Table 1.1. The updated version of WHO classification .....	12
Table 3.1. The ingredients of stacking and separating polyacrylamide gel for two .....	38
Table 3.2. Senscript cDNA converter reaction mix .....	41
Table 3.3. Quantitative PCR conditions .....	42
Table 3.4. Hypotonic solution ingredients .....	44
Table 3.5. Hypertonic solution ingredients .....	44
Table 3.6. Ingredients of top and bottom for two gels .....	45
Table 3.7. Binding reaction mix .....	46
Table 3.8. Detection and blocking buffers .....	47
Table 4.1. The sequence of the forward and reverse primers used in sequencing of TG2 native and mutant constructs .....	50
Table 4.2. Expression level of cell surface markers. ....	71

**LIST OF SYMBOLS/ABBREVIATIONS**

AML	Angiomyolipoma
APS	Ammonium persulfate
ATTC	American type culture collection
ATP	Adenosine triphosphate
BSA	Bovine serum albumin
CCRCC	Clear cell renal cell carcinoma
cDNA	Complementary deoxyribonucleic acid
CRRCC	Chromophobe renal cell carcinoma
CCPRCC	Clear cell papillary renal cell carcinoma
DMEM	Dulbecco's modified Eagle's medium
DMSO	Dimethyl sulfoxide
DTT	Dithiothreitol
ECM	Extracellular matrix
EDTA	Ethylenediaminetetraacetic acid
EGF	Epidermal growth factor
EMT	Epithelial mesenchymal transition
FAK	Focal adhesion kinase
FBS	Fetal bovine serum
FGF	Fibroblast growth factor
FH	Fumarate hydratase
FN	Fibronectin
HGF	Hepatocyte growth factor
HIF	Hypoxia inducible factor
HIF-1 $\alpha$	Hypoxia inducible factor-1 $\alpha$
HRP	Horse-radish peroxidase
HRPC	Hereditary papillary renal carcinoma
IDCS	Interdigitating dendritic cell sarcoma
ITG $\beta$ 1	Integrin beta 1
M	Molar
ml	Milliliter

μl	Microliters
mM	Millimolar
MMP	Matrix metalloproteinase
MRCC	Metastatic renal cell carcinoma
MTSCC	Mucinous tubular and spindle cell carcinoma
MTOR	Mammalian target of rapamycin
PDGF	Platelet derived growth factor
PDGFR	Platelet derieved growth factor receptor
pH	Negative log of hydrogen ion concentration
PNET	Primitive neuroectodermal tumor
PRCC	Papillary renal cell carcinoma
PVDF	Polyvinylidene difluoride
PVHL	The VHL protein
RCC	Renal cell carcinoma
RMS	Rhabdomyosarcoma
P/S	Penicillin, streptomycin
QPCR	Quantitative polymerase chain reaction
RT	Reverse transcriptase
SD	Standard Deviation
SDC	Syndecan
SDS-PAGE	Sodium dodecyl sulfate polyacrylamide gel electrophoresis
SHDB	Succinate dehydrogenase B
TCC	Transitional cell carcinoma
TEMED	N,N,N',N'- Tetramethylethylenediamine
TG	Transglutaminase
TG2	Tissue transglutaminase
TNM	Tumor-node-metastasis staging guideline
TSC	Tuberous sclerosis complex
VEGF	Vascular endothelial growth factor
VHL	Von Hippel Lindau
WST-	Water soluble tetrazolium salt
WHO	World health organization



## 1. INTRODUCTION

### 1.1. ANATOMY, PHYSIOLOGY, AND BASIC FUNCTIONS OF THE KIDNEY

The kidneys are the core members of the urinary system that are externally surrounded by the three main layers such as the renal fascia known as the outermost layer made up of connective tissue layers, the perirenal fat capsule, the middle layer to help fasten the kidneys in position and the renal capsule itself in the innermost layer. Internally, kidneys are also separated into three regions such as an outer cortex, a middle region called medulla and lastly a region called hilum of the kidney, the renal pelvis [1]. Kidneys are located on either side of the spine at the lowest stage of the rib cage, just behind the posterior abdominal wall in the anterior side of the peritoneal cavity. Kidneys could describe as the bean-shaped organs with a color of reddish-brown range and an approximate size of a human fist. The exact position of kidneys can be pointed by using the external poles of the kidneys such as the upper terminal of each kidney placed in the exactly opposite side of the 12<sup>th</sup> thoracic vertebra and the lowest terminal of each kidney located on the exactly in the 3<sup>rd</sup> lumbar vertebra (Figure 1.1) [2].

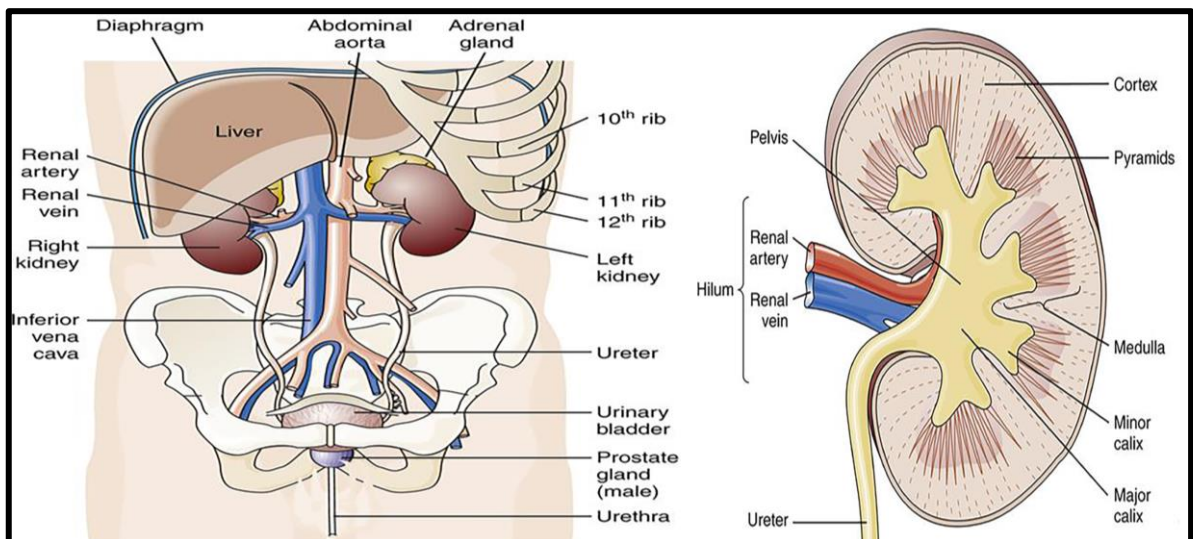


Figure 1.1. Position and basic anatomy of the kidney [3].

The urinary system is composed of the kidneys and their additional accessories, in the renal physiology. Kidneys could not just defined as one big filtering sponges in the body because each kidney posses a complicated system in their own structure. They composed of millions of tiny functioning filter units called as nephrons with their own tiny blood vessels named as glomerulus conjoined to a tubule. The basic mechanism of the nephrons is a two-step process. Initially, the glomerulus pass the fluids and waste products through the nephrons while preventing the entrance of blood cells and large molecules such as proteins. Afterwards, filtered fluid transmits through the tubule in order to send the essential minerals straight back to the bloodstream whilst removing the wastes with the help of the final product called urine. Then, urine is urged into two tubes called ureters following down to the bladder and leaves the body via the urethra.

Kidneys posses a multi-functional powerhouse of activity including the removal of metabolic wastes when the toxic level was reached and the disturbance of the blood volume and ion levels which cause serious medical issues in human systems. Besides the kidney could also be termed as the homeostatic regulator in the body by balancing the water and ion ingredient of the blood, which could briefly called as the salt-water balance or fluid-electrolyte balance.

General functions of the kidney can be divided into six general categories. Kidneys are responsible from the adjustment of extracellular fluid volume as well as the blood pressure that is crucial for the maintenance of the sufficient blood flow to the brain and also to the other organs. Kidneys are also the main player in the homeostasis process of the body especially in the term of keeping stable the concentrations of the key ions by reabsorption. They take part in the regulation of the osmolarity in the body and maintenance of ion balance. For example, sodium ( $\text{Na}^+$ ) is considered as one of the major ions in the regulation of the osmolarity in the body, additionally, concentration of potassium ( $\text{K}^+$ ) and calcium ( $\text{Ca}^+$ ) ions in the body is also regulated by the renal control system. Another important function of kidneys is the homeostatic calibration of pH in order to maintain the pH of the plasma in the narrow ranges. In the case of acidosis, kidneys start to absorb  $\text{H}^+$  ions from the blood and conserve  $\text{HCO}_3^-$  ions to neutralize the pH, on the other hand in the case of alkalosis, kidneys, this time remove the  $\text{HCO}_3^-$  and conserve the  $\text{H}^+$  ions. Excretion process of wastes is also considered as the one of the momentous functions of the kidneys as they are responsible for the removal of the metabolic waste products like creatinine

which is produced from the muscle metabolism or nitrogenous wastes such as urea and uric acid, and foreign substances that were entered into the body. In last, the production of essential hormones is accepted as important as the other functions of the kidneys because, even though kidneys are not endocrine glands, they take major part in three endocrine pathways. First of all kidney regulates the red blood cell synthesis by producing the cytokine called erythropoietin, secondly, kidney are responsible from release of an enzyme called renin, which is important for the regulation of blood pressure and sodium balance. Finally, kidneys are the organs where vitamin D3 (1,25-dihydroxycholecalciferol), a hormone that regulates the  $\text{Ca}^+$  balance in the system, is produced [4].

According to the National Kidney Foundation, 33 per cent of American adults are at high risk for developing kidney disease during their lifetime but poor kidney genetics or even care could cause the kidney health issues wide range. Chronic kidney failure is diagnosed when the functioning of the kidneys stop slowly. The cause of the kidney diseases could vary including type 1 and 2 diabetes, high blood pressure as well as the inflammation of the different parts of the kidneys or the obstructions in the urinary tract. It is momentous to mention that kidney failure is the severest stage of the kidney disease and in such cases, kidney transplantation and dialysis processes are the two main remedies for patients to survive. According to the U.S. National Library of Medicine, kidney transplantations are the most commonly performed surgeries in the United States [5]. Other kidney problems could be itemized as cancer, kidney stones, infections such as pyelonephritis and cysts [6].

## **1.2. KIDNEY CANCER**

Cancer could be elementarily explained as the commencement off-leash cell growth in the body and the spread of this uncontrolled cell growth to the other parts of the body. It was presumed that there exist over hundreds of diversified types of cancer and in order to categorize each of them a very basic method was used which was based on the location where the cancer cells were originally arose Hereby, kidney cancer could be basically summarized as the type of cancer that starts initially in the kidney.

According to 2015 data of American Society of Clinical Oncology, kidney cancer was the seventh commonly encountered type of cancer worldwide and in the year of 2015, 61,560

adults were diagnosed with both renal pelvic cancer and kidney cancer in the United States.

### **1.3. TYPES OF KIDNEY CANCER**

#### **1.3.1. Transitional Cell Carcinoma**

Transitional cell carcinomas (TCCs) were generally seen in the five to seven per cent of the upper urinary tract in kidney. These tumors associated often with the urothelial tumors with the renal pelvic lesions. TCCs were seldomly seen under the age of 50 but in the case of the incidence, the surgical resection of tumor is favorable through a therapy known as the radical nephroureterectomy but due to technological advances in the area less invasive techniques now being performed for the TCCs [7, 8].

#### **1.3.2. Wilms Tumor**

Wilms tumors also known as nephroblastomas were most commonly seen in young children from nephrogenic rests. This type of kidney cancer generally occurs because of the failure in the parts of the developing kidney during the complete differentiation process. Additionally, the mass of the Wilms tumor ingenerates from few components that have the resemblance to the tissue structures of the fetal kidney such as mesencynmal stroma, tubular structures and blastema. Unlike other types of kidney cancer, Wilms tumor can be successfully treated with radiation and chemotherapy when combined with the surgical approaches [9].

#### **1.3.3. Renal Sarcomas**

Renal sarcomas constitute 0.8-2.7 per cent of the malignant kidney tumors and because of the rarity and infrequency of the condition, it is very difficult to diagnose. However, based on the clinical features and case reports about renal sarcomas it was known that renal sarcoma has been primarily derived form the other anatomic sites and consist of several histological subtypes including synovial sarcoma, osteogenic sarcoma, malignant

fibrosarcoma, carcinosarcoma, rhabdomyosarcoma (RMS), angiosarcoma, myeloid sarcoma, anaplastic sarcoma, interdigitating dendritic cell sarcoma (IDCS), Ewing's sarcoma/primitive neuroectodermal tumor (PNET), and malignant hemangiopericytoma [10].

Another genuine characteristic of sarcomas was their capacity to arise from the mesenchymal components because of the absence of the natural barriers, so they could expand in size. Eventhough, it was reported that sarcomas typically possess pseudocapsule, they were seen as the unreliable barriers that can be infiltrated by the tumor [11].

#### **1.3.4. Benign (Non-Cancerous) Kidney Tumors**

Angiomyolipoma (AML), renal adenoma and oncocytoma are the relatively most frequent benign renal tumors.

AML is one of the most commonly seen mesenchymal tumor of the kidney with a frequency of 0.1–0.22 per cent in the general population. It consists of smooth muscle, vascular and fat elements [12]. Interestingly, the lesions might be seen in sporadic cases and could be associated with the tuberous sclerosis complex (TSC). TSC was diagnosed in almost 20 per cent of the all AML cases. It was mentioned that TSC was an autosomal dominant disorder that generally affects multiple organs including kidney. In addition, AMLs and renal cysts together represent the kidney manifestation of this syndrome [13].

Renal adenoma and oncocytoma have specific genitourinary symptoms and initially detected as small renal masses. According to the radiological case reports it was suggested that the lesions couldn't be differentiated from renal cell carcinoma only by consideration of pathological features [14, 15]. Additionally, renal adenoma often histologically indistinguishable from renal cell carcinoma and renal oncocytoma. Therefore, diagnosis approaches such as needle biopsy and aspiration cytology were limited for these lesions. However, because of the similarity characteristics of these lesions to the renal cell carcinoma, the only reliable diagnosis and treatment were considered as the surgical excision for this type of kidney tumors [14].

### **1.3.5. Renal Cell Carcinoma**

RCC termed as the renal cell cancer or renal cell adenocarcinoma is one of the subtype of the kidney cancer with a high mortality rate. According to American Cancer Society, approximately nine kidney cancer cases out of ten were assigned as the renal cell carcinomas. It was seen that in the most medical cases, RCC was listed as the sixth severe cause of cancer death that usually grown in a single tumor but sometimes in some cases more than one might grow in a single or in both kidneys at the same time with an incidence of 60,000 cases. According to Cancer Research UK London Research Institute, RCC is an epithelial neoplasm that was mainly arisen from the parenchyma of the kidney. 95 per cent of RCC was determined as the renal neoplasm where three per cent were stated as the adult malignancies [16, 17]. Even though, the prognosis of the RCC usually depends on the clinical cases itself, there were some traditional approaches that could be used in the prognosis level such as tumor stage, nuclear grade and histological tumor necrosis. If RCC was detected in early stages, it is possible to cure with a surgical resection approach but unfortunately no absolute treatment exist for the metastatic RCC yet. However, the patients whom have the disease confined to the kidney or even in the regional lymph nodes could be treated with a partial or radical nephrectomy in the intent of goodwill. However, one third of the patients were diagnosed with the metastasis at the time of the diagnosis and the other one third of the patients were developed secondary site metastatic tumors including lymph nodes, lung and bone within five years interval [18, 19].

#### ***1.3.5.1. Pathological and Molecular Assortment of RCC Subtypes***

Approximately two decades ago, RCCs were divided into two subgroups including clear cell carcinoma and granular cell variants. However, in 2004, WHO system identified several RCC subtypes that were accepted by the scientific comity. According to WHO classification, the major histological subtypes were categorized as clear cell renal cell carcinoma (ccRCC), papillary renal cell carcinomas type 1 and type 2 (pRCC), chromophobe renal cell carcinomas (crRCC), and collecting duct cancers which were represented the 90 per cent of the whole RCCs (Figure 1.2.) [7, 8].

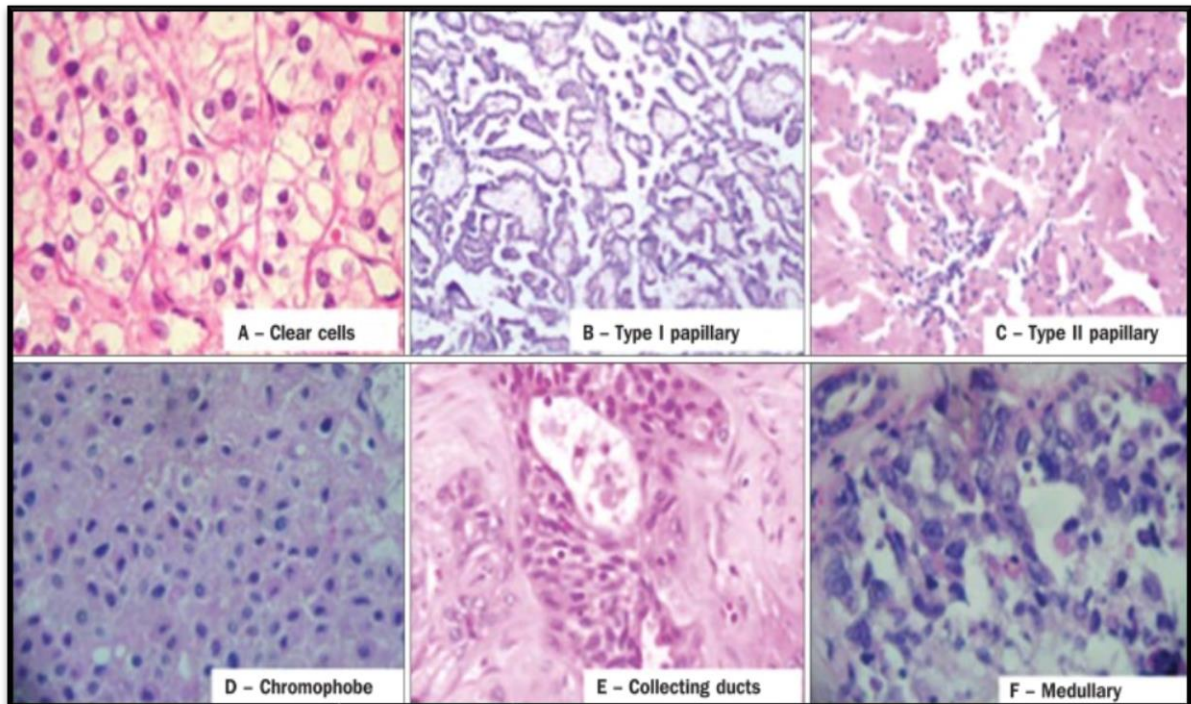


Figure 1.2. Histological representation of the RCC subtypes [20]

#### ***1.3.5.2. Clear Cell Renal Cell Carcinoma***

ccRCC was accounted for almost 70 per cent of malignant kidney tumors and one ninth of this type of RCCs showed the metastatic potential. So far, ccRCCs were recognized histologically by the clear cell cytoplasm and in the terms of morphology, granularity and sarcomatoid characteristics. On the other hand, the diagnosis of the ccRCC could be successfully carried out by the hematoxylin and eosin-stained microscopy techniques. Another typically used approach based on the immunohistochemical pattern was simply done with vimentin, cytokeratin and CA-IX staining [21].

About the genetic profile of ccRCC, it can be said that the characteristic property was the lack of the DNA in the short arm of the third chromosome, which normally contains a tumor suppressor gene called Von Hippel-Lindau (VHL) gene in its structure. In the presence of somatic mutation or hypermethylation, sporadic clear cell tumors occurs within 80 per cent of frequency through the inactivation of VHL gene [22]. In the term of tumor pathogenesis, it was understood that at least 60 per cent of the RCC cases were related with

the VHL, a tumor suppressor gene, in which its inactivation indorses tumorigenicity. It is a component of an E3 ubiquitin ligase complex and it is mainly responsible for the ubiquitination and proteasome mediated degradation of a momentous transcription factor named hypoxia-inducible factor [23]. The VHL protein (pVHL) had an utmost devoire in the regulation of hypoxia-inducible factor (HIF) [23] due to the ubiquitin-mediated destruction. Moreover, in the absence of the functional pVHL, several hypoxia response genes including erythropoietin [24], vascular endothelial growth factor (VEGF), platelet-derived growth factor (PDGF) [25], TGF- $\alpha$  and TGF- $\beta$  were activated by HIF itself. Additionally, it also has been confirmed that these mentioned factors are associated with tumor growth and angiogenesis [26, 27]. Increase in HIF gene expression contributes to angiogenesis through the activation of mTOR pathway specifically involved in the part of the complex PI3 kinase/Akt pathway [28]. Increase in HIF gene expression contributes to angiogenesis through the activation of mTOR pathway specifically involved in the part of the complex PI3 kinase/Akt pathway. However, in the case of the oxygen and nutrient depletion, cancer cells must adapt to the hypoxic stress conditions in order to maintain tumor development and growth. During the adaptation of hypoxic stress, two main features has been observed including the increased in anaerobic glycolysis and the secretion of the proangiogenic factor known as VEGF. Thus the molecular mechanism of the cellular response against to the hypoxic stress considered to be relevant with the cancer biology. Interestingly, under the normoxic conditions, one of the subunit of HIF gene, which is HIF-1 $\alpha$  gene, is continuously transcribed and translated but, the levels of HIF-1 $\alpha$  gene was found to be very minimal because of the rapid degradation through the ubiquitin-proteasome pathway, which was mediated through the interaction between HIF-1 $\alpha$  and the E3 ubiquitin ligase complex under normoxic condition [28]. On the other hand, it has been showed that the tumor suppressor function of VHL gene deregulated the HIF-1 $\alpha$  expression and inhibited the promotion of the tumor development. Several groups showed that in the lack of pVHL mRNA expression levels of hypoxia-inducible gene overproduced and in the case of the restoration of pVHL and in the presence of oxygen, the mRNAs expression levels of the hypoxia-inducible gene suppressed [29, 30]. Therefore, it can be said that under normoxic conditions, the continuously accumulated mRNA levels of the hypoxia-inducible gene is a molecular sign of the inactivated pVHL. Moreover, as it was mentioned before, HIF gene expression contributes to the angiogenesis by activating the mTOR pathway including the activation of complex PI3 kinase/Akt pathway. Interestingly,



the contribution of the PI3 kinase/Akt pathway to the tumorigenesis process was associated with the PTEN, which was known as the major tumor suppressor gene that was inactivated in various human cancers [31]. In addition, recently, it was shown that the PTEN-deficient cells indicate an excess activation of HIF-1 in response to the hypoxia conditions [32].

#### ***1.3.5.3. Papillary Renal Cell Carcinoma***

pRCC was sub-grouped into types one and two that were morphologically and biologically different from each other. pRCC approximately covers 15 per cent of the malignant kidney tumors. It was demonstrated that the most of the malignant kidney tumors, almost 60-70 per cent were diagnosed as type 1-papillary tumors [33, 34]. Hereditary papillary renal carcinoma (HRPC) was related with the activation of the mutation in the MET gene on chromosome 7. Furthermore, the oncogene encodes a membrane tyrosine kinase receptor including a ligand of hepatocyte growth factor (HGF), which has multiple downstream signaling pathways. One of the important receptor of this pathway was known as the PI3K, which was responsible for the cell proliferation, cell survival and even the cell mortality. Therefore, the constitutive activation of this pathway was considered as the path breaking factor for the carcinogenesis [35]. On the other hand, type 2 pRCC accounts for 30-40 per cent of papillary tumors that could occur in both hereditary and sporadic forms. Contrarily to type 1 pRCC, these type of tumors were seen to be high graded and complex in the cytogenetical manner, making the prognosis difficult. Patients suffering from this disease possessed a mutation in Krebs Cycle enzymes, fumarate hydratase (FH) and succinate dehydrogenase B (SHDB), leading to the accumulation of fumarate and succinate [36]. In addition to the inactivating mutations in the Krebs cycle, other cell signaling pathways like the over activation of myc pathway might be also closely related with the aggressive type 2 pRCC [37].

#### ***1.3.5.4. Rare Renal Cell Carcinomas Subtypes***

Eventhough, the several rare subtypes of the RCC has been identified and newly entered in the WHO classification 2016, the exact molecular characteristics of these newly entered subtypes of RCC were remained unclear.

Collecting duct carcinomas do not share the same molecular abnormalities or mutations with the urothelial carcinomas, even though they both share the same embryological origin as the ureter. The tumors that were caused by collecting duct have been identified due to the loss of chromosome 8p. Likewise, the genetic anomalies that could be seen in mucinous tubular and spindle cell carcinoma (MTSCC) exhibited heterogeneity and required further investigations [38]. Another example for the rare subtypes could be the tumors that were firstly included in the WHO classification in 2004 known as Xp11 translocation tumors, and mostly children and adolescents were suffered from this mentioned disease. Because of their unique histological appearance, they were defined through a breakpoint at the Xp11 chromosome and gene fusions that was joined TFE3 transcription factor with the several other genes [38, 39].

### **1.3.6. Recent Renal Tumor Oncogenes**

The WHO classification was updated over years, and according to the fourth edition of WHO classification published in 2016 illustrated in Table 1.1, significant updates in the literature has been made by pathologists and the list of the RCC subtypes has been expanded by adding newly recognized RCC subtypes such as epithelial renal tumors, which were classified as renal cell carcinoma syndrome associated RCC (HLRCC), tubulocystic RCC, hereditary leiomyomatosis, acquired cystic disease associated RCC, succinate dehydrogenase deficient RCC (SDH-deficient RCC), and lastly clear cell papillary RCC [40-44]. HLRCC was characterized as an autosomal dominant disorder with a mutation in the fumarate hydratase (FH) gene. It is located at 1q42.3-q43 chromosome and plays a role in the tricarboxylic acid cycle by catalyzing and hydrating fumarate to malate. SDH-deficient RCC was categorized as the rare renal neoplasm because of the dysfunction in the mitochondrial complex II. Great majority of the patients suffer from these tumors have a high risk in the development of paragangliomas and gastrointestinal stromal tumors and approximately entire reported cases have been related with the germline mutation in the SDH genes. Clear cell papillary RCC (ccpRCC) is quite likely one of the newly recognized renal tumor oncogenes. It generally consists of low-grade neoplasm of clear epithelial cells in the form of tubules or papillae. Interestingly, it was identified as a pain-free tumor and it was hard to distinguish from ccRCC. According to

the recent clinical cases, the diagnosis of ccpRCC was really difficult because it might arisen from the mix population of the ccp- and cc- conventional RCC cells.



Table 1.1. The updated version of WHO classification for the kidney tumors [42].

<b>WHO Classification of Kidney Tumors</b>	
<b>Renal Cell Tumors</b>	<ul style="list-style-type: none"> <li>• Clear Cell Carcinoma</li> <li>• Papillary Renal Cell Carcinoma</li> <li>• HRPC</li> <li>• Chromophobe Renal Cell Carcinoma</li> <li>• Collecting Duct Carcinoma</li> <li>• SDH-deficient Renal Cell Carcinoma</li> <li>• Acquired Cystic Disease associated RCC</li> <li>• Clear Cell Papillary Renal Cell Carcinoma</li> <li>• Papillary Adenoma</li> <li>• Oncocytoma</li> </ul>
<b>Metanephric Tumors</b>	
<b>Nephroblastic and Cystic Tumors occurring mainly in children</b>	
<b>Mesenchymal Tumors</b>	<ul style="list-style-type: none"> <li>• Mesenchymal Tumors occurring mainly in children</li> <li>• Mesenchymal Tumors occurring mainly in adults</li> </ul>
<b>Mixed epithelial and stromal tumor family</b>	
<b>Neuroendocrine Tumors</b>	
<b>Miscellaneous Tumors</b>	
<b>Metastatic Tumors</b>	

#### 1.4. GRADING OF RENAL TUMORS

In the 2016, WHO classification was updated and a new grading system (ISUP/WHO) entered into the literature. It was way much improved and simpler compared to the previously used Fuhrman grading system [45]. The Fuhrmann grading system was basically based on the tumor-node-metastasis (TNM) staging guidelines (Figure 1.3.) and in mentioned Fuhrmann grading system, the nucleolar size and appearances by avoiding the estimation of nuclear size were considered. However, in ISUP/WHO classification, there is four-tiered grading steps that is defined as follows; first grade; unnoticeable or absent nucleoli at 400X magnification, second grade; nucleoli becomes noticeable at 400X magnification and also visible yet not prominent at 100X magnification, third grade; nucleoli becomes remarkable at 100X magnification and lastly, fourth grade; multi-nucleated giant or sarcomatoid cells could be seen together with the extreme nuclear pleomorphism. This grading system has not been verified yet for the rarely seen tumor subtypes, therefore it could not be applied in every single types of tumors yet [46].

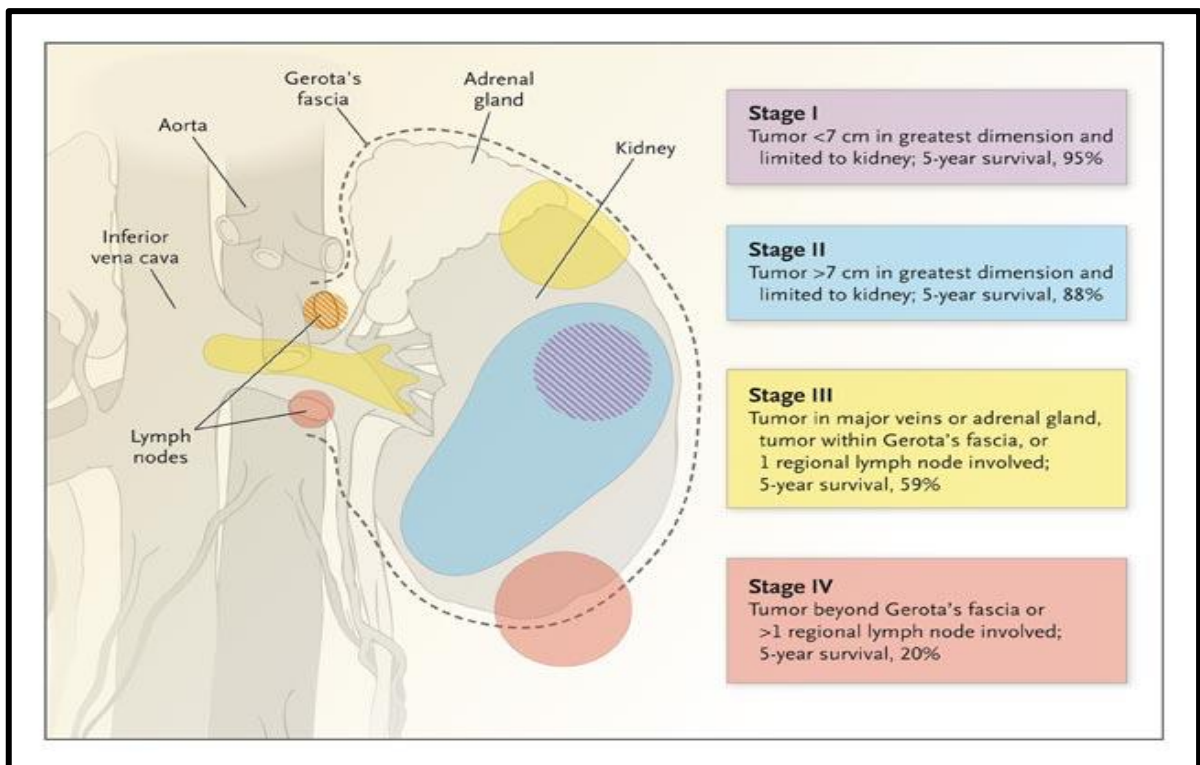


Figure 1.3. The basic illustration of renal tumor grading system stages [47].

## 1.5. MOLECULARLY TARGETED THERAPIES OF RCC

RCC was considered as the most resistant tumors against to the radio- and chemotherapies. Until recently, high-dose interleukin-2 (aldesleukin) and interferon were used as the standard treatment approved by the FDA for the metastatic renal cell carcinoma (mRCC) patients. Although previously mentioned agents were used for more than twenty years, it was known that the high-dose therapy with these agents was quite toxic and, in the most cases their benefits remain unclear with controversial reports on the effectiveness of the therapy [48]. Therefore, present investigations try to describe the molecular phenotype of the tumor cells based on its biological pathways in order to maximize the benefit and develop a targeted therapy. Thanks to the discoveries of the molecular biology of RCC, it was suggested that the VEGF and mTOR pathways could be the ones for the relevant therapeutic targets. In RCC and other solid tumors, the deficient pVHL was not able to bind to HIF in hypoxic conditions as a result of that the activated HIF translocates into the nucleus and promotes the transcription of some genes that took crucial role in the tumor progression [49]. Additionally, another pathway called as mTOR pathway activation also leads to HIF production as well, and the targets of HIF were PDGF, bFGF, VEGF and TGF- $\alpha$  genes. In this context, advanced metastatic RCC was aimed to primarily treated through the chemotherapeutic agents that systematically inhibits the several signaling pathways by targeting the multiple factors including VEGF, its receptors and mTOR. Moreover, in mTOR pathway, the accumulation of HIF activates initially, phosphoinositide 3-kinase (PI3K)/Akt (protein kinase) pathway through the cellular stimuli. Afterward the phosphorylation of mTOR, in turn activates p70S6 kinase (p70S6K) in order to ignite the translation of several important proteins including HIF. Meanwhile, the phosphorylation of 4E binding protein-1 (4E-BP1) was triggered for the dissociation of the complex to stimulate the eukaryotic initiation factor-4 subunit E (eIF-4E) which shown to play a momentous role in tumor development leading to mRNA translations in regulating the cell cycle involving c-myc and cyclin D1.. Following, activated HIF was entered into the nucleus and started a large range transcription of HI genes including VEGF and PDGF. Cell migration, proliferation, survival and even the cell permeability processes were triggered through the binding of ligands to their specific receptors on the endothelial cells. Hence forth, chemotherapeutic drugs inhibiting VEGFR (sorafenib) and

mTOR (everolimus) pathways were used as a first-line treatment in metastatic RCC (Figure 1.4.).

In order to advance forward in the systemic treatments and the understanding of the biology of RCC, the researchers try to uncover the molecular genetics and also identify the novel therapeutic targets that can be used against RCC [3, 48].

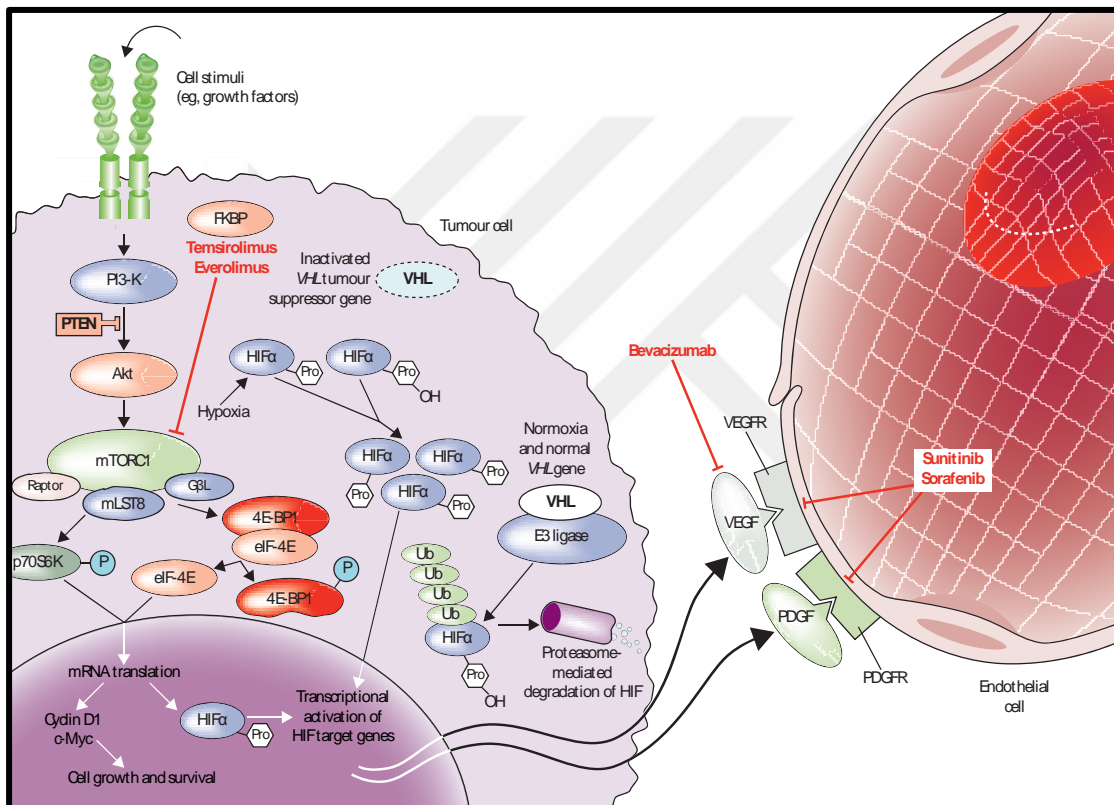


Figure 1.4. Biological pathways of the therapeutically targeted agents used in RCC [3].

## 1.6. TRANSGLUTAMINASES

Transglutaminases (TGs) are a big family with nine members of either structurally or functionally related proteins that are responsible for the catalyzing the  $\text{Ca}^{2+}$ -dependent posttranslational modification and crosslinking activities of proteins through the covalently binding to the free amine groups or carboxamide groups of peptide-bound glutamines [50]. TG2 was initially isolated from the liver of guinea pig in 1959 [51]. Researchers

discovered nine TG genes in humans; eight of them were identified as the catalytically active enzymes and the ninth gene was defined as the inactive erythrocyte membrane protein. TG proteins act as scaffolds [52], maintain membrane integrity [53], adjust cell adhesion and migration potency [54] and alter signal transduction [55]. Moreover, TGs also serve as catalyzers in the posttranslational modification of proteins. Likewise, TG-catalyzed integration of amines into proteins can also shift the function, stability and also immunogenicity of the substrate proteins and lead to the development of autoimmune disease [56]. Out of nine TGs were entered in the literature, TG2 is on the front burner and widely studied so far due to its ubiquitous expression [50].

### **1.7. TISSUE TRANSGLUTAMINASES TYPE II (TG2)**

TG2 also known as TGc or Gh, a multifunctional protein, widely spreaded in tissues and cell types. It was mainly referred as the cytosolic protein but it is a protein that could also localized in the multiple cellular compartments such as mitochondria, nucleus, plasma membrane, endolysosomes, cell surface and extracellular matrix (ECM). TG2 is located on the chromosome 20q11-12 in humans entirely composed of 13 exons and 12 introns. It is responsible from the encoding of totally 687 amino acids with a molecular weight of around 78 kDa [57]. It consists of four domains such as  $\beta$ -sandwich domain, catalytic core domain including TGase catalytic triad,  $\beta$ -barrel 1, and  $\beta$ -barrel 2 [58].



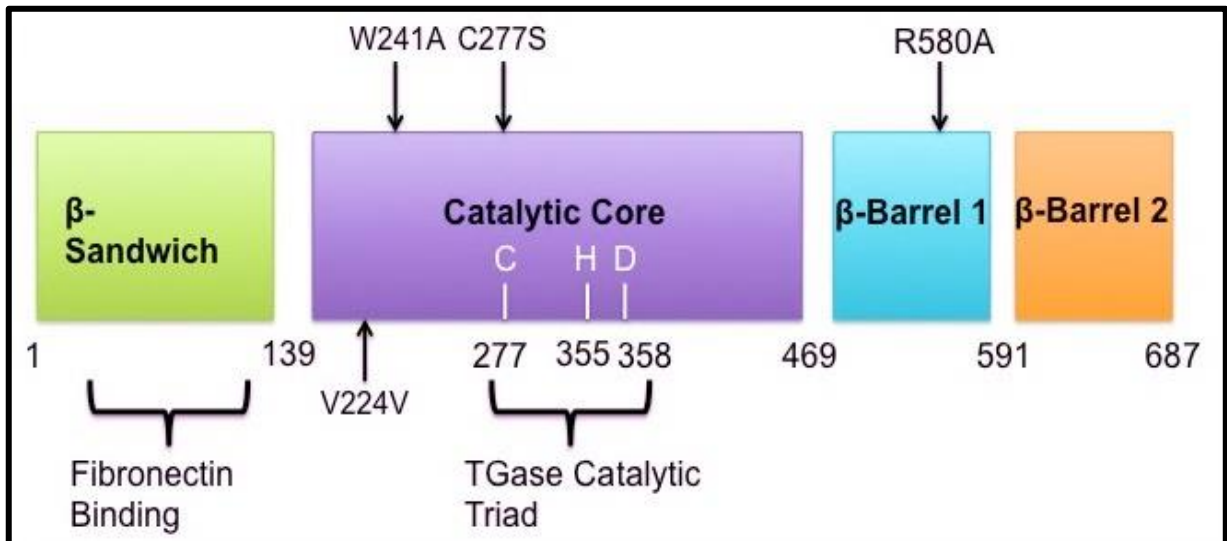


Figure 1.5. Simple illustration of the TG2 structure. The black arrows indicated the mutagenized sites on the catalytic core domain and  $\beta$ -barrel 1 domain. TGase: transglutaminase activity.

TG2 is a complex protein both in structural and functional manner with dual actions including intra- and extra-cellular functions. For example, N-terminal  $\beta$ -sandwich domain is responsible for the high-affinity binding site for fibronectin and enables the attachment of the cells to the ECM either directly or indirectly. Studies done over the course of many years revealing the crystal structure of TG2, facilitated the understanding of how the activity of this crucial protein was regulated in the cellular manner through open to closed confirmation [55, 59, 60]. For TG2 to exist in 'extended' (open) form,  $\text{Ca}^{2+}$  binding is required while the 'compact' (closed) conformation in which the active site (center of the protein) was unmasked and also GTP, GDP and ATP functions were inhibited (Figure 1.6.). In the extended form of TG2 the catalytic core domain was the blame for the cross-linking activity of various cellular proteins by providing highly stable isopeptide bonds. Probable function of catalytic core domain was accepted as the apoptotic cell death of the cell and inflammation.  $\beta$ -barrel 1 domain possess a GTP/ATP-binding site through which several crucial functions such as cell survival, cell growth and invasion were involved in TG2-mediated signaling pathways [61]. Lastly, the  $\beta$ -barrel 2 domain promotes the activation of phospholipase C under certain conditions and takes action in the pro-inflammatory processes of the TG2 protein [57, 62].

In the structure of TGM2, the retinoic acid response element located in the 1.7 kb upstream in the TGM2 promoter, a specific *cis*-regulatory element, interleukin-6 (IL-6), substantially located on the upstream of the promoter, a transforming growth factor-1 (TGF-1) response element and two AP2-like response elements found respectively 634 and 183 base pair away from the transcription initiation site. There are several factors that can induce TG2 expression including retinoic acid, TGF-1, IL-6, vitamin D, tumor necrosis factor (TNF), epidermal growth factor (EGF), NFκB, oxidative stress responses, phorbol ester and Hox-A7 [50]. TG2 is a multifunctional protein as it is not only serve in the transamidation reactions but also it offers protein kinase, GTPase/ATPase and protein disulfide isomerase activities. In the literature, it was proven that TG2 protein dysfunction directly or indirectly contributes to the development of some diseases such as celiac disease, neurodegenerative disorders and cataract formation. In addition, *in vivo* studies performed on TG2 knockout mice showed a delay in the wound healing and a poor response to the stress [63]. Moreover, TG2 was also shown to be involved in various pathological states including in inflammation, autoimmunity, tumor growth, metastasis, tissue fibrosis and vascular remodeling. On the other hand, the biochemical activity of TG2 protein was involved in several cellular processes including cell adhesion, growth, survival, migration, differentiation, apoptosis and the organization of the ECM. Additionally, TG2 protein was mostly abundant in fibroblast, osteoblast, endothelial cells, smooth muscle cells and macrophages.

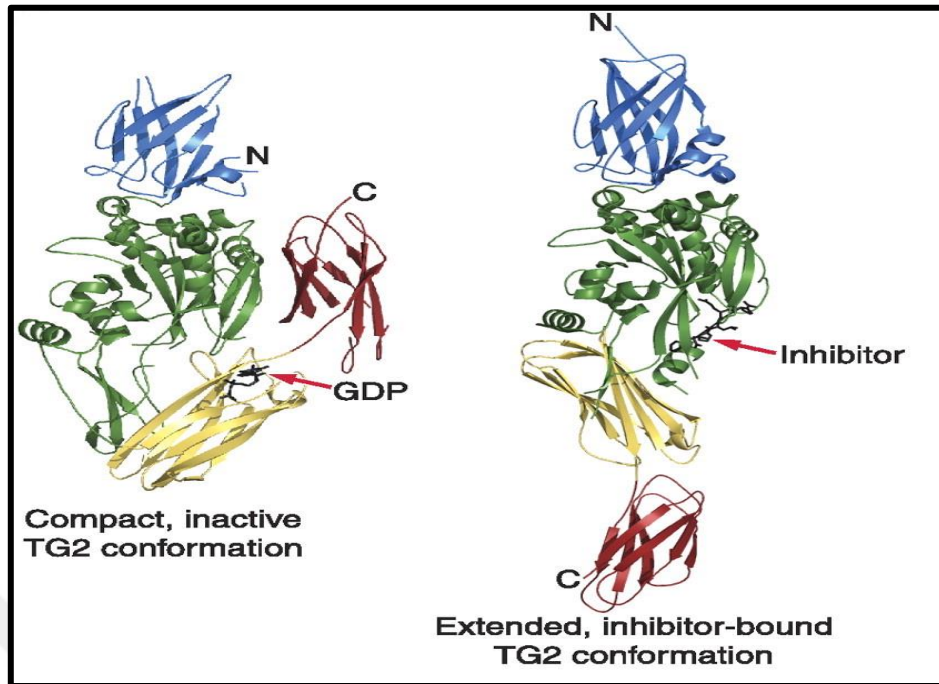


Figure 1.6. 3D structures of compact ‘closed’ and the extended ‘open’ form of TG2 [50].

### 1.7.1. TG2 in Tumor Progression

Over the past decades, the interrelation between the tumor malignancy and TG2 has been an active research field and hot topic among the researchers. Under normal circumstances, liver, bladder and adrenal gland display prominent expression and activity of the protein TG2 [64, 65]. On the other hand, TG2 expression is limited in other normal tissues in which TG2 was generally restricted to the epithelium or in adjacent stroma. The transcriptional target of HIF-1 $\alpha$ , TG2 is involved in the induction of cell survival in hypoxic cells [66].

TG2 was shown to be involved in various biological behaviors including cell growth, survival, migration, invasion and apoptosis by modifying cell’s interaction with its microenvironment. Generally, TG2 was shown to be downregulated in primary tumors but during the tumor progression it was observed to be upregulated in metastatic and chemo-resistant cancers [67, 68]. Even in some malignancy cases, epigenetic mechanisms were involved in the modulation of TG2 expression [50, 69, 70]. In addition, the presence of TG2 was suggested to be crucial for cancer cells to release micro vesicles which were

taken by epithelial and fibroblasts, an important process in the alteration of microenvironment for tumor growth [72]. Therefore, TG2 expression was not only involved with the activation of various oncogenic pathways but also in tumor progression via the regulation ECM and tumor microenvironment to facilitate of malignancy motility and invasion [71-73].

### **1.7.2. TG2 in Cell Adhesion, Migration and Invasion**

It is known that the distant site metastasis is the main cause of death in cancer patients. The metastasis is a multi-step mechanism that involves initially, the local infiltration of the original tumor cells into the adjacent tissues, followed by the migration of the cancer cells through trans-endothelial process, entrance into the blood stream known as intravasation. Then, cancer cells which were managed to survive in the circulatory system extravasated and colonized in the competent organs [9]. However, there is no clear proof for the molecular alterations by which the progression of the primary tumor cells ended up into metastasis. Therefore, the endorsement of the novel proteins and their pathways are needed to be introduced for better clinical management and treatment. In consideration of previously published studies, the direct link between TG2 and metastasis were shown in several different cancer cells such as breast [74], cervical [75], ovarian [76], pancreatic [77], colorectal [78], liver [79], lung [80], melanoma [81] and prostate [82]. It was hypothesized that the TG2 plays a momentous role in conferring the metastatic phenotype to various cancer cells by contributing to their increased survival potency, motility and invasion [83-85]. On the other hand, TG2 could also be secreted outside the cell where it contributes to the regulation of cell to matrix interactions [79, 86-91]. Moreover, due to the expression of the TG2 on the cell membrane in association with  $\beta$ -integrins, TG2 tends as a co-receptor for fibronectin [87]. Therefore, it can be said that cell surface TG2 could be assigned as an important protein in the cell functions including attachment, motility, spreading and survival [71, 83, 84, 86, 92-94] .

### 1.7.3. Epithelial to Mesenchymal Transition and TG2

EMT is a developmentally regulated program that was characterized by the breakdown of the cell junctions, loss of cell polarity and providing cell motility and invasiveness to the epithelial cells [95]. For example, for most epithelial tumors, the tumor progression toward the malignancy was associated by the loss of epithelial differentiation and the shift toward the mesenchymal phenotype [58]. Recent studies indicated that EMT was closely associated with the drug resistance and cancer cell metastasis [12]. Cancer cells lose the expression of proteins, which was mainly responsible from the cell-to-cell contact such as *E-cadherin*. The down regulation of *E-Cadherin* in cancer cells at transcriptional level by various transcriptional repressor such as *Zeb1/Zeb2* [96] and *Snail1/Snail2* [97] was responsible from the disruption of epithelial homeostasis together with the augmentation of cell invasiveness [98]. In turn, several mesenchymal markers including fibronectin, *vimentin* and *N-cadherin* were upregulated in order to enhance the cell migration and invasion [99-101]. Even though, the molecular mechanism of ‘cadherin switching’ remains unknown, TG2 was suggested to be involved in diverse tumor biological behaviors including EMT via both intra- and extracellular pathways [102]. Intracellularly, TG2 was associated with the deamination of various cytoskeleton-related components, regulating the actin-actin and myosin-actin cross-linking, reconstruction of  $\beta$ -tubulin and troponin polymerization [103]. On the other hand, in term of extracellular regulation, TG2 was responsible from the junctional stability and reconstruction of ECM by forming collagen-collagen and fibronectin-collagen cross-linking (Figure 1.7.).

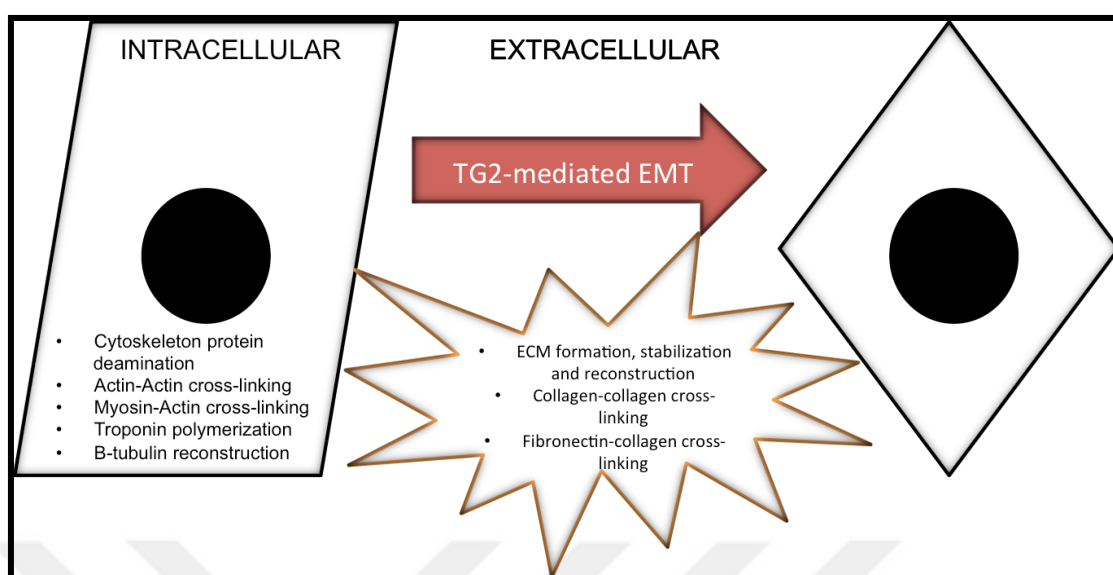


Figure 1.7 Intra- and extracellular regulation of TG2-mediated EMT adapted from Huang *et al.* [64].

Pleiotropic nature of TG2 owing to its multifunctional roles led to the implication of TG2 in the process of inflammation. It was claimed that the upregulation of TG2 enhanced the inflammatory signals including  $\text{TNF}\alpha$ ,  $\text{TGF}\beta$ ,  $\text{NF-}\kappa\text{B}$  which could in turn induce EMT together with cancer progression [104]. Concomitantly, it was suggested that there is a strong interrelation between the TG2-mediated EMT and chemo-/radio-resistance. In that, elevated expression of TG2 results in the increased invasiveness and chemo-resistance phenotype by activating various proteins and  $\text{NF-}\kappa\text{B}$  pathway [105, 106].

### 1.7.3.1. Interplay Between $\text{NF-}\kappa\text{B}$ and TG2 in EMT

Nuclear factor-  $\kappa\text{B}$  proteins are members of transcription factor family in which both heterodimer and homodimer forms of Rel homology domain (RHD) – containing polypeptides are present [107] and with the subsistence of  $\text{NF-}\kappa\text{B}$  stoichiometric inhibitor proteins ( $\text{I}\kappa\text{Bs}$ ),  $\text{NF-}\kappa\text{B}$  signaling system is constituted. In most types of cells,  $\text{NF-}\kappa\text{B}$  hetero- and homo- dimers are predominantly cytoplasmic and under normal conditions,  $\text{NF-}\kappa\text{B}$  is in transcriptionally quiescent form in a complex with inhibitor protein  $\text{I}\kappa\text{Bs}$  ( $\text{I}\kappa\text{B}\alpha$ ,  $\text{I}\kappa\text{B}\beta$  and  $\text{I}\kappa\text{B}\epsilon$ ) to prevent DNA binding and transcriptional activation. However, in the

case of stimulus-responsive activation of the I $\kappa$ B kinase (IKK), I $\kappa$ Bs are degraded which results in the release and activation of NF- $\kappa$ B. NF- $\kappa$ B activation generally responsible for the induction of a variety of inflammatory, survival and developmental genes [108].

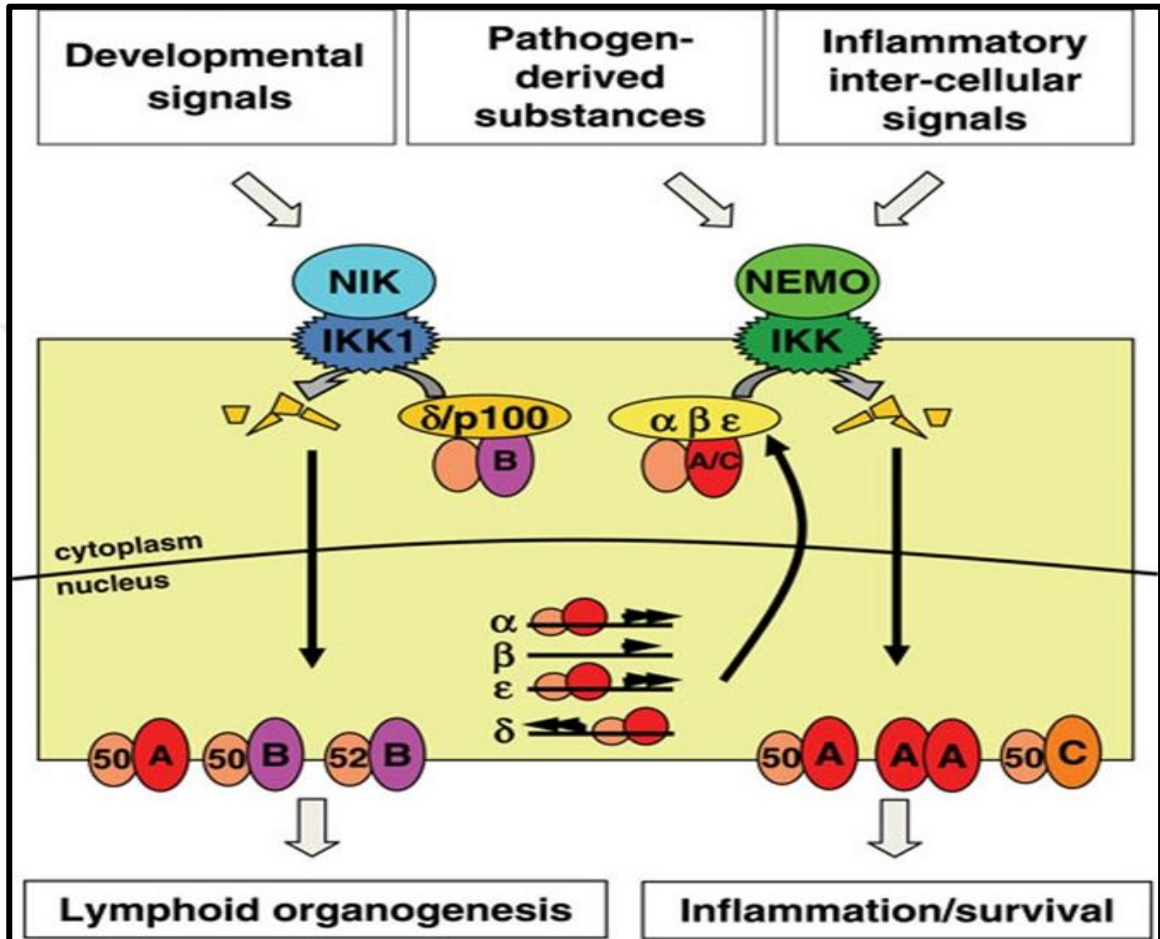


Figure 1.8. Canonical and non-canonical signaling pathway of NF $\kappa$ B system in which the canonical pathway is activated through inflammatory and survival signals while the non-canonical pathway is activated through the genes that are responsible for the organ development [108].

The canonical pathway is activated through the instantaneous and reversible inflammatory and immune responses while the non-canonical pathway is activated through slower and irreversible developmental stimulus (Figure 1.8.). Furthermore, the canonical NF $\kappa$ B pathway is mediated by a NEMO-dependent IKK complex [109]. In contrast, the non-canonical pathway is mediated by NEMO-independent kinase complex involving IKK1 together with the NF $\kappa$ B-inducing kinase (NIK) [110].

Once canonical IKK is activated, I $\kappa$ Bs proteins are phosphorylated which targets them to ubiquitylation and hence degradation via 26S proteasome. As a result of this designated degradation of I $\kappa$ Bs, NF $\kappa$ B is released into the nucleus and starts the transcriptional activation of genes that are involved in various functions like cell growth, cell adhesion, cell migration and apoptosis inhibition [111].

Even though the underlying mechanism of constitutively activated NF- $\kappa$ B was not well understood, recent evidence indicated that the upregulation of TG2 in aggressive and metastatic cancer cells was associated with constitutive NF $\kappa$ B activation by forming ternary complex with NF $\kappa$ B- I $\kappa$ B $\alpha$  in a NEMO-dependent manner [97, 112]. In addition, it was also demonstrated that the treatment with the TG2-specific inhibitors caused a significant inhibition of NF $\kappa$ B activation in breast [57] and pancreatic [97] cancers. The direct link between TG2 and NF $\kappa$ B activation was further supported by the same research group via the usage of TG2-specific small interfering RNA (siRNA). However, some of the follow up studies suggested that ectopic expression of TG2 induced the activation of NF- $\kappa$ B via a non-canonical pathway in breast [113] and ovarian [114] cancer.

#### ***1.7.3.2. Drug Resistance and TG2***

Recent studies indicated that the high levels of TG2 expression were associated with the drug resistant phenotype in cancer cells [89, 115-117]. Interestingly enough, studies showed that TG2 knockdown and the usage of enzymatic inhibitors of TG2 could reverse the drug resistance and make cancer cells sensitive against the stress- or drug-induced apoptosis [89, 96, 105, 118-121]. Furthermore, studies suggested that the overexpression of TG2 was momentous in the induction of drug resistance in multiple drug resistance mechanism. The exact mechanism for TG2-induced drug resistance was not completely understood, however, it was suggested that TG2 expression might be involved either in the development of drug resistance phenotype by inducing constitutive NF- $\kappa$ B activation [97] or in the activation of the c-Src mediated PI3-kinase pathway leading to cell survival [122].

Several studies indicated that the constitutive NF- $\kappa$ B activation in many cancer cells also responsible for the malignant cells to escape apoptosis [123-126], there against, the activation of NF- $\kappa$ B is transient in normal cells in order to prevent the normal cells from the abnormal cell growth. Starting from this point of view, it was suggested for the first



time that TG2-contributed activation of NF- $\kappa$ B might be responsible for the development of the drug resistance in cancer cells through the attenuation of the apoptotic response of cancer cells in the face of anticancer drugs (Figure 1.9.) [97]. Interestingly, a study suggested that the NF- $\kappa$ B-induced expression of the anti-apoptotic Bcl-xL and BFL1 genes resulting in a chemoresistance phenotype in lung carcinoma [80].

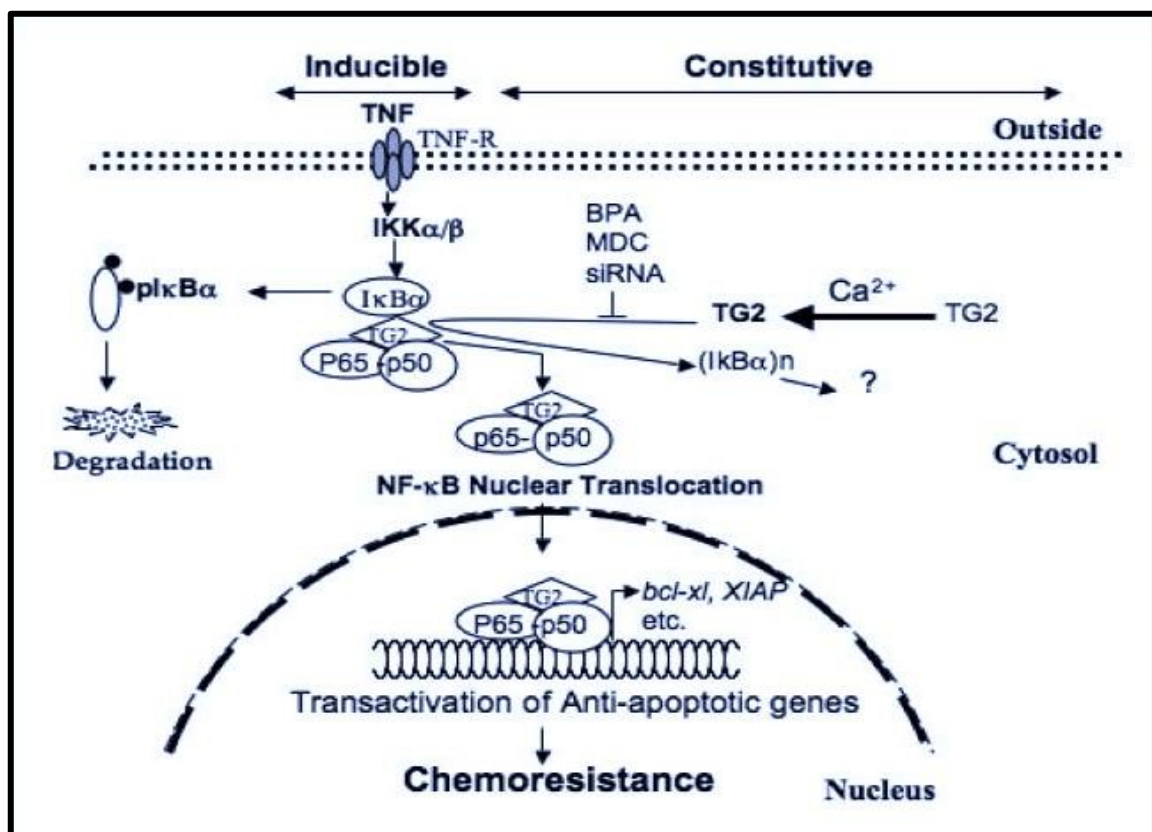


Figure 1.9. Illustration of TG2-dependent NF- $\kappa$ B activation pathway through which constitutive activation of NF- $\kappa$ B occurred via the catalyzed cross-linking of I $\kappa$ B $\alpha$  together with the destabilization of the p65:p50 complex by TG2. Therewithal, TG2-mediated activation of NF- $\kappa$ B also ended up with the constitutive expression of anti-apoptotic target genes including Bcl-xL, XIAP and etc. for the chemoresistance phenotype [97].

Recently, it was also showed that ectopically expressed TG2 was responsible for the increase activity of c-Src by forming a complex with c-Src kinase and PI3K. Once the TG2/c-Src/PI3K complex was formed, the regulatory subunit of PI3K (p85) was phosphorylated in c-Src-dependent manner to activate the p110 catalytic subunit together

with the downstream effectors of mTOR pathway. As a result of this activation, it was concluded that TG2 resulted in cell survival by enhancing the activation of PI3K which was followed by the activation of mTOR-p70 S6 kinase-pathway (Figure 1.10.) [122].

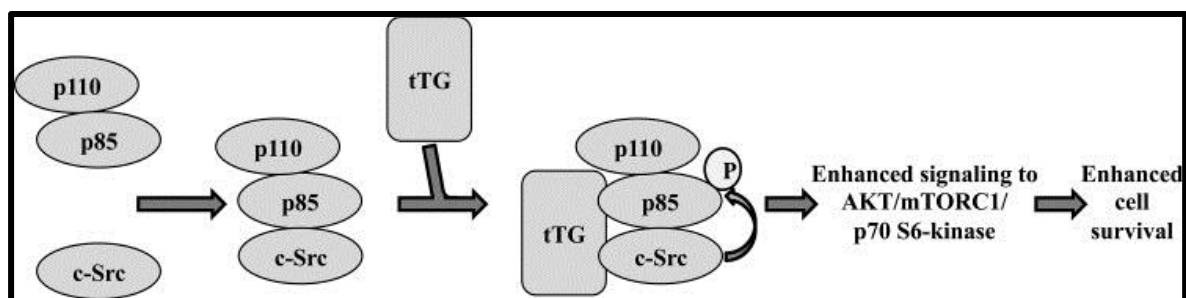


Figure 1.10. The possible activating mechanism of TG2-enhanced cell survival in c-Src mediated PI3K manner [122].

Additionally, in other studies, it was observed that TG2 induced integrin-mediated cell survival signaling was shown to not only enable melanoma cells to gain resistance against cisplatin and dacarbazine [81], but also doxorubicin resistance in lung cancer cells [127]. Taken together, it was concluded that the TG2 induced drug resistance of cancer cells could exist in multiple mechanisms [128].

#### 1.7.4. TG2 in RCC

Several studies showed that the expression of TG2 enzyme was upregulated in RCC and it was suggested that the increased expression of enzyme was closely related with the decrease in tumor necrosis in RCC [93, 129, 130]. It was shown that the overexpression of TG2 in ccRCC was assigned with the high grade of Fuhrman system but not suited with the TNM stage guideline [131]. Furthermore, it was concluded that the significantly up-regulated expression of TG2 levels in RCC was interrelated with the poor cancer specific survival outcome [132]. Even though, previous studies mentioned the strong relationship between the TG2 and the VHL gene in RCC, in 2000, It was showed that TG2 is the utmost critical regulator and target gene of the VHL [133]. In the forthcoming years, researchers started to investigate the role of TG2 in RCC in detail in order to understand

the underlying mechanism of TG2 regulation and its side-effects in RCC. Thus, recent study showed that miR-1285 is one of the microRNAs that was reduced in RCC specimens by inhibiting cancer cell proliferation, invasion and migration through the direct regulation of TG2 expression [134]. However, preliminary studies suggested that TG2 may play momentous role in the pathogenesis and progression of RCC and could be a therapeutic target in the treatment of kidney cancer yet, there is a limited knowledge about the role of TG2 specifically in kidney cancer.

### **1.8. AIM OF THE STUDY**

TG2, multifunctional protein, acts as a cross-linking enzyme, GTPase/ATPase, protein disulfide isomerase, and protein kinase hence was implicated to play a fundamental role in cell adhesion, migration, invasion, cell growth, and epithelial mesenchymal transition (EMT) [135]. In addition several evidence suggest that TG2 plays a vital role in malignancy progression mainly through the regulation of two major cellular processes including EMT and cancer stem cell (CSCs) maintenance [136]. Starting from this point of view and together with our previous findings showing that the increased expression of TG2 in RCC results in the RCC tumor metastasis with a significant decrease in disease- and cancer-specific survival outcome [130], it was aimed in the present study to investigate the relative contribution of TG2's transamidase and GTPase activity in the cell migration, invasion, EMT and cancer stemness of RCC with specific emphasis on NF $\kappa$ B activation.

## 2. MATERIALS

### 2.1. INSTRUMENTS

CO<sub>2</sub> incubator (In-Vitro Cell ES NU-5800, NuAire, USA), Laminar flow cabinet (ESCO Labculture Class II Biohazard Safety Cabinet, Singapore), Centrifuge (MICRO 22R, Hettich, Germany), Centrifuge (Sigma 2-5, England), Carl Zeiss PrimoVert Microscopy with Axio Cam 105 colour (GmbH 37081, Göttingen, Germany), Fluorescence Microscope (Nikon 80i Eclipse Fluorescence Microscope), 80 °C freezer (Thermo Forma -86 C ULT Freezer, USA), pH meter (Hanna instruments PH211, Germany), Vortex (Stuart SA8, UK), Magnetic Stirrer (Heidolph MR 3004, Germany), Heater (Bioer, MB102, China), Analytical Balance (Ohaus Explorer Pro EF214C, USA), ELISA Plate reader (Bio-Tek, USA), Mini-PROTEAN Tetra Cell Electrophoresis System (Bio-Rad, USA), Mini Trans-Blot Cell Blotting System (Bio-Rad, USA), ChemiDOC XRS+Gel Imaging System (Bio-Rad, USA), CFX96 Touch Real-Time PCR (Bio-Rad 1855195, USA), FACS Calibur (BD Biosciences, USA)

### 2.2. EQUIPMENTS

Falcon tubes (15 mL, 50 mL Isolab, Germany), Polypropylene eppendorf tubes (2mL, 1.5 mL, Germany), Electronic pipette (CAPP aid, Denmark), Micropipettes (10 $\mu$ L, 20 $\mu$ L, 100 $\mu$ L, 200 $\mu$ L, 1000 $\mu$ L, Thermo Scientific, USA), Serological pipettes (2 ml, 5 ml, 10ml, 25ml, SPL Life Sciences, USA), Cell culture flasks (T-25, T-75, T-150), cell culture plates and cryovials (TPP Switzerland, Germany), Filter 0.22  $\mu$ m (TPP, Switzerland), 0.45  $\mu$ m (Biotech, Germany), Ultra-Low Attachment 24-Well Plate Polystyrene, Flat Botrom (Corning-Costar,CLS 3473, USA), Ultra-Low Attachment 96-Well Plate Polystyrene, Flat Botrom (Corning-Costar,CLS 3474, USA), Cover Slip (Sigma Aldrich, USA), Bright-Line Hemacytometer (Sigma Aldrich, USA), Graduated Cylinder (50 mL, 250 mL, 500 mL, 1000 mL Isolab, Germany), Whatman Paper (Isolab, Germany), Amersham Hybond- ECL Nitrocellulose Membrane (GE Healthcare, USA), Amersham Rainbow Protein Marker (GE

Healthcare, USA), PVDF membrane 0.45  $\mu\text{m}$  (ThermoFisher Scientific, USA), Tumor Invasion System 24-multiwell Insert Plate 8.0  $\mu\text{m}$  Biocoat (Corning, USA)

## **2.3. CHEMICALS**

### **2.3.1. Cell Line:**

Human embryonic kidney cell line (HEK293FT, ATCC CVCL-691), Mouse renal adenocarcinoma cell line (RenCa, ATCC CRL-2947)

### **2.3.2. Cell Culture Media:**

AIM-V Medium (Gibco, 12055-091, UK), Dulbecco's Modified Eagle's Medium (DMEM) high glucose (Gibco 41966, UK), RPMI-1640 Medium (Gibco, BE12-702F, UK)

### **2.3.3. Growth Supplements:**

B27 Supplement (50X) (Gibco, REF15504-044, UK), Epithelial-Growth Factor EGF (200  $\mu\text{g}/\text{ml}$ ) (Invitrogen, REFPHG0313), Fetal Bovine Serum (FBS) cell culture tested (Sigma F9665, Germany), Fibroblast- Growth Factor (100  $\mu\text{g}/\text{ml}$ ) (Gibco, AA-10-155, UK), Insulin Transferrin Selenium (ITS) (Gibco, 41400-045, UK), N2 Supplement (100X) (Gibco, REF17502-048, UK), Penicillin-Streptomycin (Sigma-Aldrich, , 6SLBJ7114U, USA),

### **2.3.4. Other Reagents:**

2-Propanol (AppliChem A3928, Germany), 4-(2-hydroxyethyl)-1-piperazineethanesulfonic acid (HEPES) (Multicell 600-032-EG, Canada), Absolute Ethanol (AppliChem A3928, Germany), Acrylamide/ Bis-acrylamide (29:1) (Sigma A3574, USA), Ammonium Persulfate (APS) (BioRad, 1610700, USA), Bovine Serum Albumin (Santa Cruz, sc-2323, USA), Collagen Type-I from Human Placenta (Sigma C7774, USA), Dimethyl sulfoxide (Santa Cruz sc-202581, USA), Dithiothreitol (DTT) (Appllichem A1101, USA), Dulbecco's

Phosphate Buffered Saline (DPBS) (PAN Biotech P04-53500, Germany), Ethylenediaminetetraacetic acid (EDTA) (Merck, K40173218 946, Germany), Ethylene glycol tetraacetic acid (EGTA) (Fluka 03779, USA), ExtrAvidin Peroxidase (Sigma, E2886), Everolimus, 2X HPS, Glycine (Merck 104169), IgePal (5CS402, Sigma, USA), LB Agar (Fluka, B6768), LB Broth (Sigma, L3522, USA), Methanol 99per cent (Sigma, 34885, USA), Mounting media (F4680-25, Sigma, USA), PBS (10X) (Lonza, BE17-517Q, Belgium), Phenylmethanesulfonylfluoride (PMSF) (Sigma 78830, USA), Protease Inhibitor (PI) (Sigma, P8340, USA), Protein Assay Reagent A (BioRad, 5000113), Protein Assay Reagent B (BioRad, 5000114), Puromycin dihydrochloride (Santa Cruz, sc-108071), Polybrene (Santa Cruz, sc-134220), Sodium orthovanadate ( $\text{Na}_3\text{VO}_4$ ) (Sigma, S6508, USA), Sodium orthovanadate ( $\text{Na}_3\text{VO}_4$ ) (Sigma, S6508, USA), Sorafenib (HY-1/CS-016-), N,N,N',N'-Tetramethylethylenediamine (TEMED) (Sigma, T7024, USA), Tris-base (Merck 108387), Tris-HCl (Merck 108219), Triton-100X (Biomatik Corporation, A4025), Trizol (Invitrogen, 15596-018), Tween-20 (Merck, 822184), Trypan Blue (%0. 4) (Sigma-Aldrich, T8154), %0.05 Trypsin (Lonza, BE02-007E, Belgium), WST-1 Cell Proliferation (13489900, Roche, Germany)

## 2.4. KITS and SOLUTIONS

Albumin Fraction V (2Z008164, AppliChem Germany), Bovine Serum Albumin, Protein Standard (Sigma P0834, USA), Clarity™ Western ECL Substrate, (BioRad, 1705061, USA), EMSA LightShift Optimization Kit (QF219950, Thermo Scientific, USA), RIPA Lysis Buffer (Santa Cruz sc-24948, USA), QuantiTect SYBR Green PCR Kit (Qiagen, 204145, USA), Sensiscript RT Kit (Qiagen, 205213, USA), Peq-Gold Ultra Competent Kit (Agilent technologies), Ultrapure Plasmid Isolation Kit (Invitrogen), Mm\_MMP3\_1\_SG QuantiTect Primer Assay (208679793, USA), Mm\_MMP9\_1\_SG QuantiTect Primer Assay (208679794, USA), Mm\_MMP2\_1\_SG QuantiTect Primer Assay (208679792, USA), Mm\_MMP1a\_1\_SG QuantiTect Primer Assay (208679791, USA), Mm\_MMP13\_1\_SG QuantiTect Primer Assay (208810906, USA), Mm\_Vim\_1\_SG QuantiTect Primer Assay (208810905, USA), Mm\_Cdh1\_1\_SG QuantiTect Primer Assay (202689402, USA), Mm\_Cdh2\_1\_SG QuantiTect Primer Assay (202689403, USA), Mm\_Zeb1\_1\_SG QuantiTect Primer Assay (174899188, USA), Mm\_Zeb2\_1\_SG QuantiTect Primer Assay (174899189, USA), Mm\_Twist1\_1\_SG

QuantiTect Primer Assay (174899194, USA), Mm\_Twist2\_1\_SG QuantiTect Primer Assay (174899191, USA), Mm\_Snail1\_1\_SG QuantiTect Primer Assay (174899193, USA), Mm\_Snail2\_1\_SG QuantiTect Primer Assay (174899190, USA), Mm\_TGM2\_1\_SG QuantiTect Primer Assay (110786097, USA), Hs\_TGM2\_1\_SG QuantiTect Primer Assay (202689401, USA)

## **2.5. ANTIBODIES**

### **2.5.1. Primary Antibodies**

Mouse- anti-TG2 Antibody (ThermoFisher Scientific, Labvision Cub 7402, MS-224-P, USA), Monoclonal mouse anti- $\beta$ -Actin antibody (Sigma, USA), Monoclonal mouse anti-Integrin  $\beta$ 1 Antibody (Santa Cruz, sc-8978, USA), Anti-Syndecan 4 antibody (Abcam, ab24511, USA), Mouse anti-I $\kappa$ B- $\alpha$  Antibody (H-4, Santa Cruz, sc-1643, USA), Mouse anti-p-I $\kappa$ B- $\alpha$  Antibody (B-9, Santa Cruz, sc-8404, USA), Mouse anti-NF- $\kappa$ B-p65 (H-286, Santa Cruz, sc-7151, USA), Anti-mouse CD11b Flow Antibody (B192967, Biolegend, USA), Anti-mouse Sca-1 Flow Antibody (B163257, Biolegend, USA), Anti-mouse CD44 Flow Antibody (B193068, Biolegend, USA), Anti-mouse CD45 Flow Antibody (B187805, Biolegend, USA), Anti-mouse CD73 Flow Antibody (B182619, Biolegend, USA), Anti-mouse CD29 Flow Antibody (B181560, Biolegend, USA), Anti-mouse CD106 Flow Antibody (B178443, Biolegend, USA)

### **2.5.2. Secondary Antibodies**

Anti- rabbit IgG Peroxidase (Sigma A0545) and anti- mouse IgG Peroxidase (Sigma A4416) Conjugates

### **3. METHODS**

#### **3.1. CELL CULTURE METHODS**

##### **3.1.1. Cell Lines and Culturing Conditions**

The Human embryonic kidney cell line HEK293FT and the renal cell adenocarcinoma cell line RenCa were obtained from ATCC. HEK293FT cell line was cultured with DMEM (100 units/ml Penicillin and 100 µg/ml Streptomycin and 10 per cent (v/v) FBS) media. RenCa cell line was culture in RPMI-1640 (100 units/ml Penicillin and 100µg/ml Streptomycin and 10 per cent (v/v) FBS) media. All cell lines were incubated at 37°C, five per cent (v/v) CO<sub>2</sub> and 95 per cent (v/v) air conditions.

##### **3.1.2. Cell Subculturing**

Cell subculturing procedure was passaged whenever cells reached to 70-80 per cent confluency. The cell monolayer was rinsed once with 1X DPBS (pH 7.4) prior to the treatment with 0.05 per cent (w/v) trypsin and incubated at 37°C for 3 minutes. To eliminate trypsin activity, growth media was added and cells were collected. Obtained cell suspension was centrifuged at 300 g for 5 minutes and cells were resuspended in their pre-defined growth media.

##### **3.1.3. Calculation of Cell Number**

Following the cell subculturing procedure, as the cells were detached from the cell culture plates and re-suspended in fresh media as described in Section 3.1.2. 10 µl of cell suspension was loaded into the center of the hemocytometer, which was assigned as the cell counting area and counted under the inverted light microscope using 4x objective.



### **3.1.4. Cryopreservation of Cell Lines**

While the subculturing procedure, cells were dislodged by trypsin and counted as it was described in Section 3.1.2. Meanwhile, 10 per cent (v/v) of Dimethyl sulfoxide and 90 per cent (v/v) FBS was mixed to prepare freezing mix solution. Cell pellet was resuspended in prepared freezing mix solution with a density of  $1 \times 10^6$  cells/mL per one cryovial. Cells were then stored at  $-80^\circ\text{C}$  overnight before move to a liquid nitrogen for the long-term stocking.

### **3.1.5. Cell Thawing**

Previously stocked cells were taken from the liquid nitrogen and rapidly warmed up to  $37^\circ\text{C}$ . Then, cell suspension was collected into a sterile falcon tube and 5 ml of pre-warmed growth media was added drop wise drop onto the cell with a continuous mixing gesture in order not to harm the cells with sudden increase in the osmotic pressure. Afterward, cell suspension was spinned at 300 g for 5 minutes with the aim of discarding DMSO that present in the freezing mix solution. Pellet was resuspended in growth media and plated into a tissue culture flask. The very next day, the medium was changed to remove any residual of DMSO, which is known to be toxic substance for the cells. Cells were passaged at least once before the experiment begins.

## **3.2. ISOLATION OF TG2 CONSTRUCTS PLASMID DNA**

Wild-type (WT) TG2 gene was sub-cloned into Plenti CMV BLAST DEST (706-1) vector and the other related mutant TG2 constructs including C277S, W241A and R580A were produced via side directed mutagenesis at Debrecen University by Ajna Bihorac under the supervision of Dr.Robert Kiraly.

### **3.2.1. Plasmid Isolation**

After observing the colonies on the LB Agar, single colony was selected from the agar plates and transferred to the 100 ml of LB broth in which ampicillin was already added and

left for the overnight. 16-18 hours later, when the bacterial culture was grown, samples were transferred to the 50 ml falcon tubes and spun at 4000 g for 10 minutes to harvest the cells and the obtained bacterial pellet was used for plasmid isolation. 4 ml of resuspension buffer in which RNase A was added, was used and gently mixed with the obtained pellet until the solution became homogenous. four ml of lysis buffer was added onto the mixture and immediately inverted several time. Then incubated at room temperature for 5 minutes. After the incubation process, four ml of precipitation buffer was mixed into the suspension and centrifuged at 12000 g for 15 minutes at room temperature. Meanwhile, equilibration columns were washed with 10 ml of equilibration buffer. After the centrifugation step, obtained supernatant was loaded into the equilibrated column and it was allowed to drain by gravity flow. 10 ml of wash buffer was then introduced into the column. In order to collect the purified DNA, first five ml of elution buffer was added into the column, and then 3.5 ml of isopropanol was placed into the collection tube to elute DNA. Following another centrifugation process at 12000 g for 30 minutes at 4°C. Supernatant was discarded and the remained pellet was washed with 3 ml of 70 per cent ethanol. Afterward, the pellet was left to dry and suspended in 100 microliter of TE buffer. After the isolation process, the concentration was nanodropped and plasmid DNA was stored at -20°C.

### **3.3. LENTIVIRAL PARTICLE PRODUCTION OF TG2 CONSTRUCTS AND TRANSDUCTION**

#### **3.3.1. Transfection of HEK293FT with DNA of Interest**

HEK293FT cells were seeded into the 10-cm cell culture dishes ( $1 \times 10^6$  cells/well) and incubated overnight. The very next day, the media was replaced with the fresh preheated media was replaced two hours before the transfection. Two hours later, the gene of interest, packaging plasmid (pPAX2) and enveloped plasmid (PMD2G) were mixed according to the concentration obtained from the plasmid isolation process in the 15 ml falcon tube. Meanwhile, other reagents were prepared in the following order. 0.1X TE, water and 2.5 mM  $\text{CaCl}_2$  were gently mixed into the same 15 ml falcon tube and then, 2X HBSS with a pH of 7.12 was added drop wise under the agitation by aerating the mixture by 2 ml

serological pipette. The mixture was incubated for 20 minutes at room temperature and then cell monolayers were treated drop by drop and gently mixed by rotating the plate back and forward. 14 hours later, media was removed, cells were washed with 1X PBS and 9 ml of fresh pre-heated media was placed. 24 hours later, media was collected into the falcon and kept at 4°C. Another 9 ml of fresh pre-heated media was added into the plates. 48 hours later, the media was again collected and unified with the previously collected media. After 48 hours later, cells were killed with bleach and also left under UV. Meantime, collected supernatants were filtered and aliquoted and stored at -80°C.

### **3.3.2. Transduction of RenCa Cells with Obtained Lentiviral Particles**

RenCa cells were seeded as 25.000 cells/well in 24 well tissue culture plate and left overnight incubation. The very next day, cells were pre-treated 8 µg/ml polybrene in two per cent (v/v) FBS and one per cent (v/v) pen/strep (v/v) containing growth media for 2 hours and followed by the lentiviral particles addition, gentle stirred, and incubated for 24 hours. 24 hours later, lentiviral particles were discarded and growth media was added into wells in order to recover for the next day. Cells were incubated for another 24 hours and after that selection process was started by using 6 µg/ml blasticidine for RenCa cells and in the following several days wells are replaced with fresh blasticidine containing media until the non-transduced control RenCa cells were completely dead because of the non-resistance against the blasticidine.

## **3.4. IDENTIFICATION OF CANCER STEM CELL PROFILE OF TG2 IN RENCA CELL LINE TRANSDUCED WITH LENTIVIRAL PARTICLES**

### **3.4.1. Detection of Cell Surface CD Markers Using Flow Cytometer**

Cells were seeded on 6-well plate at a density of  $3 \times 10^5$  cells/well and incubated overnight. Then, cell monolayers were washed with PBS and dislodged from the 6-well plate using trypsin. Cell suspension was centrifuged and the pellet was washed twice with 1 ml PBS for 5 minutes. Then, cells were counted, the same amount of cells were collected and fixed with 4 per cent paraformaldehyde. After fixation steps, fixed cells were incubated with

FITC- or PE- conjugated flow antibodies for one hour at room temperature. Following with the two sets of washing steps with PBS and the mesenchymal stem cell marker expression profile of the TG2 mutants were determined using Becton Dickinson FACS Calibur flow cytometer. 10000 events per samples were acquired and the results were analyzed with the CellQuestPro Program.

### **3.4.2. Spheroid and Sub-spheroid Formation Assay**

RenCa cells were plated in Costar 24-well ultra-low flat bottom attachment plates at  $2.5 \times 10^2$  cells/well density in the prepared spheroid media including RPMI-1640 supplemented with 1 per cent penicillin/streptomycin, 1 per cent N<sub>2</sub>, 2 per cent B27 serum-free supplement, 1 per cent ITS, 0.5 per cent methyl cellulose, 20 ng/ml EGF and 20ng/ml FGF. Seeded cells were incubated for 24 hours and the first images of cell suspension were taken under the light microscope at 20x objective at the end of the 24<sup>th</sup> hour. Spheroid size and colony numbers were closely surveyed every 24 hours and images of each colonies were taken if the spheres were larger than 50  $\mu\text{m}$  using Carl Zeiss Primovert microscope equipped with camera system Axiocam 105 Digital color microscope. Every four days, 100  $\mu\text{l}$  of spheroid media was added into each well to avoid the evaporation problem. Imaging procedure was realized everyday until the end of the 11<sup>th</sup> day. Then, on the 11<sup>th</sup> day, the cell suspension containing the spheroids were collected into the falcon tubes, and centrifuged at 125 g for 7 minutes by treating them as a suspension cells. Followed by the collection of the pellets into the 1.5 mL eppendorf tubes. In order to get the homogenous cell suspension, 500  $\mu\text{l}$  of trypsin was added in each eppendorf tube and tubes were placed into the incubator for 10 minutes. After the incubation process, 50  $\mu\text{l}$  of trypsin inhibitor was added which was followed by the centrifugation at 300 g for 10 minutes at 4°C. The obtained supernatant was discarded and the pellet was resuspended in 100  $\mu\text{l}$  of spheroid media for the counting procedure. For the sub-spheroid step of the experiment, 25 cells/well were aimed to seed in each well yet, as the cell number was too small for the plating just in case, 25 cells were seeded in ultra-low attachment 96-well plate and 125 cells per well were seeded into ultra-low attachment 24-well plate. They were incubated for 24 hours and the first imaging procedure was realized. Whenever, the spheroid formation was observed which was around fourth day, the images of sub-spheroids were taken as described above. Lastly, at the end of the experiment, in order to prove the

viability of the spheres, tryphan blue staining was performed and live and dead cells were determined and counted.

### **3.5. DETECTION OF PROTEIN LEVELS IN RENCA MUTANT CELLS**

#### **3.5.1. Preparation of the Cell Lysate**

Non-transduced wild type RenCa, mock control RenCa and TG2 mutant RenCa cells (TG2-C277S, TG2-W241A, TG2-R580A and TG2-V224A) were seeded into 6-well plate with a density of 300.000 cells/well. Cells were brought to the quiescent state by incubation in serum-free media for 4 hours. Next, cells were immediately placed on ice, the media was discarded and cells were scraped from the surface using RIPA lysis buffer (50 mM NaCl, one per cent (v/v) Igepal CA-630, 0.5 per cent (w/v) sodiumdeoxycholate, 0.1 per cent (w/v) SDS in 50 mM Tris pH 8.0) containing 1mM Na<sub>3</sub>VO<sub>4</sub>, 1 mM PMSF and 1 per cent (v/v) protein inhibitor cocktail. Following the mechanical shearing of DNA that was carried out by the sonication process with a power of 60 per cent with five-second pulses on ice. Then cell lysates were centrifuged at 12000 g for 10 minutes at 4°C. The obtained supernatant was transferred into new eppendorfs and for the storage they were placed at -80°C.

#### **3.5.2. Measurement of Protein Concentration by Lowry Assay**

Protein content of cell extracts was determined using Bio-Rad Lowry assay. From 0.05 to 0.75 mg/ml of protein content of BSA were used as a standard. Stored cell lysates were diluted in 1:5 and added into the 96-well plates in triplicate. Samples were mixed initially with 25 µl of Reagent A and 200 µl of Reagent B and incubated at room temperature for 15 minutes. The absorbance values were taken using Elisa Micro plate reader at 750 nm.

### 3.5.3. SDS-PAGE

Denatured proteins were spared according to their molecular weight via SDS-PAGE method. Four per cent (w/v) stacking gel and six, eight, ten and twelve per cent (w/v) separating gels were poured according to the proportion shown in the Table 3.5.

Table 3.1. The ingredients of stacking and separating polyacrylamide gel for two

Stock solutions	Stacking Gel	Separating Gels			
	4 per cent	6 per cent	8 per cent	10 per cent	12 per cent
30 per cent (w/v) acrylamide / 0.8 per cent bisacrylamide	0.65 ml	3 ml	4 ml	5 ml	6 ml
0.5 M Tris-HCl containing 0.4 per cent (w/v) SDS, pH 6.8	1.25 ml				
1.5 M Tris-HCl containing 0.4 per cent (w/v) SDS, pH 8.8		3.75 ml	3.75 ml	3.75 ml	3.75 ml
dH <sub>2</sub> O	3.05 ml	8.25 ml	7.5 ml	6.25 ml	5.25 ml
10 per cent (w/v) APS	25 µl	100 µl	100 µl	100 µl	100 µl
TEMED	5 µl	20 µl	20 µl	20 µl	20 µl

After performing Lowry assay that was described in the Section 3.5.2, equal amount of proteins from calculated cell extracts were taken and mixed with 2x Laemmli buffer in 1:1 ratio. Meanwhile, SDS-PAGE gel was prepared according to the ingredients and amount

that was given in the Table 3.5. Then, initially, prepared separating gel was poured from the edge and in the middle of the thick and thin glass, the top of the gel was covered with isopropanol to avoid oxidation and facilitate the formation of an even gel surface, and left to polymerize at room temperature. After polymerization was completed, isopropanol was removed and the gel surface was washed with dH<sub>2</sub>O until the smell of alcohol was discarded completely. The excess amount of dH<sub>2</sub>O between the glasses was removed gently with the help of filter paper. Then, the stacking gel was directly poured on the separating gel and 10-well combs with 1.0 mm thickness were placed into the stacking gel by avoiding the bubble formation while inserting the comb and left to polymerize at room temperature. At the time for the running the gel, the comb was carefully removed. Prepared protein samples were loaded into the wells together with the full range molecular weight marker. The gel-casting apparatus was positioned as required and filled with the prepared 1X running buffer (25 mM Tris, 192 mM glycine, and 0.1 per cent (w/v) SDS). Electrophoresis was started at 70V through the stacking gel for 15 minutes and then performed at 100 V until the Bromophenol Blue sodium salt tracking dye front reached to the bottom of the separating gel.

#### **3.5.4. Immunoblotting**

After completion of electrophoresis procedure, samples were transferred onto nitrocellulose or PVDF membrane with 0.22 µm or 0.45 µm pore size using Bio-Rad wet blot system. Whatmann papers, fiber pads and membrane were soaked in ice-cooled in 1X transfer buffer with a pH of 8.3 (25 mM Tris-Base, 192 mM glycine and 20 per cent (v/v) methanol) at least 15 minutes and PVDF membrane was activated with methanol for 5 minutes. Followed by the gel sandwich method, the blocking cassette was inserted into the U shaped apparatus in a position that membrane was faced to the anode side electrode. The apparatus was filled with 1X transfer buffer and in order to avoid the overheating, an ice block was also placed into the apparatus. The transfer process was performed at 175 mA for 90 minutes on ice. Then, the blocking of the membrane was performed with five per cent (w/v) non-fat milk prepared in TBS-Tween, pH 7.4 for 1 hour followed by the addition of probed either with mouse monoclonal anti-TG2 Cub7402, mouse monoclonal anti-β-Actin, rabbit monoclonal anti-syndecan-4, mouse monoclonal anti-IκB-α or mouse monoclonal anti-p-IκB-α antibodies dissolved in 5 per cent (w/v) non-fat milk in TBS-

Tween, pH 7.4 and incubated overnight at +4°C. Approximately, eighteen hours later, membrane was washed three times with TBS-Tween, pH 7.4 for five minutes. Then, secondary antibodies were prepared either anti-mouse IgG and anti-rabbit IgG and incubated for 2 hours at room temperature. After performing, another washing steps, development of the membrane was performed using Amersham ECL Advance Western Blotting Detection Kit and visualization was realized via Bio-Rad Molecular Imager ChemiDoc XRS+

### **3.6. DETECTION OF TG2 ACTIVITY IN RENCA CELLS EXPRESSING TG2 MUTANT CONSTRUCTS**

#### **3.6.1. TG2 Activity Assay**

TG2 activity assay was performed using TG2 specific CovTest colorimetric microassay kit. Cells were lysed using three cycles of freeze-thaw process and 100 µg of protein from each sample which was determined by performing Lowry assay as described in Section 3.5.2. was added into pre-coated 96-well plate and samples were incubated in biotinylated T26 peptide in the presence of spermine at 37°C for 30 minutes. Then, streptavidin labeled peroxidase (Sav-HRP) was added in order to visualize the reaction and the optical density of each well was measured using Elisa Micro plate reader at 450 nm.

### **3.7. DETECTION OF GENE EXPRESSION LEVELS IN RENCA CELLS EXPRESSING TG2 MUTANT CONSTRUCTS**

#### **3.7.1. Total RNA Isolation**

TG2-expressed mutant cells and non-transduced parental cell, mock control RenCa cells were counted and seeded into 6 well plates at a density of 300.000 cells/well in growth media and incubated overnight. Next day, cells were incubated with serum-free media for 4 hours to induce the quiescence. Four hours later, cells were dislodged using 250 µl of Trizol reagent and transferred into sterile 1.5 ml eppendorf tubes, and 50 µl of chloroform was added on the top of the mixture and inverted several times. Then, samples were



incubated at room temperature for 15 minutes followed by the centrifugation process at 12000 g for 15 minutes at 4°C. The clear phase containing the required part, which was the RNA, was collected, transferred into the new sterile 1.5 ml eppendorf tubes, mixed with isopropanol and incubated in ice for 15 minutes. Afterward, another centrifugation process was done in order to get the RNA precipitation that was recognized as the white-yellowish pellet present at the bottom of the tubes. By adding, 75 per cent (v/v) ethanol, the pellet was aimed to clarify and centrifuged at 7500 rpm for 10 minutes. Supernatant was discarded and the remaining ethanol solution was dried out at room temperature. Then, pellet was dissolved in RNase-DNase free water. RNA concentration was nanodropped and stored at -80°C.

### 3.7.2. Reverse Transcriptase Polymerase Chain Reaction

Isolated RNA extracts were used to get the cDNA products via Sensiscript Reverse Transcriptase kit purchased from QIAGEN. PCR reaction was carried out at 37°C for 1 hour according to manufacturer's protocol (Table 3.2.). cDNA samples were nanodropped.

Table 3.2. Senscript cDNA converter reaction mix

Reagents	Volume per reaction
10x Buffer	2 µl
dNTP (5mM)	2 µl
Oligo-dT primer (10 µM)	2 µl
Senscript Reverse transcriptase enzyme	1 µl
Rnase-Dnase free water	Variable
Template	Variable
Total reaction volume	20 µl

### 3.7.3. Quantitative Polymerase Chain Reaction

The mRNA expression levels were detected for the following *hTGM2*, *Zeb1*, *Zeb2*, *Snail1*, *Snail2*, *Twist1*, *Twist2*, *18 S RNA*, *MMP1a*, *MMP2*, *MMP3*, *MMP9*, *MMP13*, *E-cadherin*, *N-cadherin* and *Vimentin* genes using Qiagen QuantiTect Primer Assay and SYBR PCR Kit. Reaction mixture contains 500 ng of cDNA converter from each sample, 1.25  $\mu$ l primer, 3  $\mu$ l RNase-DNase free water and 6.25  $\mu$ l Syber Green PCR mix, according to the reaction conditions listed in Table 3.3. Samples were studied in triplicate. During the analysis relative quantification was normalized using 18S rRNA housekeeping gene and the analysis were done using the obtained standard curve from the cycler.

Table 3.3. Quantitative PCR conditions

Cycle	Temperature	Time	Phase
1	94°C	15 min	
2	95°C	5 min	Initial denaturation
3 (39 repeat)	95°C	60 sec	Denaturation
	55°C	60 sec	Annealing
	72°C	60 sec	Extension
4	72°C	10 min	Final extension
5 (80 repeat)	50-80°C 0.5 °C increase /12 sec		Melt curve
6	4°C	$\infty$	Cooling

### **3.8. DETECTION OF ACTIVE NUCLEAR PROTEIN NF-KB VIA ELECTROPHORETIC MOBILITY SHIFT ASSAY (EMSA)**

#### **3.8.1. Protein Extraction for EMSA**

TG2-expressed and non-transduced control and mock control Renca cells were seeded into 10cm culture dishes at a density of  $2 \times 10^6$  in 9 ml growth media and cells were incubated overnight. Next day, 2 per cent FBS containing RPMI-1640 media was added into each well in order to keep cells in quiescent state and prevent proliferation. In the morning, cells were washed with 3 ml cold PBS pH 7.4 and cells were harvested with scraper then collected in 15 ml falcon tube. Cell suspension was centrifuged at 400 g for 5 minutes. Supernatant was discarded and 400 ul of hypotonic solution (Table 3.4.) was added onto the pellets and vortexed well before putting on ice and incubated on ice for 10 minutes. Meantime, 1 per cent IgePal was prepared and placed at 37°C to dissolve. After incubation on ice samples were vortexed and 1 per cent IgePal was added into samples. Samples were vortexed and then incubated on ice for another 20 minutes. Samples were centrifuged at 450 g for 3 minutes in order to participate the cell membrane. Supernatant of the samples were transferred to new tubes without disturbing the pellet and transferred supernatants were centrifuged at 10000 rpm for 10 minutes. Supernatant of the samples which was known as cytosolic fraction was transferred to another eppendorf tubes and kept at -80°C. Meanwhile, 25 ul of hypertonic solution (Table 3.5.) was added onto the pellets and incubated on ice for 30 minutes by vortexing the samples every 5 minutes for 1 minute. Then, samples were centrifuged at 10000 rpm for 10 minutes and supernatant, which was known as nuclear fraction was transferred to new sterile 1.5 ml eppendorf tubes without disturbing the pellets. Lowry assay was performed as described in the Section 3.5.2. to measure the protein content of the samples. At least 8 ug of nuclear extract was used for the following steps of the EMSA.

Table 3.4. Hypotonic solution ingredients

<b>Hypotonic Solution</b>	<b>Stock Concentration</b>	<b>Final Concentration</b>	<b>Volume for 2 ml</b>
HEPES (pH 7.9)	40 mM	10 mM	500 ul
EDTA (pH 8.0)	100 mM	0.1 mM	2 ul
EGTA (pH 8.0)	10 mM	0.1 mM	20 ul
DTT	100 mM	0.1 mM	2 ul
NaF	500 mM	50 mM	200 ul
Na <sub>3</sub> VO <sub>4</sub>	100 mM	1 mM	20 ul
PMSF	100 mM	0.5 mM	10 ul
β-Glycerophosphate	300 mM	30 mM	200 ul
PI (1 per cent (v/v))	-	-	20 ul
dH <sub>2</sub> O	-	-	1026 ul

Table 3.5. Hypertonic solution ingredients

<b>Hypertonic Solution</b>	<b>Stock Concentration</b>	<b>Final Concentration</b>	<b>Volume for 2 ml</b>
HEPES (pH 7.9)	40 mM	20 mM	500 ul
NaCl	4.2 M	420 mM	100 ul
EDTA (pH 8.0)	100 mM	1 mM	10 ul
DTT	100 mM	1 mM	10 ul
NaF	500 mM	50 mM	100 ul
Na <sub>3</sub> VO <sub>4</sub>	100 mM	1 mM	10 ul
PMSF	100 mM	0.5 mM	5 ul
β-Glycerophosphate	300 mM	30 mM	100 ul
PI (1 per cent (v/v))	-	-	10 ul
dH <sub>2</sub> O	-	-	155 ul

### 3.8.2. Preparation and Pre-Run of the EMSA Gels

EMSA gels were prepared just like the SDS-PAGE gels that were described above (Section 3.5.3.) with the only different of the some ingredients. The top and bottom gels for EMSA were prepared according to the following table given below.

Table 3.6. Ingredients of top and bottom for two gels

	<b>Top Gel 6 per cent</b>	<b>Bottom Gel 15 per cent</b>
30 per cent (w/v) acrylamide/0.8 per cent (bis-acrylamide (29:1))	5 ml	12.5 ml
5X TBE (450 nM Tris, 450 nM Boric Acid, 10 mM EDTA pH8.3)	2.5 ml	2.5 ml
dH <sub>2</sub> O	17.3 ml	9.7 ml
10 per cent (w/v) ammonium persulphate	175 ul	175 ul
TEMED	8.75 ul	8.75 ul

For the pre-run process, electrophoresis unit was filled with 0.5X TBE till the bottom of the wells, flushed the wells and pre-electrophorese the gel for 1 hour at 70 volts.

### 3.8.3. Binding Reaction

Equal amount from the previously prepared nuclear extracts was taken and equalized the volumes by hypertonic buffer. Then, binding reaction was performed for each samples by adding 5 ul the following reaction mix and incubated at room temperature for 10 minutes. (Table 3.7)

Table 3.7. Binding reaction mix

<b>Contents of Reaction</b>	<b>Concentration per Reaction</b>	<b>Final Amount per Reaction</b>
10 X Binding Buffer	1X	2 ul
100 mM MgCl <sub>2</sub>	5 mM	1 ul
1 per cent Non-Idet P40	0.05 per cent	1 ul
100 mg/ml Albumin Fraction V	2.5 mg/ml	0.5 ul
100 uM Poly (dI.dC)	2.5 uM	0.5 ul
Total		5 ul

Following to the incubation step, 3 pmol of biotin-labeled double-stranded oligomer probe <sup>32</sup>P-NFκB (forward 5'-AGTTGAGGGGACTTTCCCAGGC-3' and reverse 5'-GCCTGGGAAAGTCCCCTCAACT-3') was added into each sample and incubated for 40 minutes at room temperature with the aim of achieving the binding reaction to take place.

#### **3.8.4. Electrophoresis of Binding Reaction and Electrophoretic Transfer to Nylon Membrane**

20 ul of each sample was loaded onto the pre-run polyacrylamide gel. It was initiated at 90 volts for 10 minutes and then switched to 120 volts until the bromophenol blue dye was reached approximately at the end of the glass. After completion of the running procedure, nylon membrane was soaked in 0.5X TBE for at least 10 minutes. Sandwich method was performed for the gel and transferred was performed at 200 mA for 2 hours on ice. When the transfer was completed, the membrane was cross-linked using the UV-light cross-linker instrument.

### 3.8.5. Detection of Biotin-Labeled DNA by Chemiluminescence and Development of the Membrane

In order to perform the blocking procedure the following buffers were used. (Table 3.8) 10 ml of blocking buffer containing 100 mg/ml Albumin Fraction V (with 1:1000 dilution) was added onto top of the membrane and gently shaken for 15 minutes. By adding 33 ul stabilized streptavidin-horseradish peroxidase conjugate into 10 ml of blocking buffer with 1:300 dilution, the conjugate-blocking buffer solution was prepared. The blocking buffer alone was discarded and the conjugate-blocking buffer solution was replaced and membrane was incubated at room temperature while gently shaking for 30 minutes. Meanwhile, 1X wash solution was prepared by adding 19 ml of 4X wash buffer into 57 ml ultrapure water. For the rest of the washing steps, each time the tray was changed. The membrane was transferred into the new container and washed with 12 ml of 1X wash buffer. Then, membrane was washed four times for five minutes by adding 15 ml of 1X washing solution with gentle shaking. Lastly, 15 ml of substrate equilibration buffer was poured and the membrane was gently shaken for five minutes.

Table 3.8. Detection and blocking buffers

<b>Buffer</b>	<b>Volume per Membrane</b>
1X Wash Buffer	76 ml
Blocking Buffer	20 ml with 100 ug/ml Albumin Fraction v
Substrate Equilibration Buffer	15 ml

Substrate working solution was prepared (6 ml of luminol/enhancer solution with 6 ml substrate peroxide solution). The membrane was taken from the substrate equilibration buffer and covered with the prepared substrate working solution, incubated for five minute with gentle shaking and exposed for five minutes.

### **3.9. CELL MIGRATION – SCATTERING ASSAY**

RenCa cells were plated into 6-well plate at a density of  $1 \times 10^3$  in growth media and allowed to grow as a colony in the incubator. When the colony formation was visualized growth media was replaced with two per cent FBS containing RPMI-1640 to achieve cell synchronization and incubated overnight. Meanwhile, the seven- selected colonies were marked and the following day, the two per cent FBS containing RPMI-1640 media was replaced with the AIM-V media. As soon as, when the AIM-V medium was added into the wells, first images of the colonies were taken under the light microscope at 20x magnification as it was considered the 0<sup>th</sup> hour. The colonies were monitored at 4 to 24 hours by capturing the images at the specify time of interval. For data analysis, colonies in three different forms such as scattered, loose and compact were calculated in triplicate.

### **3.10. TRANSWELL MATRIGEL INVASION ASSAY**

Transwell cell invasion assay was done using 6.5 mm, 8.0- $\mu$ m pore sizes BD BioCoat inserts (Costar). RenCa cells that were present in the AIM-V media were plated on the upper chambers of matrigel coated transwell inserts with a density of  $2 \times 10^4$  cells/chamber, and the growth media was placed at the lower chamber. Then, seeded cells were allowed to migrate by incubating in the incubator for the following 24 hours and non-migrant cells were gently removed from the upper chamber using a cotton swab. Then, the cells that were attached onto the lower chamber were fixed by four per cent paraformaldehyde and stained with the DAPI. The images were captured using Carl Zeiss Fluorescence microscope equipped with Camera System AxioCam 105 Digital Color under the 10x magnification. Data analysis was performed by evaluating the total number of the cells per well using Scion Image Analysis Program.

### **3.11. THE DRUG RESISTANCY OF TG2-EXPRESSING RENCA CELLS**

RenCa cells were plated into 96-well plate at a density of  $3 \times 10^3$ ,  $5 \times 10^3$ , and  $7.5 \times 10^3$  and  $10 \times 10^3$  cells per well, respectively for the standardization process. While,  $3 \times 10^3$  cells/well were seeded into another 96-well plate and allowed to grow overnight. The very next day,



chemotherapeutic agents such as sorafenib and everolimus were added at various concentrations (1  $\mu\text{m}$ , 5  $\mu\text{m}$  and 10  $\mu\text{m}$ ) and the cells were incubated for 24, 48 and 72 hours in growth media. In order to measure the toxic effect of DMSO cells were also grown in growth media supplemented with 0.001 per cent DMSO as all the used chemotherapeutic agents were dissolved in DMSO. The cytotoxic effect of the drugs was then figured out by adding WST-1 cell viability assay. Used procedure mainly based on the tetrazolium salts, which were known to be cleaved to formazan molecule through the mitochondrial enzymes. The number of viable cells is closely related with the mitochondrial dehydrogenase activity resulting in the formation of formazan dye in viable cells, which can be logically related with metabolically active cell numbers. In order to measure the cell viability, 5  $\mu\text{l}$  WST-1 solution was dissolved in 45  $\mu\text{l}$  growth media and the total volume of 50  $\mu\text{l}$  was added onto each samples. Then, cells were incubated for one hour in dark at 37°C. One hour later, the absorbance value was measured at 450 nm using 630 nm as reference wavelength with an ELISA plate reader. The values obtained from the plate reader then analyzed by using the DMSO treated cells as the control in the experiment.

### **3.12. STATISTICAL ANALYSIS**

All values presented in the result part (Section 4.) were calculated as follows; the means  $\pm$  SE from triplicate experiments. The necessary comparisons that were done between groups via parametric statistics using the Student's t-test for parametric and Mann-Whitney test for the non-parametric distribution using GraphPad Prism and the \*p- < 0.05, \*\*p- < 0.01 and \*\*\*p- < 0.001 considered as statistically significant.

## 4. RESULTS

### 4.1. DNA SEQUENCE ANALYSIS OF TG2 CONSTRUCTS

In the context of FP-7 TRANSPATH 289964 project named ‘transglutaminase in disease: a novel therapeutic target’, wt-TG2, TG2-C277S, TG2-W241A and TG2-R580A were cloned in Plenti CMV BLAST DEST (706-1) vector in Debrecen University, Hungary. DNA sequence analysis results were showed in Figure 4.1 – 4.4 and primers used in the DNA sequencing was designed by Ajna Bihorac (Table 4.1).

Table 4.1. The sequence of the forward and reverse primers used in sequencing of TG2 native and mutant constructs.

Sequence of the Primers	Forward	Reverse
<b>V224V-W241A</b>	TGGGCAGTTTGAAGATGGGA	CGATCCAGGACATGGGGCT
<b>C277S</b>	CAAGTTCCTGAAGAACGCCG	TCTCGCTCTTGTCACCCTG
<b>R580A</b>	CCTTACGGAGTCCAACCT	ATCTCCACCGTCTTCTGC

As can be seen from Figure 4.2 the TGT codon coding for Cysteine at 277<sup>th</sup> position (wt-TG2 in Figure 4.1) was changed to AGT coding for Serine. In order to generate W241A TG2 variant, 241<sup>st</sup> site Tryptophan (TGG codon) was mutated to Alanine (GCC) (Figure 4.3.). Lastly, R580A variant of TG2 was obtained by mutating 580<sup>th</sup> site Arginine (CGC) to Alanine (GCT).

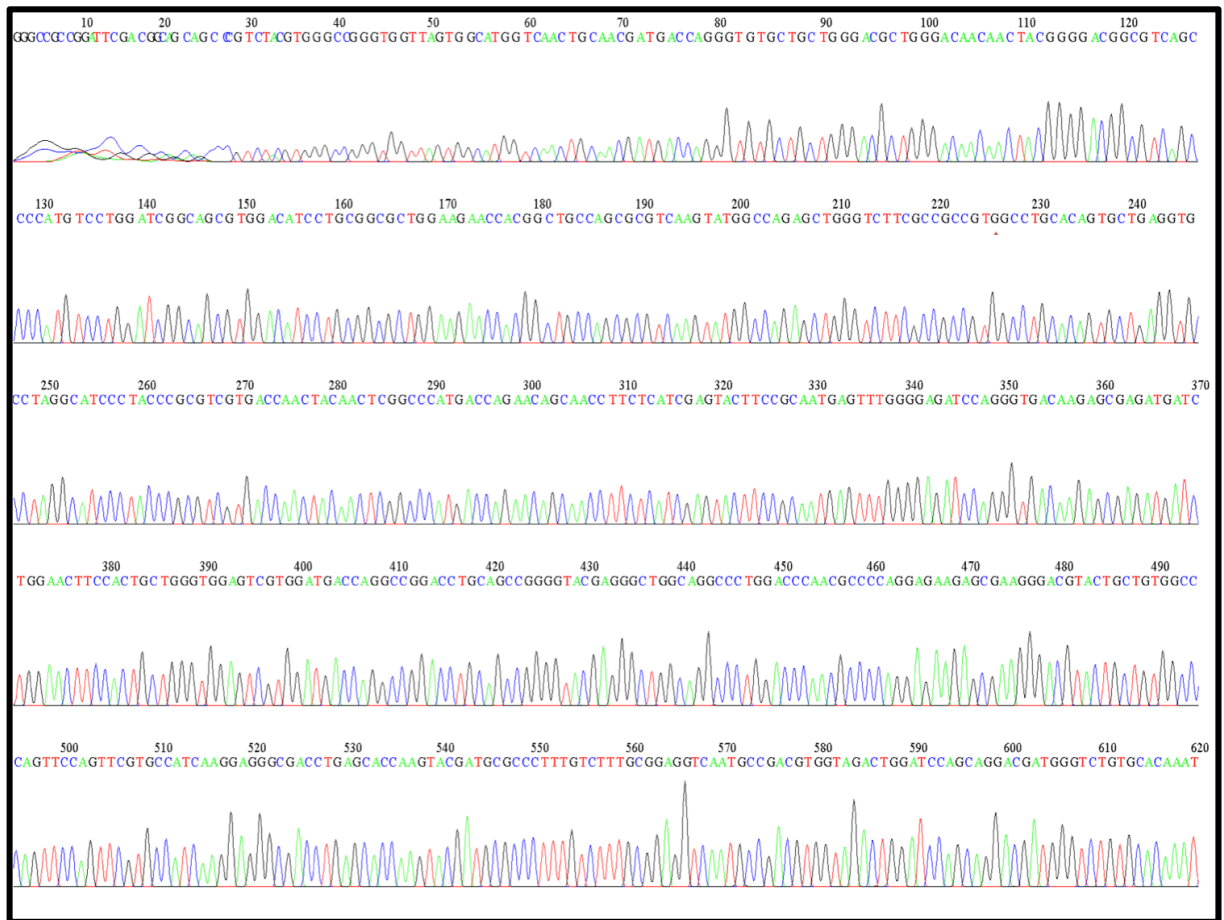


Figure 4.1. Chromatogram result of wt-TG2 cDNA.

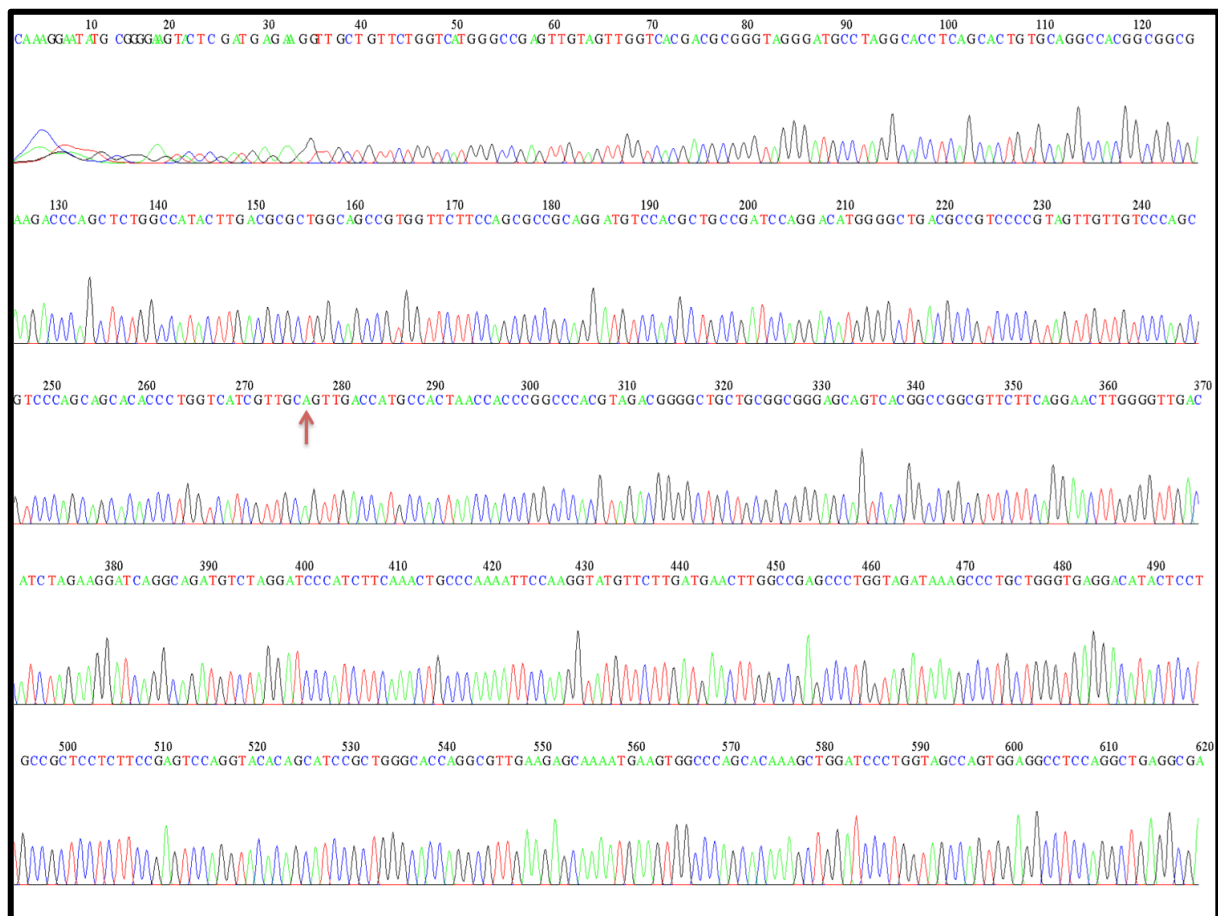


Figure 4.2. Chromatogram result of TG2-C277S, the red arrow indicates the site of the single point mutation C→S at 277 on TG2 cDNA cloned in Plenti BLAST plasmid under CMV promoter.

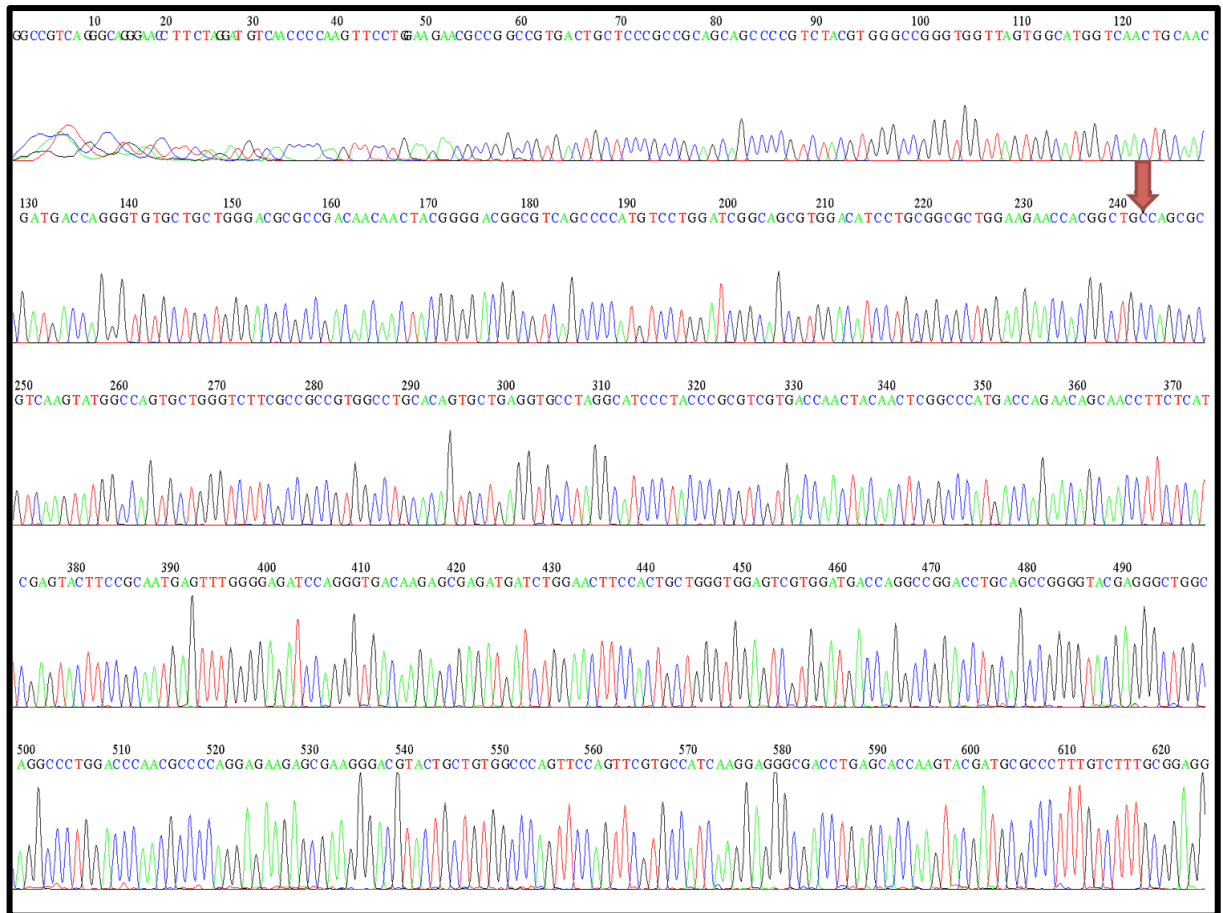


Figure 4.3. Chromatogram result of TG2-W241A, the red arrow indicates the site of mutation W→A at 241 on TG2 cDNA cloned in Plenti BLAST plasmid under CMV promoter.



Figure 4.4. Chromatogram result of TG2-R580A, the red arrow indicates the site of mutation R→A at 580 on TG2 cDNA cloned in Plenti BLAST plasmid under CMV promoter.

## 4.2. CONTROL OF TRANSFECTION EFFICACY IN HEK 293FT

In order to optimize the transfection conditions for HEK 293FT using  $\text{CaCl}_2$  method, cells were transfected with pUC19-eGFP as described in Section 3.3.1. Following 24 and 48 hours of incubation, the images captured at different time points indicated that the transfected cells were positive for the GFP fluorescence (Figure 4.5).

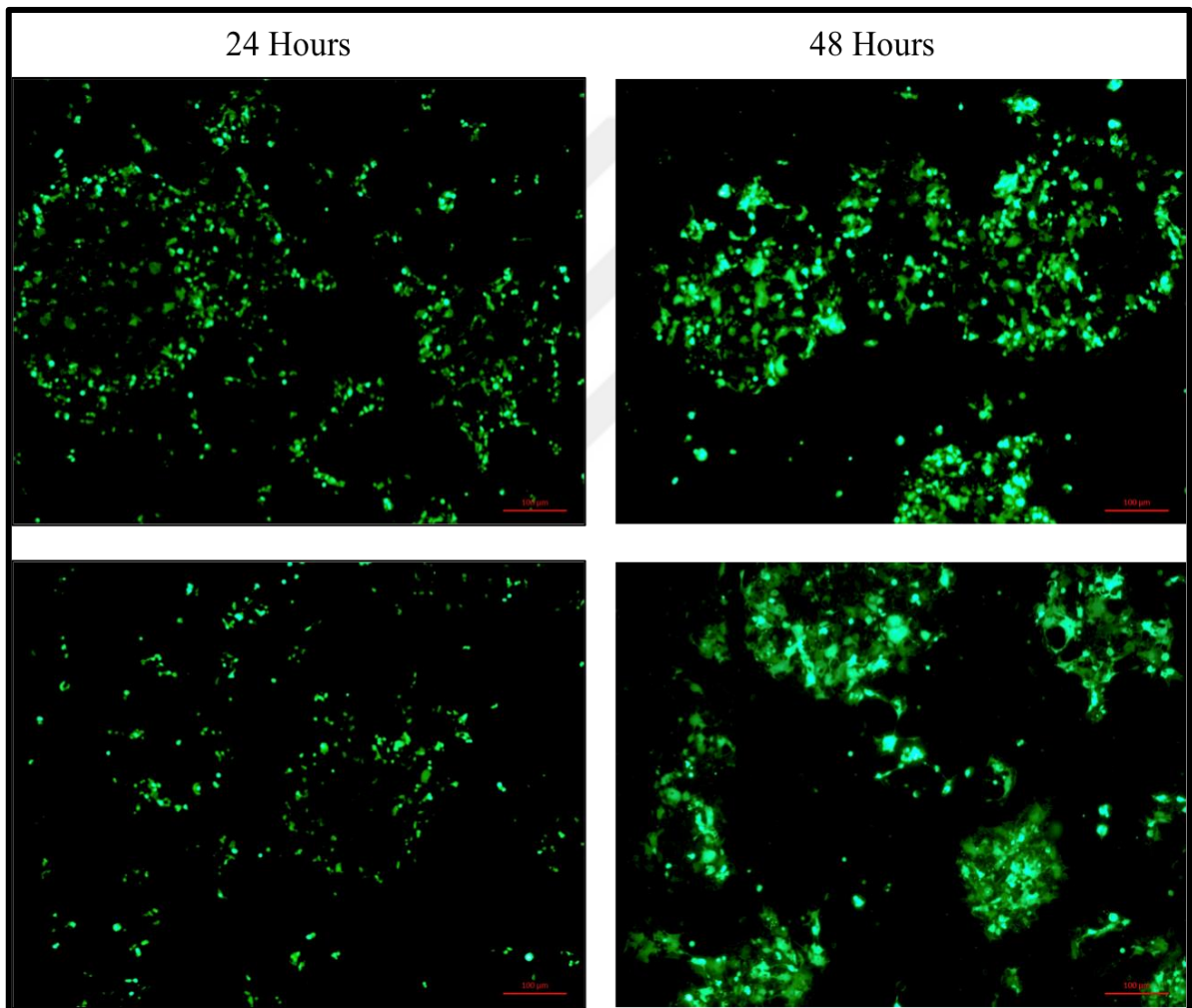


Figure 4.5. Images of transfected HEK 293FT with eGFP s were taken under a fluorescent microscope with a 10x objective at 24 and 48 hours after transfection. Representative images were performed three times independently. Scale bars 100 μm.

#### 4.3. DETERMINATION OF TG2 EXPRESSION LEVELS IN RENCA CELLS EXPRESSING TG2 MUTANT CONSTRUCTS

In order to determine which function of TG2 enzymatic activity is more essential or indispensable for tumor development in RCC, mouse model of renal adenocarcinoma cell line RenCa was transduced with lentiviral vectors encoding wild type TG2 (wt-TG2), TG2-C277S, TG2-W241A and TG2-R580A cDNA constructs as described in Section 3.3.2. Following the transduction, mRNA expression levels for *hTGM2* in TG2 constructs in RenCa cells were determined by real-time PCR as mentioned before in Section 3.7.3. Levels of *hTGM2* gene expression was found to be similar for wt-TG2, TG2-W241A and TG2-R580A transduced RenCa cells, except for TG2-C277S cells, which showed slightly lower ( $p > 0.05$ ) *hTGM2* mRNA levels (Figure 4.6).

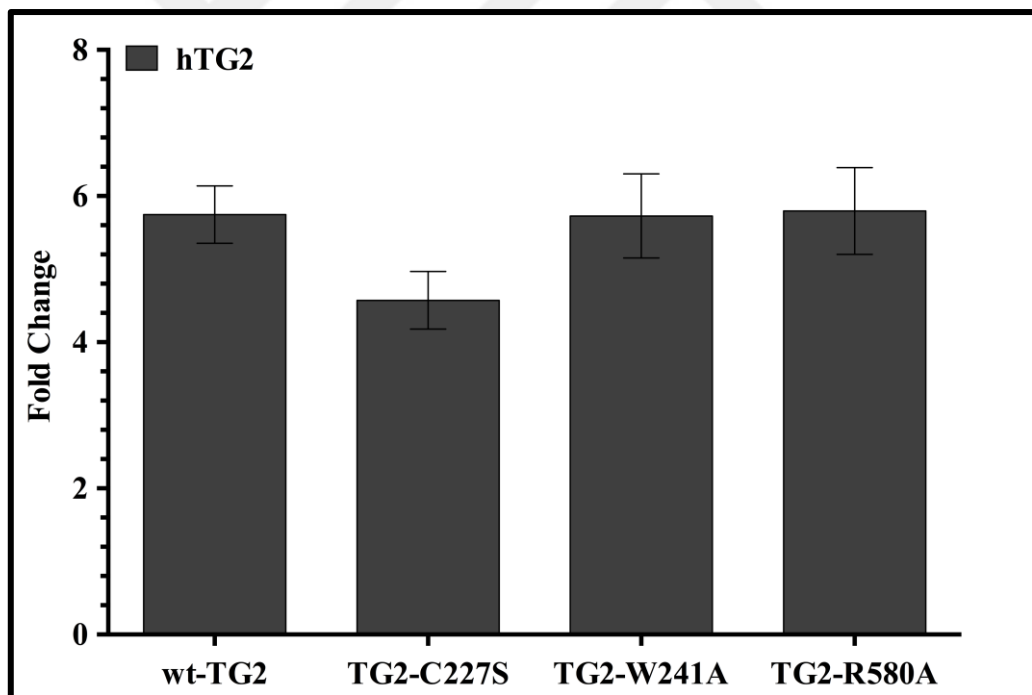


Figure 4.6. The relative *hTGM2* mRNA levels in RenCa cells transduced with wt and mutant *hTGM2* constructs was evaluated using RT-PCR. 18S RNA was used to normalize the *hTGM2* mRNA levels. Data values represent the average of three experiments independently (means  $\pm$  SD) performed in triplicate.



Western blot analysis for TG2 protein levels in transduced RenCa cells was performed as described in Section 3.5.4. using proteins isolated from whole cell lysate and membrane alone. Interestingly, analysis of TG2 protein levels in the isolated membrane fractions showed a polarized distribution of TG2 in TG2-expressing mutant RenCa cells (Figure 4.7A). It was observed that TG2-W241A and TG2-R580A cells exhibited higher protein levels of membrane-associated TG2 when compared to the wt-TG2. Densitometric analysis of TG2 protein levels in membrane and whole cell indicated that the plasma membrane distribution of TG2 was found to be minimal in TG2-C277S cells (Figure 4.7B).

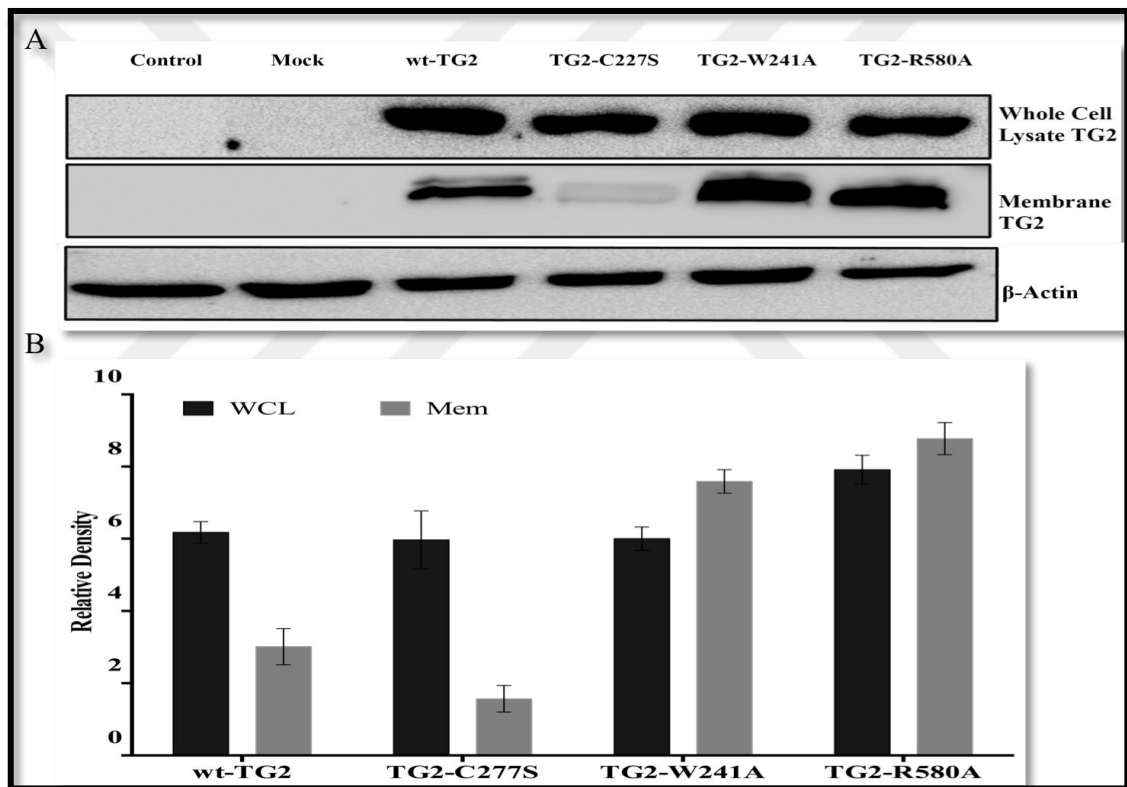


Figure 4.7. Analysis of TG2 protein levels in membrane and whole cell lysates. (a) Immunoblots demonstrating TG2 protein levels in the membrane and whole cell lysate for RenCa cells expressing TG2 mutant constructs. Mouse monoclonal Cub7402 was used to probe TG2 and  $\beta$ -actin was used as the loading control. (b) The relative density graphic of TG2 distribution in TG2-expressing mutant RenCa cells were quantified using Image Lab analysis program by dividing  $\beta$ -actin levels

In order to confirm the loss of transamidating activity in TG2-C277S and TG2-W241A mutants, analysis of TG2 cross-linking activity was performed using CovaLab (Section 3.6.1.) Results from enzyme-linked sorbent assay (ELSA) showed that the TG2-R580A, which was known as the GTP-binding defective mutant displayed similar catalytic activity with wt-TG2 expressing transduced RenCa cells (Figure 4.8). As expected, residual cross-linking activity was detected in cell lysates of both transamidating-defective mutants known as TG2-C277S and TG2-W241A.

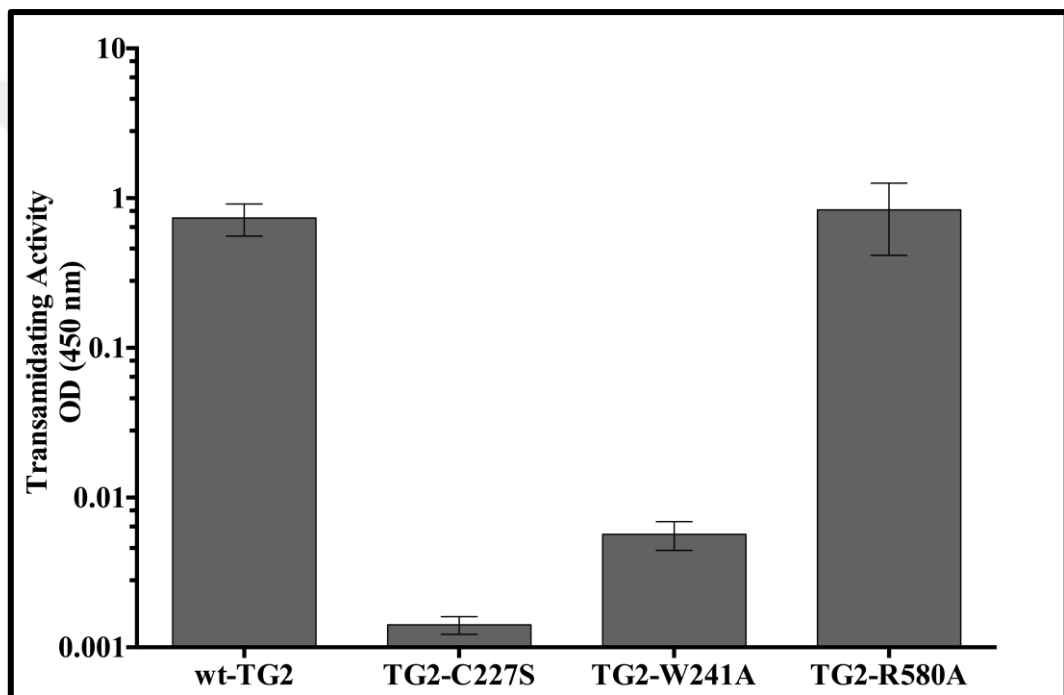


Figure 4.8. The analysis of TG2 transamidating activity in TG2 mutant transduced RenCa cells using the specific TG2-CovTest colorimetric microassay kit. Each data point represents the average of three experiments independently  $\pm$  SD performed in triplicate.

In order to prove that the obtained results did not lead to a change in the expression levels of TG2 cell surface binding partners ITG $\beta$ 1 and SDC4, control experiment was performed. Western blot analysis showed that the expression levels of ITG $\beta$ 1 and SDC4 was found to be constant in each TG2-expressing mutant cells (Figure 4.9) suggesting that the differential distribution of TG2 in RenCa mutant cells (Figure 4.7) was independent from the ITG $\beta$ 1 and SDC4.

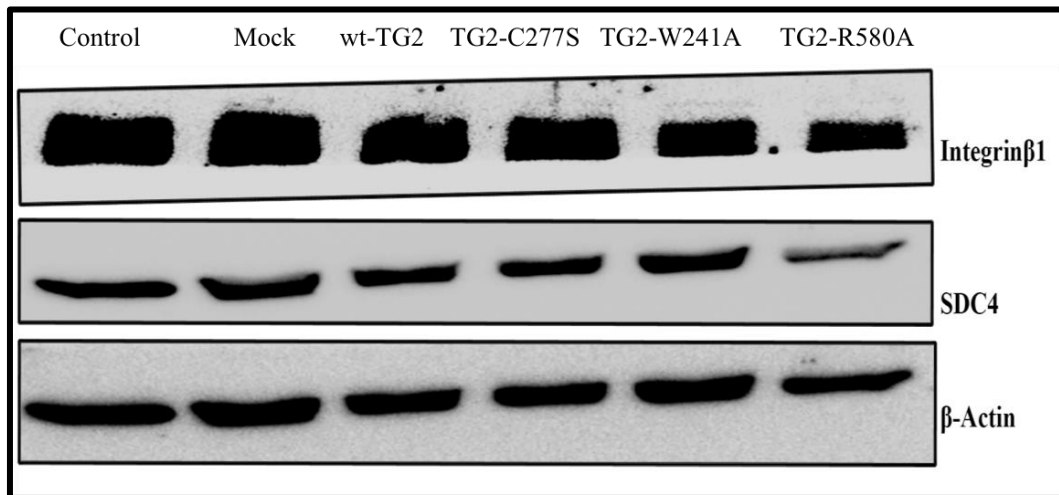


Figure 4.9. Western Blots showing the protein levels of ITGβ1 and SDC4 in RenCa cells transduced with TG2-variants. β-actin was utilized for normalization analysis.

#### 4.4. ACTIVATION OF NF-κB SIGNALLING TOGETHER WITH EMT IS DEPENDENT ON A FUNCTIONAL GFP-BINDING DOMAIN OF TG2

TG2 expression is associated with the activation of NF-κB signaling pathway, which in turn responsible for the promotion of the EMT due to the upregulation of transcription factors including *Zeb1/2*, *Snail1/2* and *Twist1/2*.

In this regard, EMSA was performed to elucidate which functional domain of TG2 was mainly responsible from the activation of NF-κB signaling inducing EMT process. Analysis of active NF-κB in nuclear fractions (Figure 4.10). showed that wt-TG2 expression had a 0.5 fold increase in nuclear NF-κB protein levels when it was compared to the non-transduced parental and mock control RenCa cells. The catalytically inactive mutant TG2-W241A exhibited a significant 1.3 fold increase, while GTP-binding deficient form TG2-R580A led to a 3.8 fold decrease in the active NF-κB nuclear antigen. Concomitantly, the transaminase-defective with low GTP-binding affinity form TG2-C277S led to a 2.4 fold decrease in the levels of active nuclear NF-κB protein.

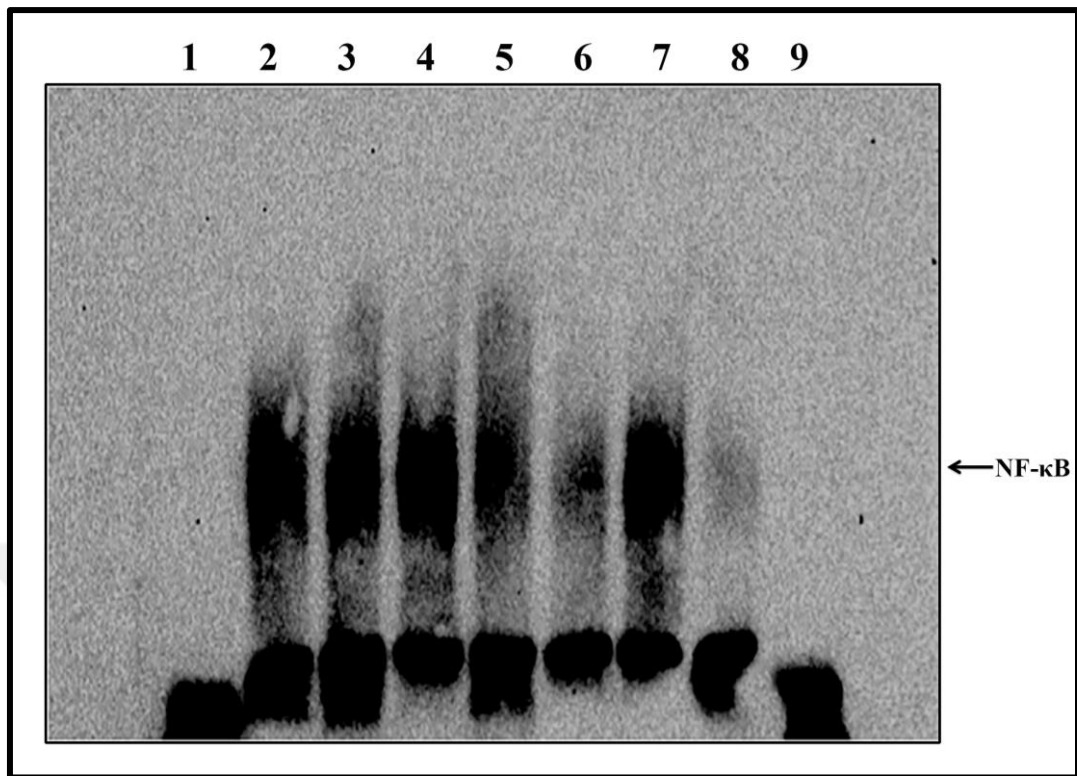


Figure 4.10. Nuclear extract prepared from the non-transduce (Lane 3) and wild-type transduced (wt-TG2; Lane 5), TG2 transaminase (TG2-C277S; Lane 6, TG2-W241A; Lane 7) and GTPase (TG2-R580A; Lane 8) mutant expressing RenCa cells were subjected to EMSA. Supershift assay was performed incubating control nuclear extracts with p65 monoclonal antibody (Lane 2). Cells transduced with lentiviral particles encoding eGFP (Mock) was used as additional control (Lane 4). Free probe (Lane 1) and cold probe (Lane 9) were used as negative control.

In order to show whether TG2 mediated activation of NF- $\kappa$ B was through canonical or non-canonical pathway, basal and phosphorylated protein levels of I $\kappa$ B- $\alpha$  was determined by Western blot analysis. In agreement with Figure 4.10, a significant reduction in the levels of p-I $\kappa$ B- $\alpha$  was observed for TG2-C277S and TG2-R580A cells, which was in parallel with the increased amount of basal I $\kappa$ B- $\alpha$  levels with a 2.5 and 4.4 fold, respectively (Figure 4.11.). While, wt-TG2 and TG2-W241A cells showed a slightly reduced levels of p-I $\kappa$ B- $\alpha$  compared to the control non-transduced and mock RenCa cells. In this context, our findings indicated TG2 mediated the activation of NF- $\kappa$ B through the canonical pathway, which was dependent on the GTP-binding ability of the enzyme.

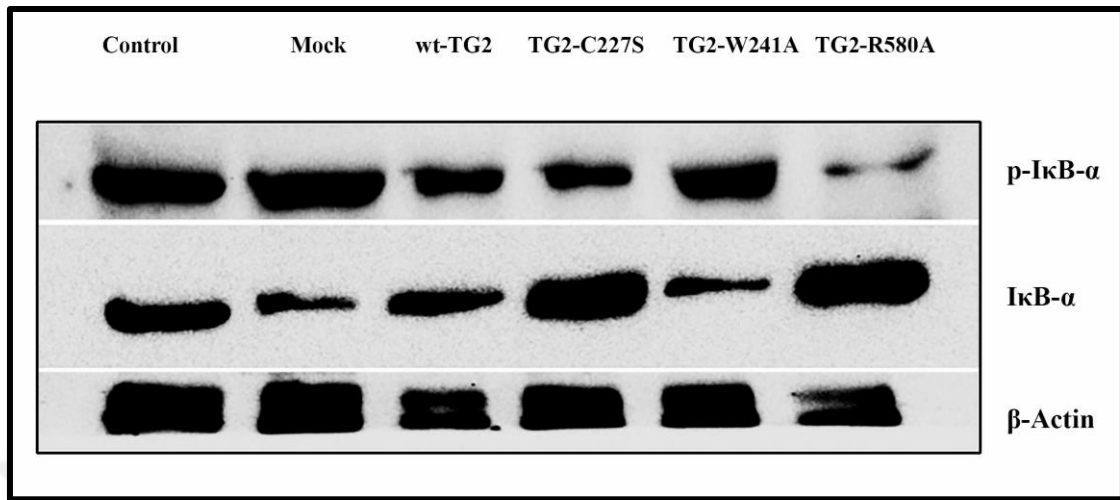


Figure 4.11. Immunoblots showing membranes probed with IκB-α and p- IκB-α in RenCa cells expressing TG2 mutant constructs for the evaluation of the protein levels, results were normalized using β-actin levels.

Given that NF-κB activation is essential for the regulation of EMT, the expression levels of EMT markers was evaluated by RT-PCR analysis (Figure 4.12-4.14.). Analysis of mRNA levels of *Zeb1* (Figure 4.12A) indicated that *Zeb1* expression was upregulated by 20.8 fold in wt-TG, by 14 fold in TG2-W241A and 5 fold in TG2-R580A compared to the non-transduced parental control cells. Interestingly, a 5.7 fold decrease in *Zeb1* mRNA levels was detected for TG2-C277S. On the other hand, no significant change in mRNA levels of *Zeb2* was recorded for TG2-mutant RenCa cells except for TG2-W241A and TG2-R580A cells, which demonstrated an increment of 11- and 4.3 fold in *Zeb2* mRNA levels (Figure 4.12B). Similarly, the expression of TG2-W241A construct in RenCa cells led to an average of 30 fold increase in *Twist1/2* whereas TG2-R580A expression resulted in only a 1.5 fold increase in *Twist1/2* mRNA levels in comparison to control RenCa cells. Meanwhile, a 6.5 fold downregulation in *Twist1/2* expression was seen in TG2-C277S cells (Figure 4.13A&B). The mRNA level of *Snail1* was downregulated in wt-TG2 and TG2-C277S by 1 fold and 6 folds, respectively, while TG2-W241A and TG2-R580A mutants exhibited a 32.5- and 2.6 fold increase in *Snail1* expression, respectively (Figure 4.14A). Figure 4.14B indicated that TG2-C277S, TG2-W241A and TG2-R580A cells displayed a 11-, 34- and 21 fold increase in *Snail2* mRNA expression, respectively. Taken

together, these results strongly suggested that GTP-binding domain of TG2 might be crucial for the upregulation of EMT markers in a NF- $\kappa$ B dependent manner.

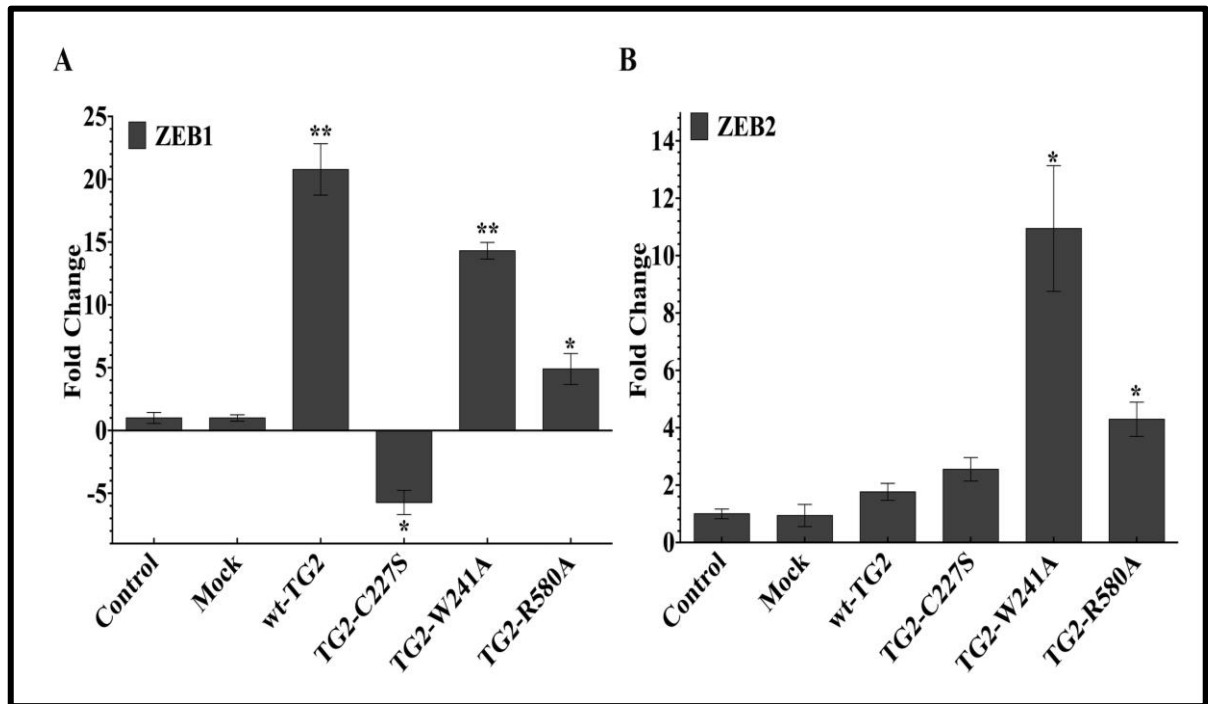


Figure 4.12. Real Time (RT-PCR) analysis for expression levels of EMT related transcription factors in non-transduced and mock control RenCa cells and RenCa cells transduced with TG2 constructs (wt-TG2, TG2-C277S, TG2-W241A and TG2-R580A), Data values recorded for the relative expression of. (a) *Zeb1* (b) *Zeb2* represent the average of three experiments independently (means  $\pm$  SD) normalized against 18 S RNA mRNA, (\* $p$ - < 0.05 and \*\* $p$ - < 0.01)

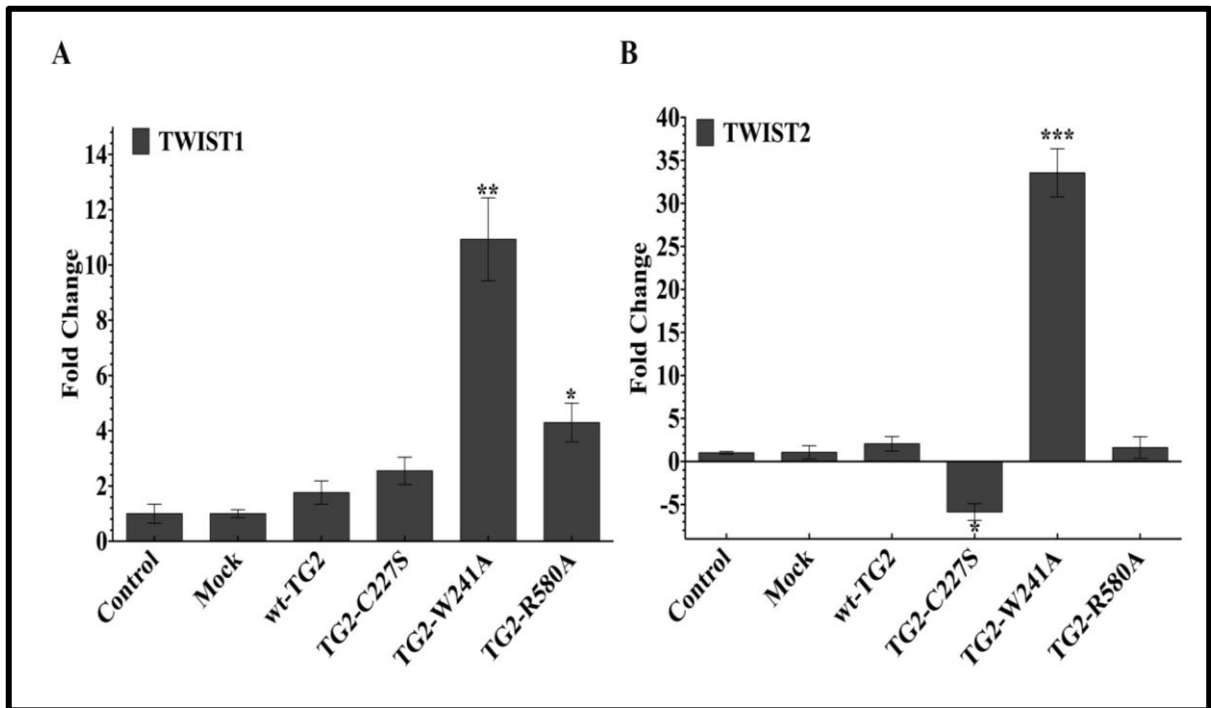


Figure 4.13. Real Time (RT-PCR) analysis for expression levels of EMT related transcription factors in non-transduced and mock control RenCa cells and RenCa cells transduced with TG2 constructs (wt-TG2, TG2-C277S, TG2-W241A and TG2-R580A), Data values recorded for the relative expression of. (a) *Twist1* (b) *Twist2* represent the average of three experiments independently (means  $\pm$  SD) normalized against 18 S RNA mRNA, , (\*p- < 0.05, \*\*p- < 0.01 and \*\*\*p- < 0.001)

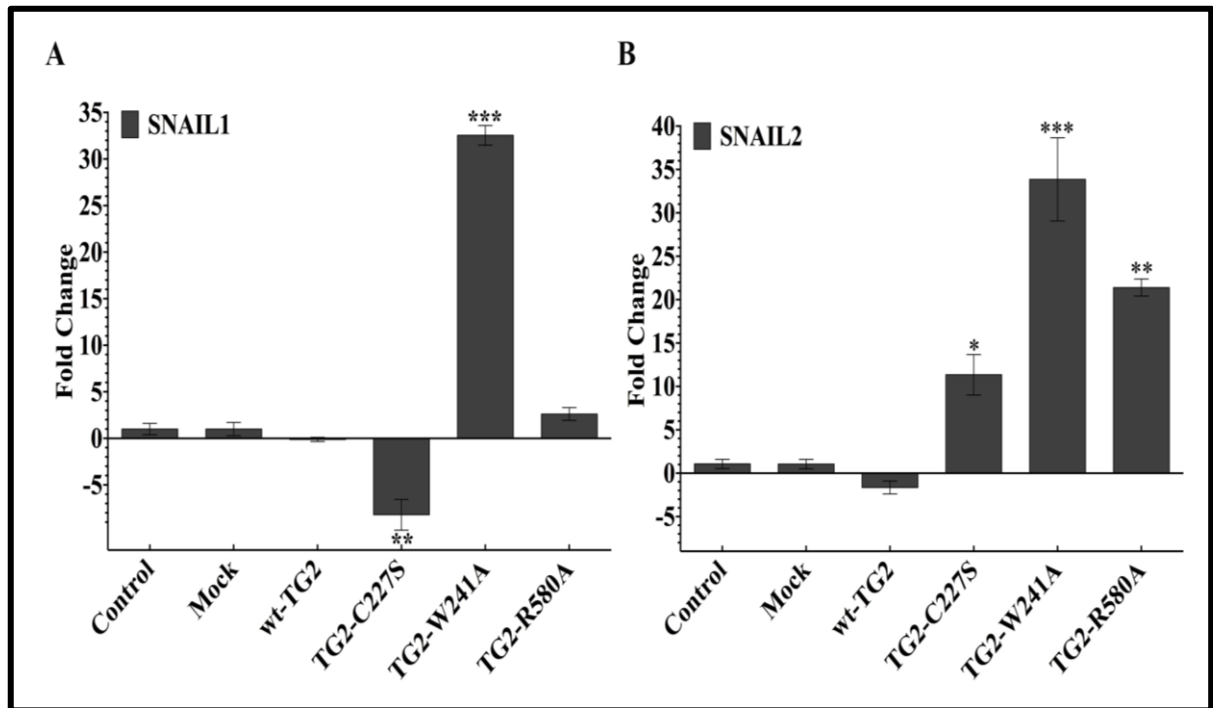


Figure 4.14. Real Time (RT-PCR) analysis for expression levels of EMT related transcription factors in non-transduced and mock control RenCa cells and RenCa cells transduced with TG2 constructs (wt-TG2, TG2-C277S, TG2-W241A and TG2-R580A), Data values recorded for the relative expression of. (a) *Snail1* (b) *Snail2* represent the average of three experiments independently (means  $\pm$  SD) normalized against 18 S RNA mRNA, (\*p- < 0.05, \*\*p- < 0.01 and \*\*\*p- < 0.001)



## **4.5. CANCER STEM CELL PROFILE OF RENCA CELLS EXPRESSING TG2 MUTANT CONSTRUCTS**

### **4.5.1. Characterization of Stemness Profile**

Previous studies indicated that TG2 overexpression in the healthy mammary epithelial cells led to the induction of cancer stem cell property and mammo-sphere formation [137]. Based on these findings, stem cell marker profile in parental RenCa (control) cells and Renca cells transduced with the lentiviral vectors encoding wild type TG2 (wt-TG2), TG2-C277S, TG2-W241A and TG2-R580A mutants was evaluated via flow cytometer (Table 4.2, Figure 4.15.-4.17.). The cell surface levels of CD44, cell-surface glycoprotein involved in cell to cell interaction, adhesion and migration, was increased by more than 85 per cent in wt-TG2 and TG2-W241A cells when compared to the parental control RenCa cells (Figures 4.15B)

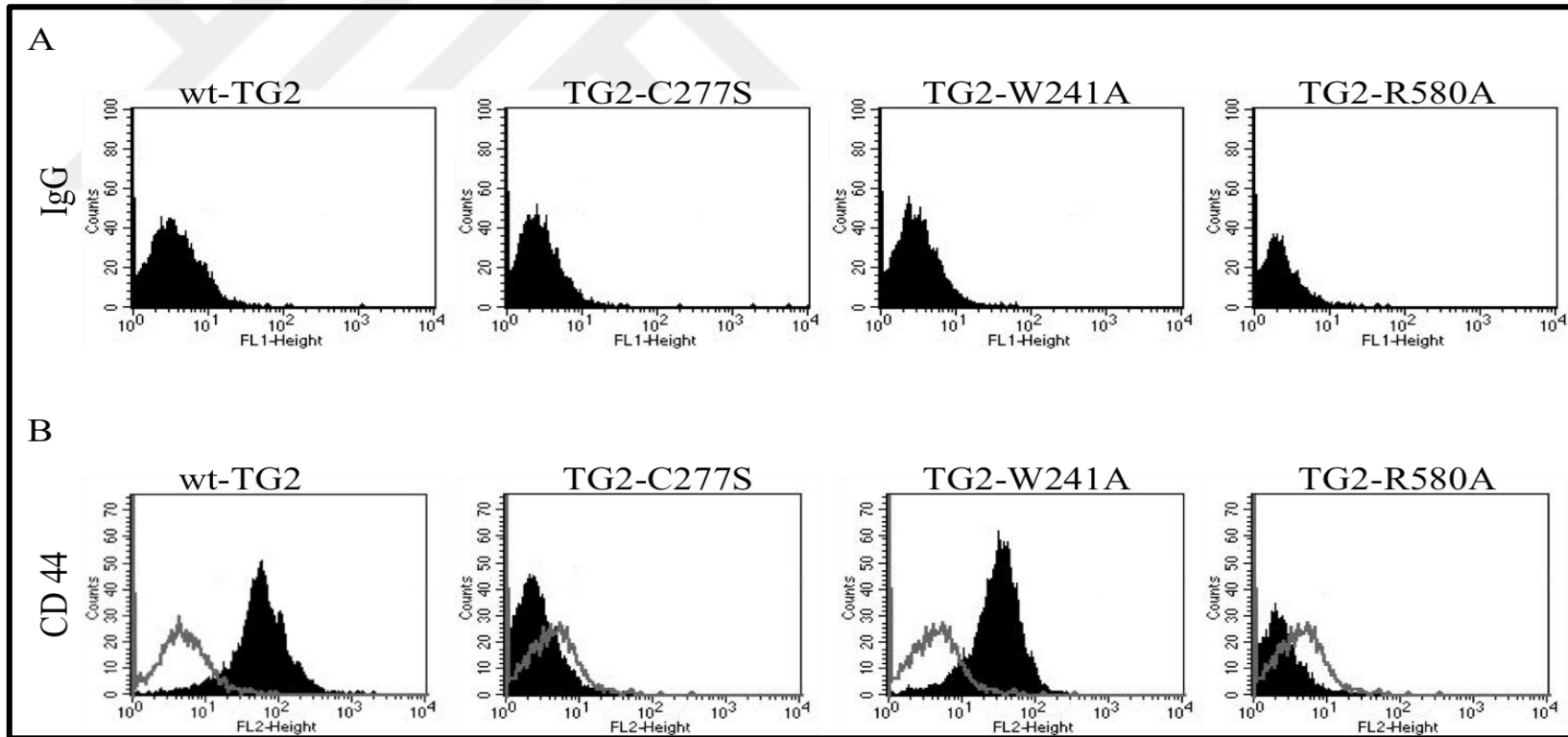


Figure 4.15. (a) Flow Cytometry analysis of mouse IgG isotype control (b) cell surface marker, mouse CD44 marker in control (grey-shaded histograms) and wt-TG2 and mutant (dark-shaded histograms) expressing RenCa cells.

Furthermore, Figure 4.16.A showed that wt-TG2 and TG2-W241A expression in RenCa cells resulted in a 60 per cent increase in the cell surface levels of CD73, a membrane-bound enzyme also known as ecto-5'-nucleotidase mesenchymal marker. On the other hand no detectable change was observed in the cell surface expression levels of CD106, vascular cell adhesion molecule 1 (VCAM-1), in transduced RenCa cells, in comparison to the control cells (Figure 4.16.B).



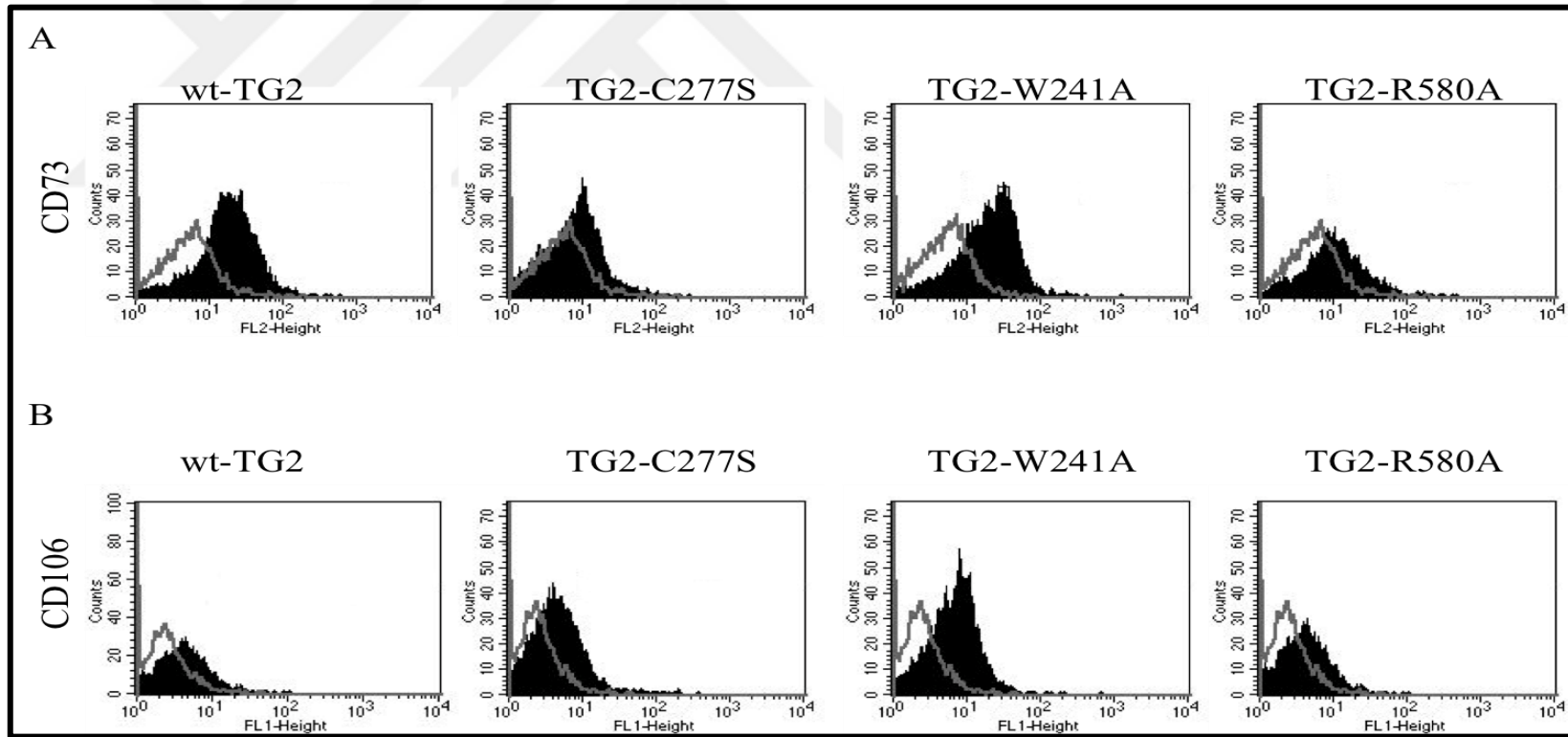


Figure 4.16. (a) Flow Cytometry analysis of CD73 and (b) CD106 cell surface mesenchymal markers in control (grey-shaded histograms) and wt-TG2 and mutant (dark-shaded histograms) expressing RenCa cells.

The expression levels of CD11b, the cell surface glycoprotein involved in integrin-mediated cell adhesion, did not show any change in TG2-expressing mutant cells and parental control RenCa cells (Figure 4.17A), while the cell surface levels of hematopoietic stem cell markers Sca-1 (Figure 4.17.B) and CD45 (Figure 4.17.C) were found to be negative in all RenCa variant with an exception of wt-TG2 cells which were found to be positive for Sca-1 with 50 per cent expression levels.



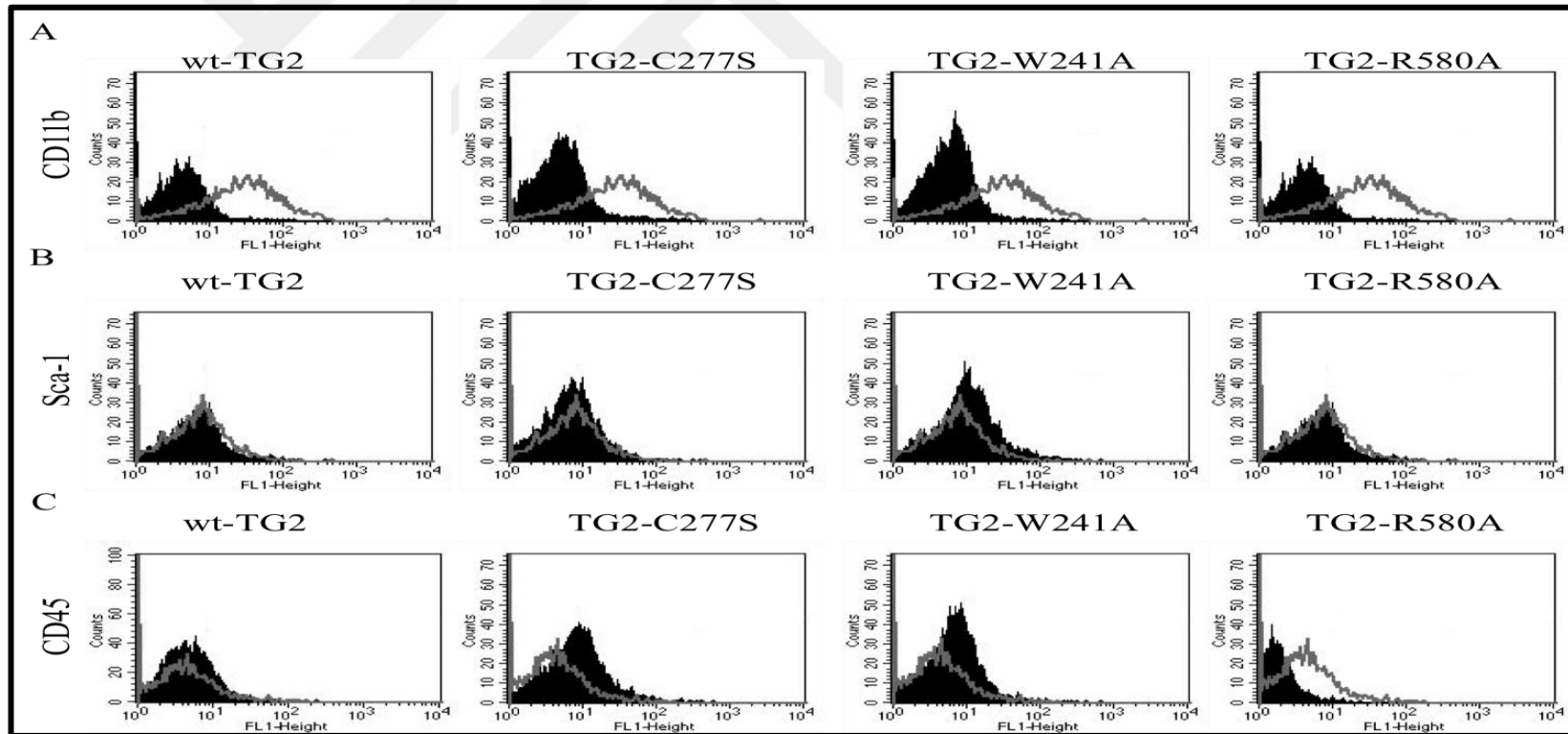


Figure 4.17. (a) Flow Cytometry analysis of mouse CD11b, (b) mouse Sca-1 and (c) mouse CD45 cell surface mesenchymal markers in control (grey-shaded histograms) and wt-TG2 and mutant (dark-shaded histograms) expressing RenCa cells.

Table 4.2. Expression level of cell surface markers with the values represent the average of three experiments independently (means  $\pm$  SD).

CD Markers	Control	wt-TG2	C277S-TG2	W241A-TG2	R580A-TG2
CD 44	2.39 $\pm$ 0.91	87.07 $\pm$ 1.34	0.49 $\pm$ 0.35	91.57 $\pm$ 3.31	0.59 $\pm$ 0.15
CD 73	31.64 $\pm$ 13	59.47 $\pm$ 3.09	25.92 $\pm$ 6.97	60.36 $\pm$ 1.46	38.19 $\pm$ 7.8
CD 106	0.28 $\pm$ 0.47	1.8 $\pm$ 0.44	2.89 $\pm$ 0.86	3.73 $\pm$ 0.04	2.27 $\pm$ 1.64
CD 11b	0.6 $\pm$ 0.09	2.94 $\pm$ 0.64	1.71 $\pm$ 1.14	39.88 $\pm$ 5.60	1.35 $\pm$ 1.18
Sca-1	2.75 $\pm$ 3.69	52.44 $\pm$ 4.92	10.10 $\pm$ 0.75	14.70 $\pm$ 1.39	6.56 $\pm$ 2
CD 45	1.23 $\pm$ 1.18	3.33 $\pm$ 1.48	8.78 $\pm$ 2.41	6.11 $\pm$ 1.83	0.23 $\pm$ 0.09

#### 4.5.2. GTP-binding Function of TG2 is Crucial in the RCC Sphere Formation

Studies indicated that the cancer cells that were positive for CD stem cell markers also possess the ability to form 3D spheroids under the ultra-low attachments conditions. In order to determine whether TG2 expression in RenCa cells, which are known to be the adherent cells, have the ability to induce self-renewal ability to form reno-spheres, spheroid and sub-spheroid *in vitro* assays were performed as described in Section 3.4.2. Figure 4.18. demonstrates the sphere formation of non-transduced parental and mock control RenCa cells together with TG2-expressing mutant cells. Following three to five days of incubation, spheroid formation was evident in all RenCa variants, albeit with a low efficiency for the parental and mock control RenCa. These cells displayed spheroid formation with an average diameter of 180  $\mu$ m in the 5<sup>th</sup> day of incubation, which were enlarged to small renal spheroids with average diameter of 710  $\mu$ m at the end of 11<sup>th</sup> day. Similarly, the number of reno-spheres was not significantly increased for TG2-C277S and TG2-R580A constructs when compared to the control cells. Interestingly, the average diameter was measured as 180  $\mu$ m for TG2-C277S and 170  $\mu$ m for TG2-R580A on the 5<sup>th</sup> day; spheres were reached with the average of 400  $\mu$ m for both TG2-C277S and TG2-R580A. However, wt-TG2 and TG2-W241A mutant cells showed a significant increase in the spheroid number with a respective of 1.3 and 2.9 fold when compared to the control RenCa cells. In the context of the size of the reno-spheres formed was measured as 250  $\mu$ m for wt-TG2 and 257  $\mu$ m for TG2-W241A in day 5 and in day 11, it was observed that the

size of the reno-spheres was enlarged 1.1 fold for wt-TG2 with an approximate diameter of 1430  $\mu\text{m}$  and 2.3 fold for TG2-W241A with a diameter of 1500  $\mu\text{m}$ .

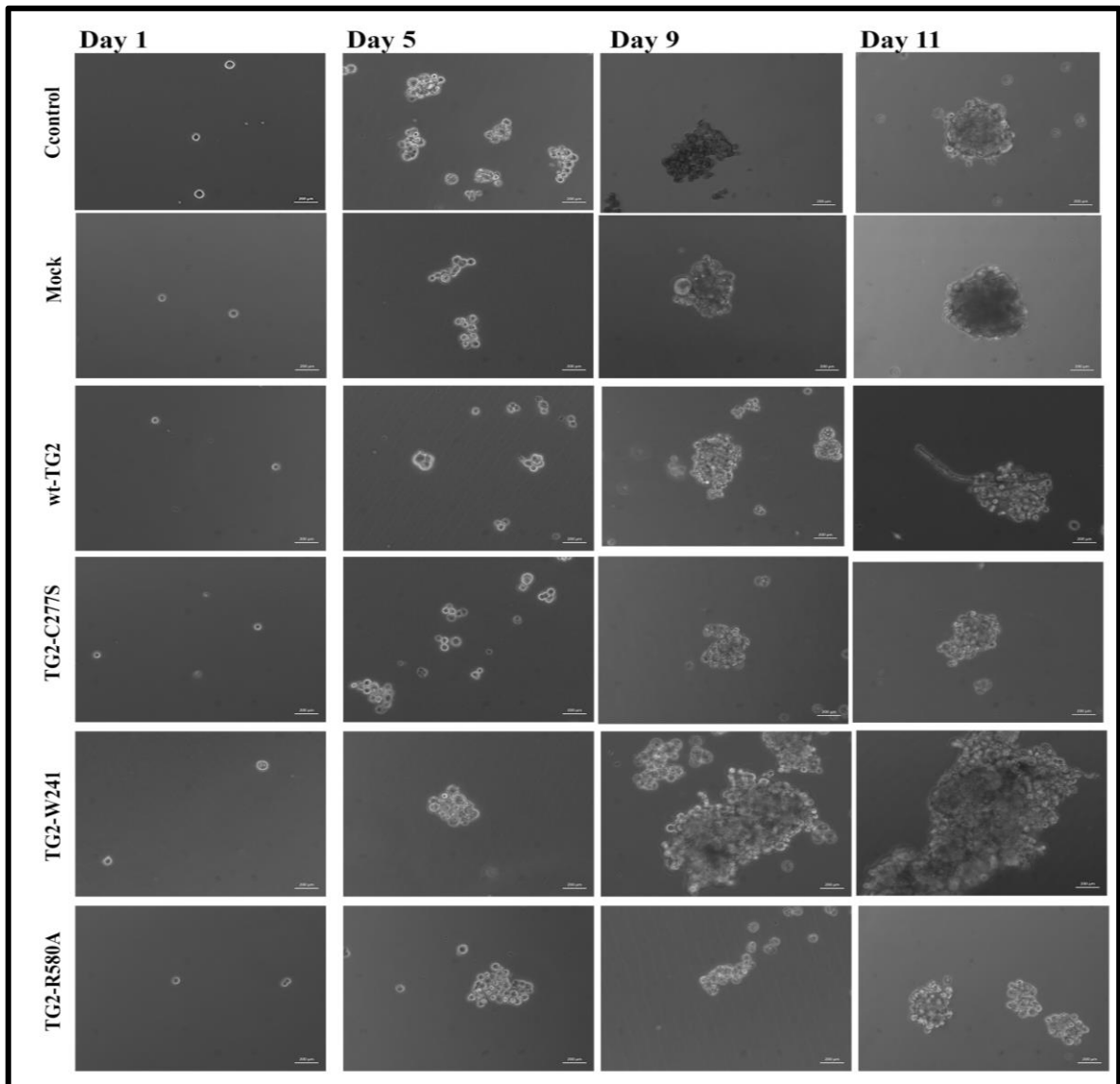


Figure 4.18. Representative images of the formed spheres by non-transduced parental and mock control and TG2-expressing mutant RenCa cells from the day 1-11. Three independent experiments were performed in triplicate. Images were captured under the light microscope with 20x magnification. Scale bars 200  $\mu\text{m}$

Similar to the first-generation spheroid assay, second-generation sub-spheroid assay was performed as described previously in Section 3.4.2. In agreement with the spheroid assay



results, similar results were obtained in sub-spheroid experiments such as parental and mock control cells were again possessed the low efficiency of forming spheres with the average diameter of 280  $\mu\text{m}$  on the 5<sup>th</sup> day and 700  $\mu\text{m}$  on the 11<sup>th</sup> day. wt-TG2 and TG2-W241A cells were showed the formation of reno-spheres with the average diameter of 290  $\mu\text{m}$  on the 5<sup>th</sup> day and were enlarged approximately to the 1580  $\mu\text{m}$  on the 11<sup>th</sup> day. TG2-R580A cells were exhibited the small sphere formation with the starting diameter of 170  $\mu\text{m}$  and at the end of the 11<sup>th</sup> day the average diameter was became 500  $\mu\text{m}$ . However, for the TG2-C277S cells the results were increased with an average diameter of 158  $\mu\text{m}$  on the 5<sup>th</sup> day and 520  $\mu\text{m}$  on the 11<sup>th</sup> day that shows that the ability to form reno-spheres led to a 1.5 fold increase for TG2-C277S cells.

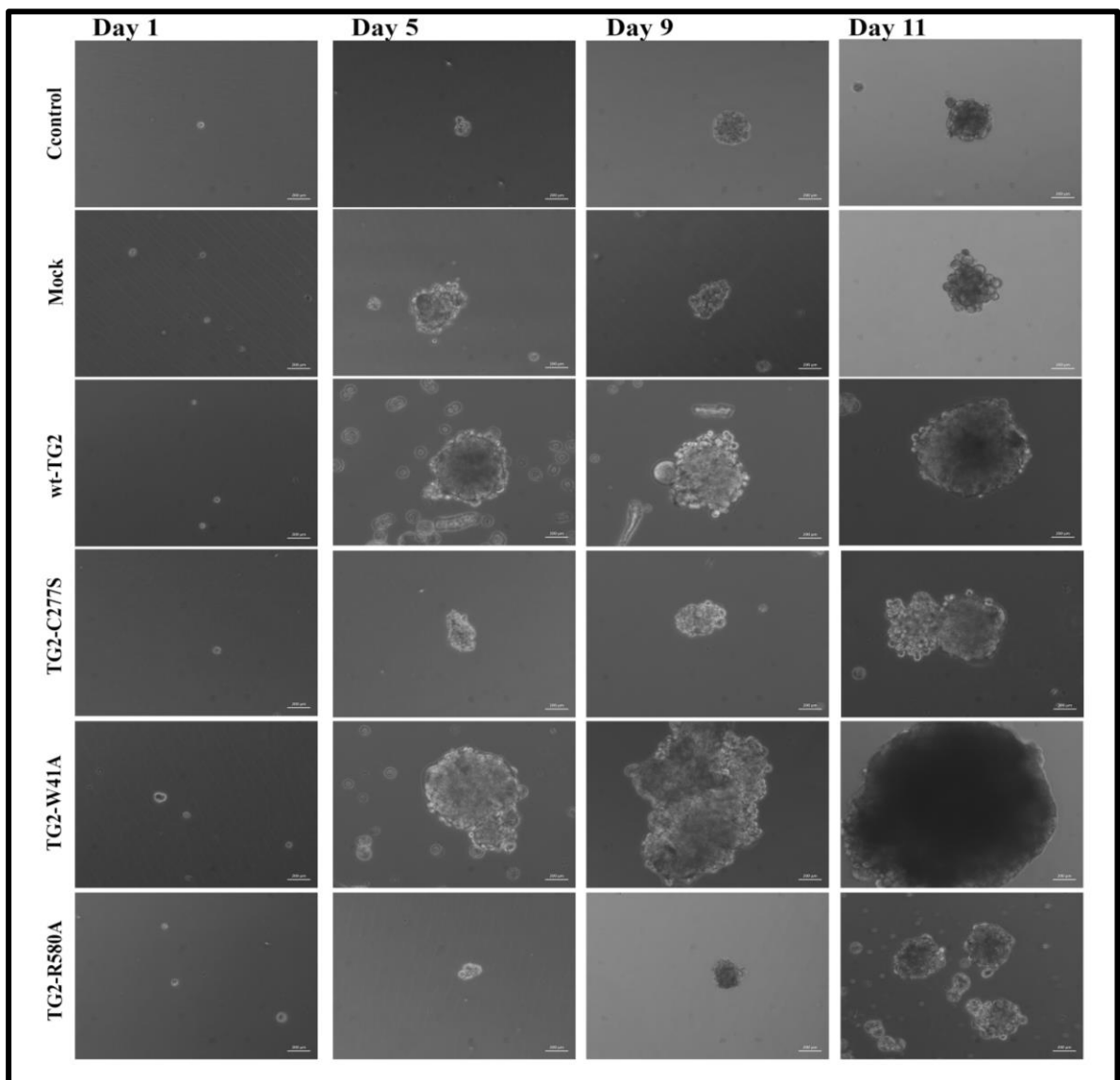


Figure 4.19. Representative images of the formed sub-spheres by non-transduced parental and mock control and TG2-expressing mutant RenCa cells from the day 1-11. Three independent experiments were performed in triplicate. Images were captured under the light microscope with 20x magnification. Scale bars 200  $\mu\text{m}$

Together with the results obtained from Figure 4.18. and Figure 4.19., it was indicated that the functional GTP-binding domain ability of TG2 is essential for stem cell characteristic and anchorage-independent self-renewal.

#### 4.6. ROLE OF GTP-BINDING ACTIVITY OF TG2 IN RCC CELL MIGRATION

During the transactivation of EMT adherent junctions are known to be disrupted and a process of switching was realized from cell to cell adhesion *E-cadherin* to *N-cadherin* together with the upregulated expression in *vimentin* levels. In order to understand the role of TG2 activity in cell mobility, the ability of TG2-expressing mutant RenCa cells was tested via the scattering assay in which, cells were observed to detach from the original colonies and spread to the near vicinity.



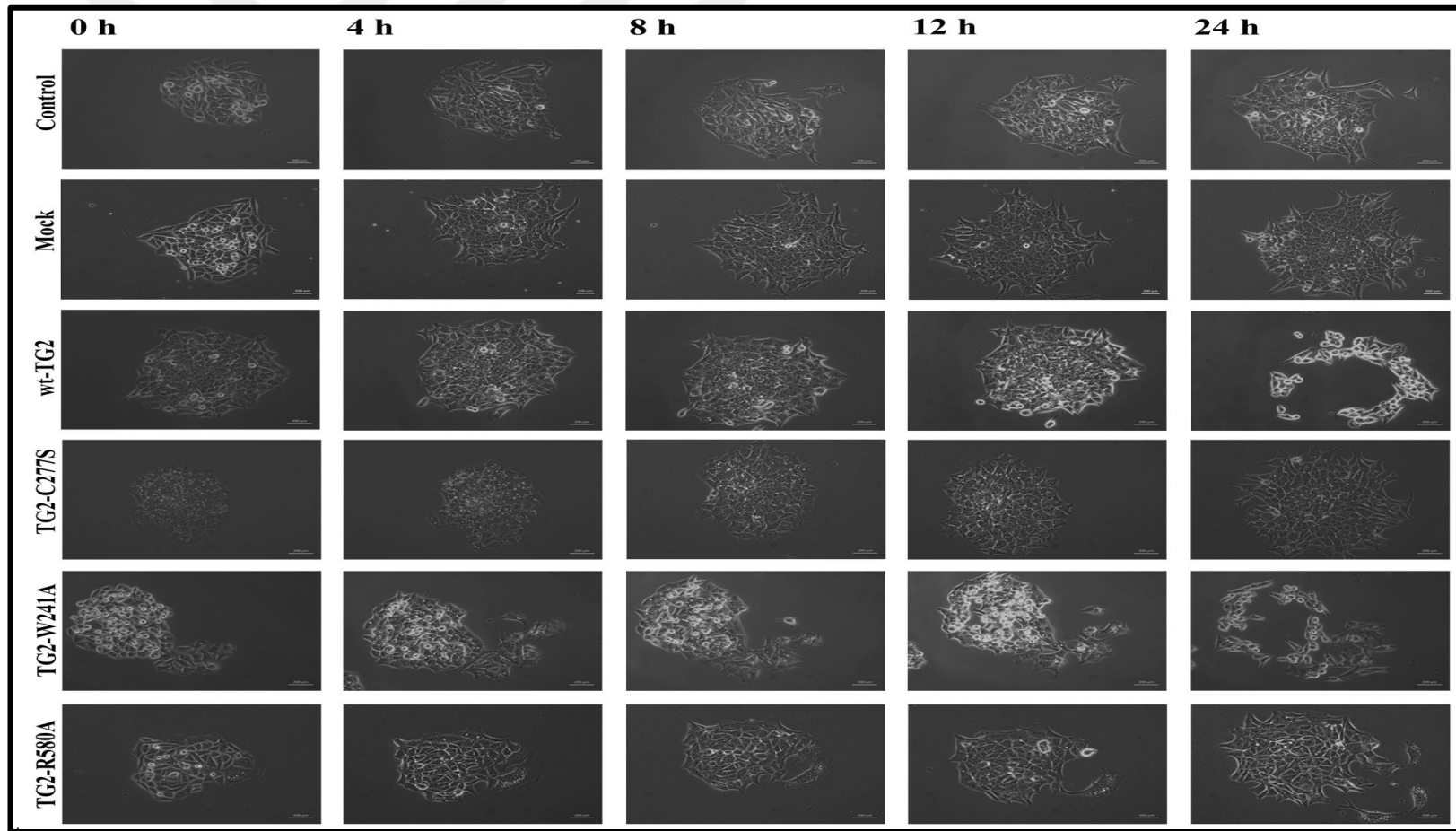


Figure 4.20. Cell motility potential of TG2-expressing transduced RenCa cells were monitored using scattering assay. Representative images were taken at 0-24 hours just after the colony formation was observed. Three independent experiments were performed. Scale bars 200  $\mu\text{m}$ .

Due to the analysis done and seen in Figure 4.21., the non-transduced parental and mock control together with TG2-C277S and TG2-R580A cells exhibited a very similar migration pattern with 45 per cent compact, 35 per cent loose and 20 per cent scattered colonies. While, wt-TG2 and TG2-W241A cells expressed 20 per cent less compact and 40 per cent more scattered colonies when compared to the control cells.

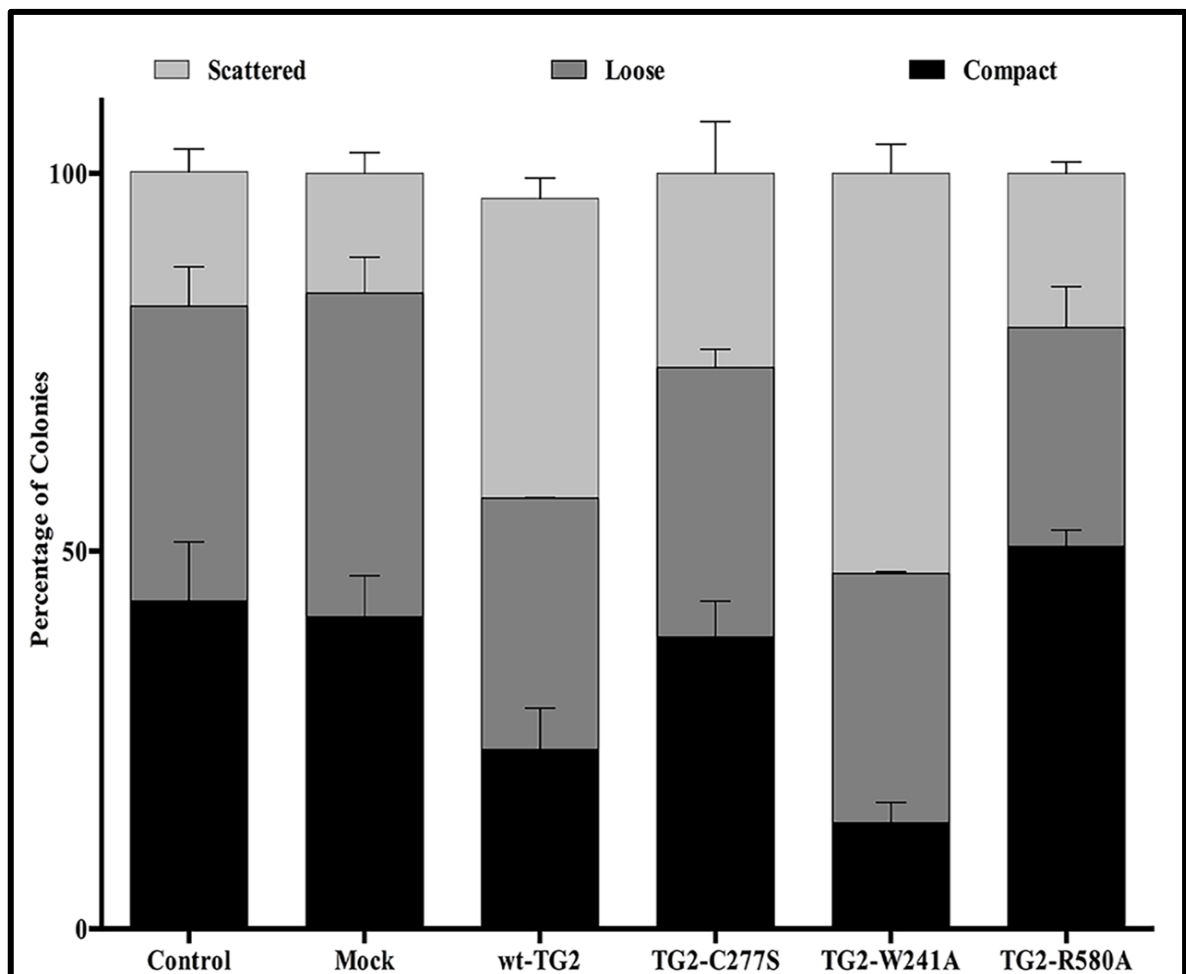


Figure 4.21. Graphic represents the colonies that were classified as compact, loose and scattered forms. Colony numbers were enounced as the percentages of control values listed for the non-transduced control RenCa cells.

Then, the mRNA expression levels of *E-* and *N-cadherins* were investigated and as it can be seen in Figure 4.22. wt-TG2, TG2-C277S, TG2-W241A and TG2-R580A constructed mutant cells showed 2-, 2-, 0.8- and 2.5 fold decreased in the *E-cadherin* levels compared to the non-transduced parental control RenCa cells, respectively. Whereas, wt-TG2, TG2-

C277S, TG2-W241A and TG2-R580A constructed mutant cells expressed 7-, 6.2-, 13- and 3.4 fold increased in *N-cadherin* mRNA levels, respectively.

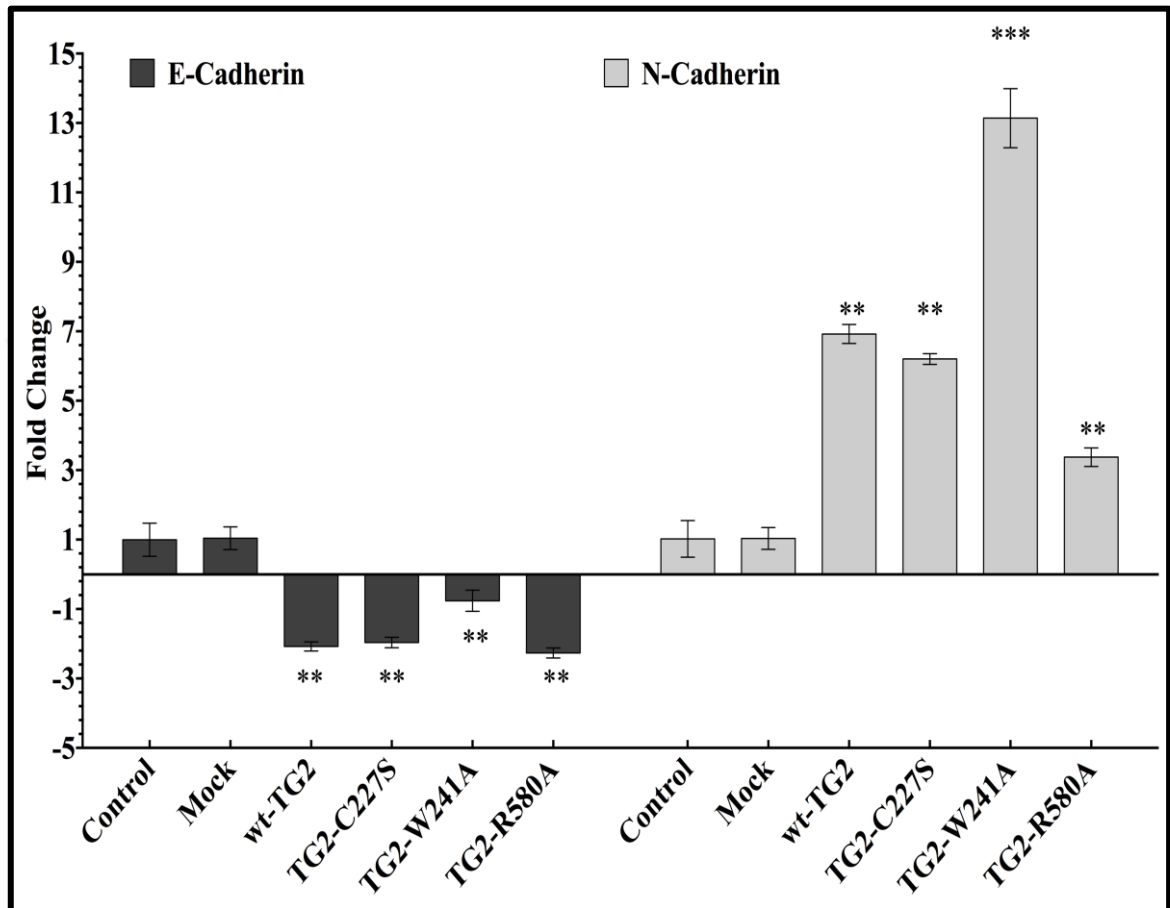


Figure 4.22. The mRNA level expression of cell-cell adhesion switching involving *E-* to *N-cadherin* was determined by RT-PCR analysis. 18 S mRNA was used for normalization.

(\*\*p- < 0.01 and \*\*\*p- < 0.001)

Similarly, the upregulated expression of *vimentin* associated with the pioneer preparation of cells to the migratory process. In Figure 4.23., it was seen that *vimentin* expression was upregulated by 1.8 fold in wt-TG2, 2.5 fold in TG2-C277S, 3.4 fold in TG2-W241A and 2.2 fold in TG2-R580A mutant cells when compared to the non-transduced parental and mock control RenCa cells.

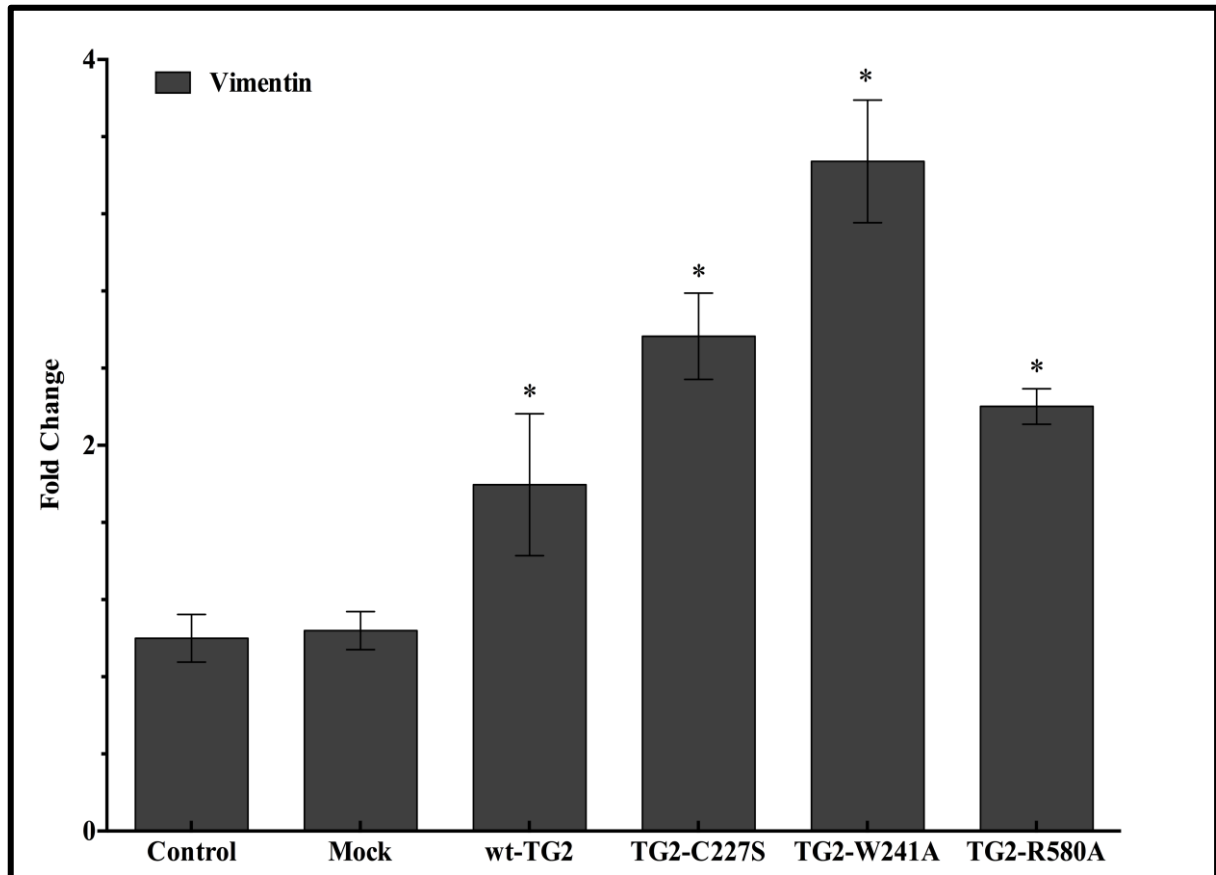


Figure 4.23. RT-PCR analysis of *vimentin* expression of transduced RenCa cells with TG2 constructs. 18 S mRNA was used for normalization. (\* $p < 0.05$ )

These results suggest that even though TG2 expression is sufficient to trigger the switch mechanism of cadherin along with the elevated expression of *vimentin* levels, GTP-binding activity is necessary to drive the cell-cell dissociation process including the migration of individual cells.

#### 4.7. ROLE OF GTP-BINDING ACTIVITY OF TG2 IN THE UPREGULATION OF MMP AND INVASIVENESS

Metastasis of primary tumors from original location to the distant sites is a multistep process in which the upregulation of matrix metalloproteinases (MMP) activities play an essential role in the invasion, intra- and extravasation, and metastatic colonization. For this purposes, the gelatinase and collagenase expression levels were detected in TG2-variant expressing RenCa cells using real-time PCR. Analysis of *MMP1a* mRNA levels showed

that expression levels was upregulated by 2 fold in all RenCa variants except for TG2-W241A which displayed a 14 fold increase in MMP1a expression in comparison to the parental RenCa cells (Figure 4.24A). When compared to the control cells, wt-TG2 and TG2-W241A cells exhibited 11 and 15 times higher levels of *MMP2* mRNA while only six fold increase in the expression levels of *MMP2* was detected for TG2-C277S and TG2-R580A cells (Figure 4.24.B). On the other hand, *MMP3* mRNA expression level was increased by 4.3 fold in wt-TG2, 2.6 fold in TG2-C277S, 6.4 fold in TG2-W241A and 1.6 fold in TG2-R580A mutant cells (Figure 4.24C). Only TG2-W241A mutant cells promoted a significant upregulation in *MMP9* mRNA expression levels in comparison to parental RenCa cells. Interestingly, stable expression of wt-TG2 cells resulted in an increase of 15 fold in the levels of *MMP13* mRNA, while the other TG2-expressing mutant cells showed an average of 6 fold increase in the expression of *MMP13* (Figure 4.24E).



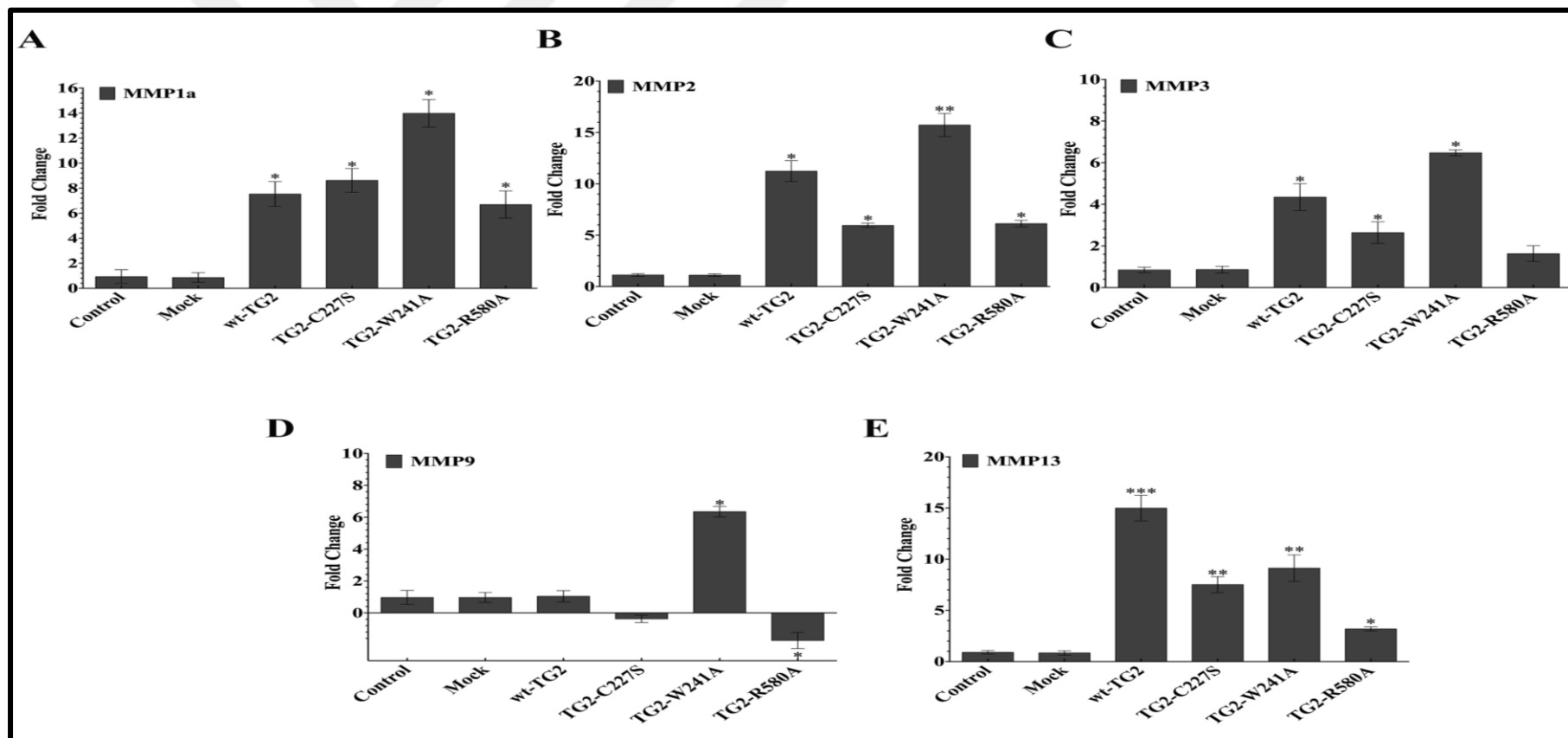


Figure 4.24. Real Time (RT-PCR) analysis indicating the changes in the mRNA expression levels of MMP in TG2-expressing RenCa cells. (a) *MMP1* (b) *MMP2* (c) *MMP3* (d) *MMP9* (e) *MMP13*, data values represent the average of three experiments independently (means  $\pm$  SD) normalized to 18 S mRNA, (\* $p$ - < 0.05, \*\* $p$ - < 0.01 and \*\*\* $p$ - < 0.001)

Given that the upregulation of MMP activity is a key factor in the regulation of the intra- and extravasation potential of cancer cells, invasive ability TG2-expressing mutant cells were determined via Matrigel transwell assay. As it was seen in Figure 4.25.A, TG2-W241A cells exhibited highest invasive phenotype when compared to other TG2 variants. In that, the number of invasive cells was 4 fold higher in TG2-W241A mutant cells (Figure 4.25.B).



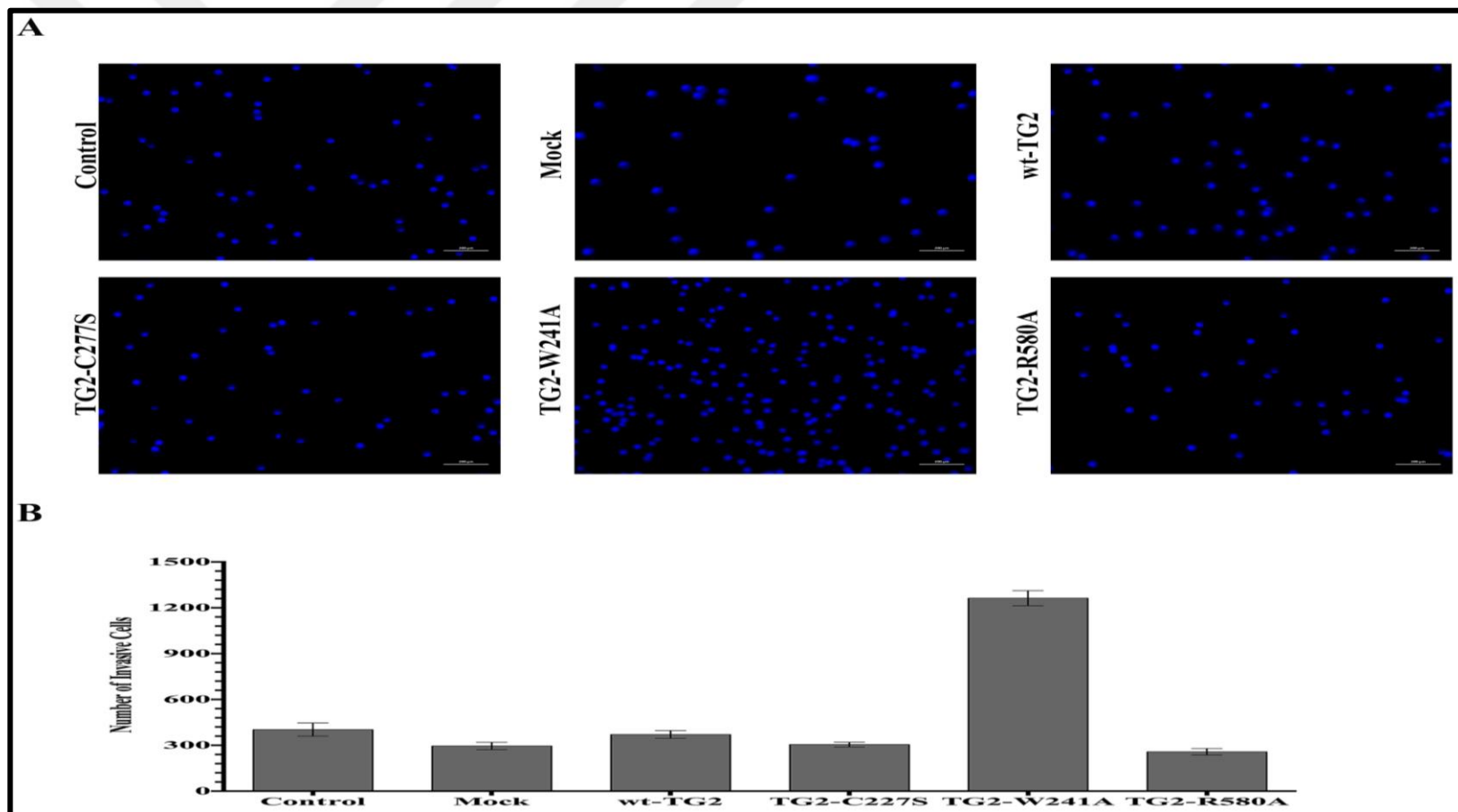


Figure 4.25. (a) Invasion potential was evaluated in parental and TG2-expressing mutant cells that were seeded on the upper chamber of Matrigel coated transwells. Following 24 hours of incubation, cells on the bottom of the transwell were stained with DAPI and 5 non-overlapping fields per samples were captured. (b) Cell number analysis was performed in Scion Image Analysis Program. Scale bars 200  $\mu$ m.

#### **4.8. GTP-BINDING ACTIVITY OF TG2 IS IMPORTANT IN ACQUIRED RESISTANCE FOR THE TYROSINE KINASE INHIBITORS SORAFENIB AND EVEROLIMUS**

Clinical and scientific studies suggested that TG2 overexpressed in many cancer cells was responsible for tumor cell invasiveness together with the drug resistance. In order to determine the role of either TG2 functional domains on TG2 mediated drug resistance, TG2-expressing mutant RenCa cells were treated with the two well-known RCC chemotherapeutic agents such as sorafenib and everolimus. Sorafenib is known to be a multi-targeted tyrosine kinase inhibitor that can block the VEGFR signaling pathway through the inhibition of VEGFR and its related receptors. On the other hand, a rapamycin derivative, everolimus is an inhibitor of mTORC1 pathway. The drug-resistance of TG2-expressing mutants was evaluated using WST-1, cell proliferation assay, which was performed following to the treatment with indicated chemotherapeutic agents in time- and dose-dependent manner (Figures 4.26-4.30).

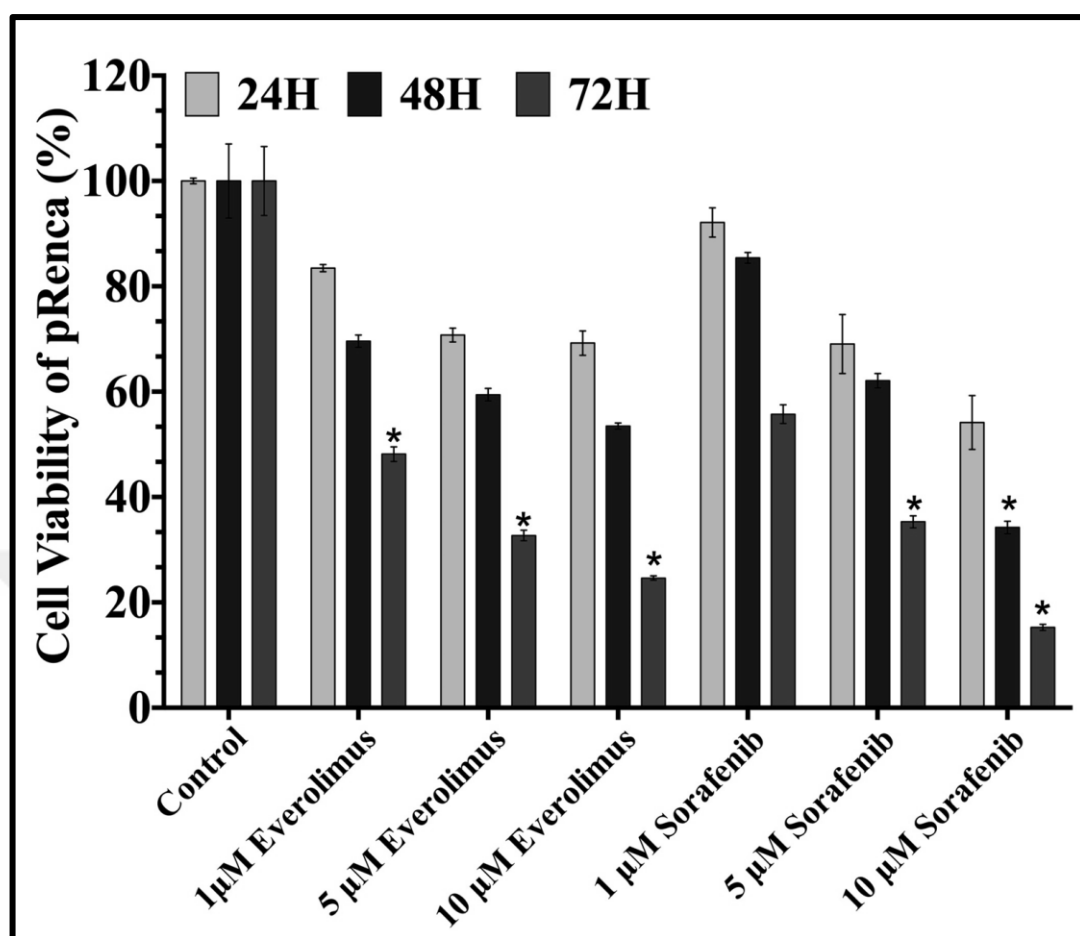


Figure 4.26. The role of TG2 functional domains on the drug resistance of non-transduced parental RenCa cells was determined with indicated concentrations of sorafenib and everolimus at 24, 48, and 72 hours using WST-1 assay. Representative data points shown are the mean percentage of viable cells from three independent experiments performed in triplicate. The cell viability of vehicle DMSO treated cells (Cnt) was considered as 100% for all time points. (\* $p < 0.05$ )

The cell viability result of non-transduced parental control cells was shown in Figure 4.26. A significant decrease in non-transduced parental RenCa cells was evident in response to both sorafenib and everolimus treatment in a dose and time-dependent manner. After 24 hours of incubation, it was observed that the viability of control cells was decrease to 17, 28 and 30 per cent in the presence of 1  $\mu$ M, 5  $\mu$ M, and 10 $\mu$ M everolimus, respectively. Additionally, the viability of parental control cells was further decreased to 71, 60 and 54 per cent on the second day and 49, 31, and 27 per cent on the third day of the everolimus

treatment. Similar to everolimus treatment, sorafenib treated control cells also expressed almost same survival profile except for the highest dose (10  $\mu$ M), as only 17 per cent cells were survived at the end of the third day.

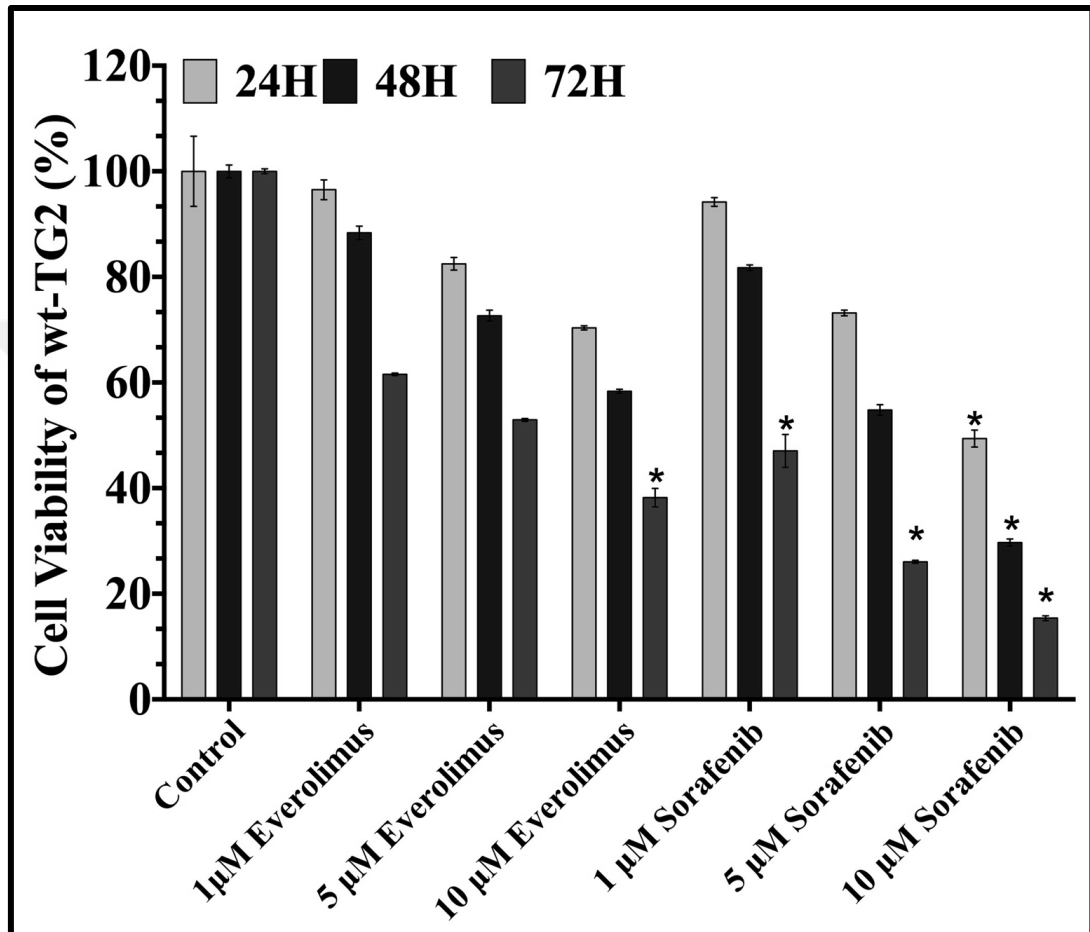


Figure 4.27. The role of TG2 functional domains on the drug resistance of wild type TG2 (wt-TG2) cells was determined with indicated concentrations of sorafenib and everolimus at 24, 48, and 72 hours using WST-1 assay. Representative data points shown are the mean percentage of viable cells from three independent experiments performed in triplicate. The cell viability of vehicle DMSO treated cells (Cnt) was considered as 100% for all time points. (\* $p$  < 0.05)

Figure 4.27. shows that the average viability recorded for RenCa cells expressing wt TG2. On the first day cell viability was 95, 88 and 60 per cent when the cells were treated with 1, 5, and 10  $\mu$ M sorafenib and everolimus. After 48 hours of incubation the average cell

viability in wt-TG2 cells was found to be 85, 60 and 45 per cent and at the end of the third day, the average cell viability of wt-TG2 cells was further decreased to 55, 40 and 23 per cent when compared to the non-transduced parental control cells.

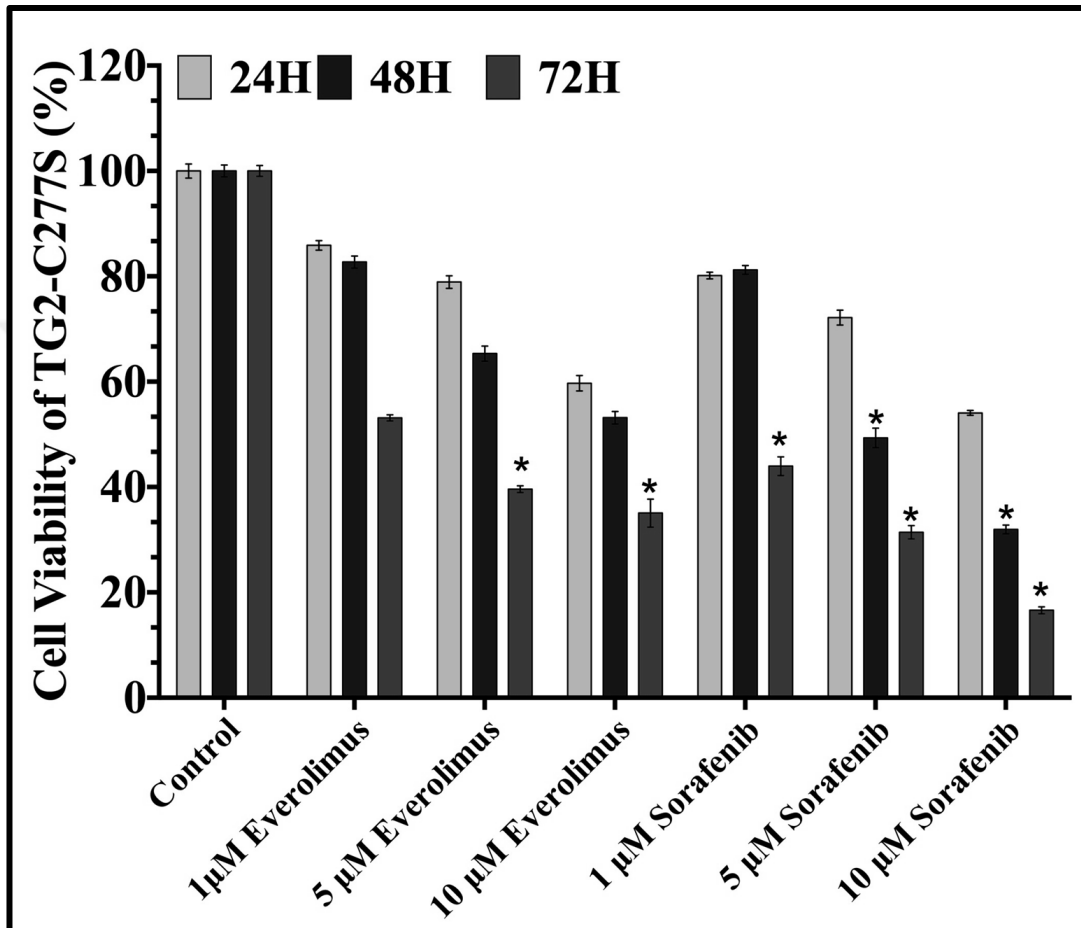


Figure 4.28. The role of TG2 functional domains on the drug resistance of transaminase null TG2-C277S cells was determined with indicated concentrations of sorafenib and everolimus at 24, 48, and 72 hours using WST-1 assay. Representative data points shown are the mean percentage of viable cells from three independent experiments performed in triplicate. The cell viability of vehicle DMSO treated cells (Cnt) was considered as 100% for all time points. (\* $p < 0.05$ )

As it can be seen in Figure 4.28. transamidating inactive mutant TG2-C277S cells was treated with 1, 5 and 10 µM sorafenib and everolimus for three days. The average cell viability of TG2-C277S after 24 hours of incubation with indicated drugs was 80, 75 and 55 per cent. The cell viability of the TG2-C277S cells was further dropped to an average of

80, 60 and 40 for 48 hours and 48, 35, 25 for 72 hours.

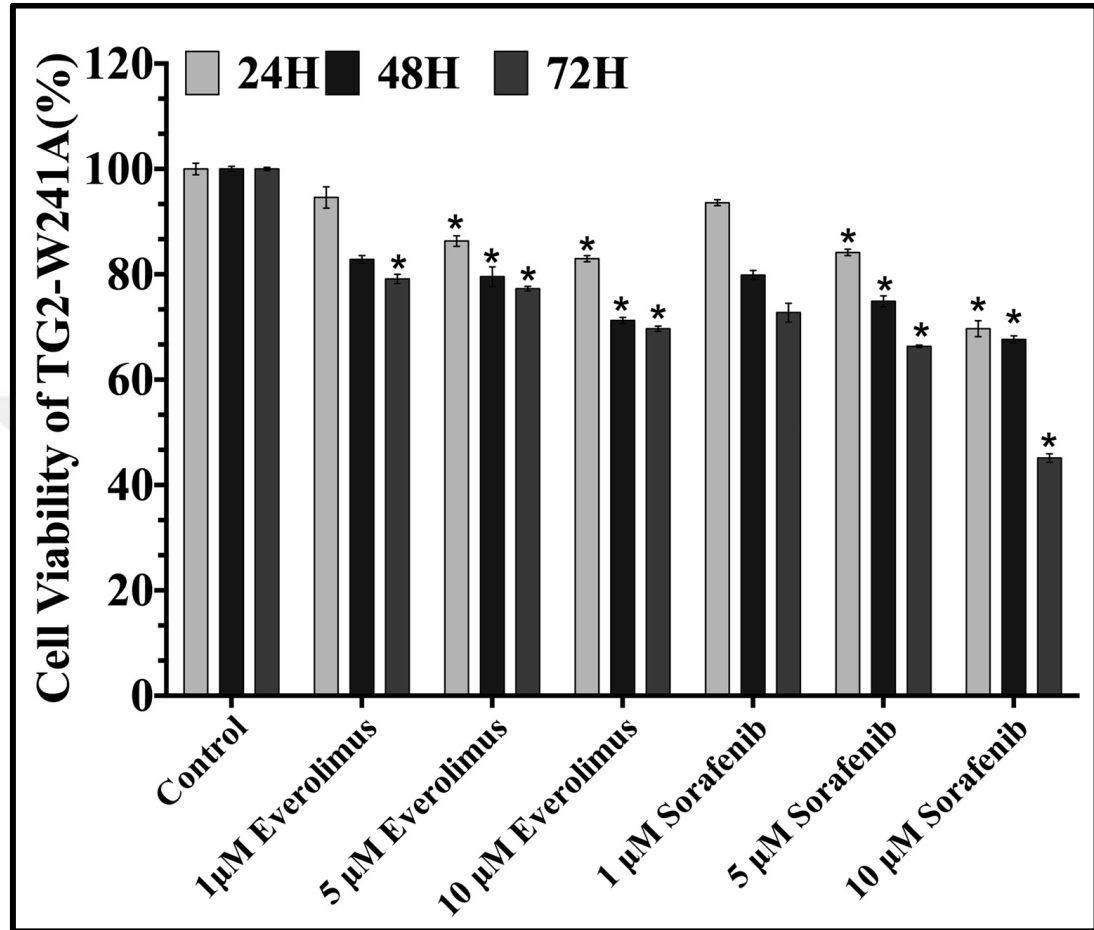


Figure 4.29. The role of TG2 functional domains on the drug resistance of transaminase inactive TG2-W241A cells was determined with indicated concentrations of sorafenib and everolimus at 24, 48, and 72 hours using WST-1 assay. Representative data points shown are the mean percentage of viable cells from three independent experiments performed in triplicate. The cell viability of vehicle DMSO treated cells (Cnt) was considered as 100% for all time points. (\* $p < 0.05$ )

The obtained result from the cell viability of TG2-expressing W241A, the transamidating defective but GTP-binding active, form of mutant RenCa cells was shown in Figure 4.29. Following 24 hours of treatment with sorafenib and everolimus and sorafenib, the average survival rates for TG2- W241A were detected as 94, 85 and 76 per cent. Interestingly, when the treatment duration was prolonged to 72 hours for 1, 5 and 10 µM sorafenib and



everolimus, the average decrease in cell viability was found to be 24, 27 and 34 per cent in contrast to the non-transduced parental control RenCa cells.

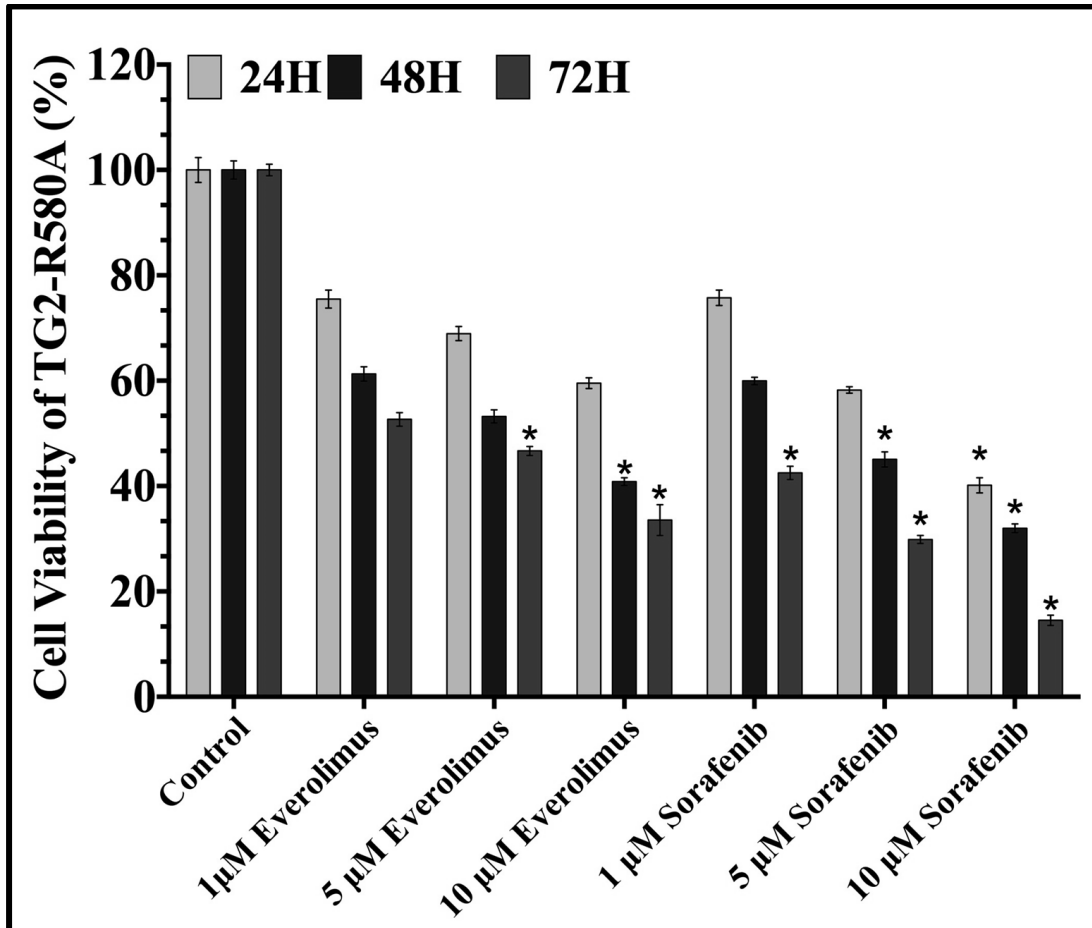


Figure 4.30. The role of TG2 functional domains on the drug resistance of GTP-binding null TG2-R580A cells was determined with indicated concentrations of sorafenib and everolimus at 24, 48, and 72 hours using WST-1 assay. Representative data points shown are the mean percentage of viable cells from three independent experiments performed in triplicate. The cell viability of vehicle DMSO treated cells (Cnt) was considered as 100% for all time points. (\*p- < 0.05)

According to Figure 4.30. the average decrease in the cell viability for the GTP-binding defective mutant TG2-R580A was determined as 25, 37 and 50 per cent for 24 hours of incubation, 40, 51 and 65 per cent for 48 hours of incubation and lastly 53, 62 and 76 per cent for 72 hours of incubation.

Together with the results obtained from Figure 4.26. - 4.28 and Figure 4.30., it was demonstrated that non-transduced parental control, wt-TG2, TG2-C277S and TG2-R580A expressing RenCa cells all had the similar cell viability pattern with a 15 per cent and 30 per cent survival against sorafenib and everolimus, respectively. However, Figure 4.29. shows that at least 3 and 2 fold increase in the cell survival was detected under the treatment of sorafenib and everolimus, respectively for the TG2-W241A cells. As a result, it was found that GTP-binding activity of TG2 is indispensable for TG2-induced drug resistance of renal adenocarcinoma cells.



## 5. DISCUSSION

RCC is one of the most common form of the kidney cancer which has been classified as highly vascular and resistant to radio- and chemo- therapies. Concomitantly, 25-30 per cent of patients have been already presented with the metastatic disease at the time of diagnosis [138]. According to recent studies the estimated worldwide incidence and mortality rates for RCC is rising with an approximate rate of two to three per cent per decade. mRCC is the most treatment-resistant malignancy among other RCCs with a poor outcome and survival chance [129, 130]. Additionally, the world population ages and the risk factors such as hypertension or obesity increase significantly from year to year, which in turn may lead to an increase in mRCC incidence rate. Therefore, novel therapies such as molecularly targeted therapies of mRCC have been under investigations in recent years [139]. One such molecular target was TG2 with a multifunctional ability to (i) posttranslationally modify proteins by catalyzing the  $\text{Ca}^{2+}$ -dependent transamidation or interchain glutamine and lysine cross-linking and (ii) to regulate GTPase mediating intracellular signalling through various G protein-coupled receptors [83-86]. However, the conformational switch between GTPase and transamidase functions has yet to be elucidated [140, 141].

Accumulating evidence suggested that TG2 might be involved in cancer progression or metastasis by regulating the tumor cell growth, cell survival, cell-ECM interaction and EMT process [113]. Hence, the downregulation of TG2 expression in tumor cells might be the answer and could have a promising potential in reversing the chemo- and drug resistance or metastasis. Moreover, it was shown that TG2 was involved in cell adhesion by forming a heterophilic complex with fibronectin, an essential ECM glycoprotein, which in turn was recognized by the syndecan-4, a heparin sulfate proteoglycan [93]. Due to the formation of this complex, a signaling cascade was triggered resulting in the enhancement of cellular adhesion and survival through the ITG $\beta$ 1 activation [78, 90-93]. A line of evidence linking ITG $\beta$ 1 upregulation with increased metastatic potential also suggested the involvement of TG2 in this process [57, 142]. On the basis of these findings, first study that investigated the role of TG2 in RCC metastasis showed that the simultaneous upregulation of TG2 with ITG $\beta$ 1 and SDC4 increased the risk of mRCC by 3 fold [129]. In follow up studies, it was found that RCC commonly shows marked increase in the expression of TG2 which was associated with a decrease in tumor necrosis in RCC

samples [129, 143-145]. However, the molecular mechanisms underlying this pro-metastatic act of TG2 is yet to be determined. In this respect, the aim of this thesis was to elucidate the relative contribution of the two-well characterized (transamidase and GTPase) activities of TG2 in promoting the oncogenic functions involving cell migration, invasion, EMT and cancer stemness of RCC with specific emphasis on TG2-NF $\kappa$ B axis.

Considering, the crucial interrelation between ITG $\beta$ 1 and TG2 in the tumor progression in epithelial cancers, several studies indicated that the TG2 overexpression together with ITG $\beta$ 1 led to invasiveness and exhibited more mesenchymal phenotype in tumor metastasis including multiple cancer types such as cervical squamous [79], breast [146], pancreatic [147], and colon cancer [148]. In contrast, our findings showed that TG2 overexpression in RenCa cells which exhibited advanced metastasis and invasiveness did not lead to any change in the expression levels of ITG $\beta$ 1 and SDC4 suggesting that TG2 induces metastatic phenotype in RenCa cells independent from its binding partners. Given the importance of ITG $\beta$ 1 as an EMT marker, the function of TG2 in EMT process became the center of recent studies in the last decade. Several studies showed that TG2 plays as the key modulator role in inducing EMT and enhancing the tumor metastasis through the activation of oncogenic signaling in multiple cancer types such as breast [23], ovarian [53, 149], epidermoid [150], pancreatic [147]. EMT was first described in 2005 and defined as a remarkable process, in which cell transitions from epithelial into the mesenchymal phenotype occurred making it possible for mesenchymal cells to become mobile and leave the epithelium and move through the extracellular matrix [95]. Later, it was showed that the EMT was also involved in the pathological states including organ fibrosis or more importantly in cancerogenesis [151]. The initiation of the molecular switch of the EMT program was associated with the changes in the expression of specific transcription factors such as *Zeb1/Zeb2*, *Twist1/Twist2* and *Snail1/Snail2*. [152]. These transcription factors act as repressors and recognize the E-box domains in the promoters of cell to cell adhesion receptors such as *E-cadherin*, *claudins* and *occludins*, hence their activation enhances the breakdown of intercellular junctional integrity and shift in cell receptor repertoire [153-155]. The first study that investigated the role of TG2 in EMT showed that TG2 induced a mesenchymal phenotype by repressing *E-cadherin* expression at the transcriptional level in ovarian cancer [156]. TG2 mediated *E-cadherin* loss at the transcriptional level was induced by upregulation of several transcriptional repressors including *Snail*. *Snail*

transcription factor was the one that firstly discovered as a transcription repressor that directly interacts with the *E-cadherin* promoter in order to repress expression of *E-cadherin* [99]. *Snail* was also responsible from the induction in the expression of the genes that were associated with a mesenchymal and invasive phenotype [154]. However, our findings showed that TG2 overexpression did not lead to a upregulation in the expression levels of *Snail* although a remarkable decrease in *E-cadherin* was recorded. This contradiction in the findings may be explained by lack of TGF $\beta$  signaling in RenCa cells [157, 158], as *Snail* mediated *E-cadherin* repression depends on TGF $\beta$  signaling [159, 160]. Functional cooperation between *Snail* and *Twist* transcription factors were highly important in inducing the expression of the *Zeb1* gene during EMT [161]. Accumulating evidence suggested that the loss of *E-cadherin* expression enhanced EMT program in mammary epithelial cells potentially through transcriptional factors such as *Zeb1/2* [162]. Recent findings showed that silenced TG2 in ovarian carcinoma resulted in the reduced mRNA expression levels of *Zeb1/2*, *Twist 1/2* [156]. In confirmation, Kumar *et al.* showed that TG2-deficient cells displayed a reversal process of EMT by gaining the expression of *E-cadherin* and losing the expression of EMT markers [146]. Further support the vital role of TG2 in EMT, Agnihotri *et al.* showed that TG2-expressing cells demonstrated a substantial elevation in the expression of *Zeb* and *Twist* transcription repressors [74]. In support of these findings, our results indicated an increase mRNA expression levels of *Zeb1/2* and *Twist 1/2* in overexpressed TG2 cells when compared to parental non-transduced RenCa cells.

To understand relative contribution of two-best studied functions (transamidase and GTPase) of TG2 in EMT, EMT marker analysis was performed in RenCa mutants. Kumar *et al.* and Eckert *et al.* showed that GTP-binding activity of TG2 was essential and required for the expression of transcriptional factors during EMT. In agreement, our findings also indicated that GTP-binding activity was required for the induction of the EMT process (Figure 4.12.- 4.14.) as the catalytically inactive TG2-W241A cells showed a significant upregulation in the expression of *Snail 1/2*, *Zeb1/2* and *Twist 1/2* while GTP-binding null TG2-R580A cells did not show a significant decrease in these EMT markers when compared to the parental control RenCa cells.

Since, the inhibition of NF- $\kappa$ B signaling prevented the process of EMT in epithelial cells, EMT markers associated with the increased NF- $\kappa$ B activity [163]. EMT process is tightly

controlled in the downstream of NF- $\kappa$ B signaling which was well known due to its involvement in the regulation of EMT together with drug resistance and metastasis processes in epithelial cells. Recent studies demonstrated that the aberrant expression of TG2 resulted in the constitutive activation of NF- $\kappa$ B pathway by inducing an increase in the p-I $\kappa$ B- $\alpha$  levels [164]. Mehta *et al.* demonstrated that GTP-binding function of TG2 was essential for NF- $\kappa$ B activation [137], in accordance our results also indicated that GTP-binding activity of TG2 was essential for the activation the NF- $\kappa$ B signaling by significant decreasing the basal protein expression level of I $\kappa$ B- $\alpha$  (Figure 4.10-11). A parallel increase in the amount of p-I $\kappa$ B- $\alpha$  levels for TG2-W241A cells indicated that the TG2-mediated the activation of NF- $\kappa$ B was through the canonical pathway. These results were however contradicted with the findings of Yakubov *et al.* which showed that TG2 activated NF- $\kappa$ B signaling through a non-canonical pathway in order to promote metastasis in ovarian cancer [114]. Similar to our findings, Eckert *et al.* demonstrated that transamidating activity of TG2 was not found to be as effective as GTP-binding function of TG2 for the activation of NF- $\kappa$ B.

Activation of NF- $\kappa$ B results in the cadherin switch from *E-cadherin* to *N-cadherin*, which is essential in the initial process of cancer cell dispersal from the main tumor body [165]. Consistent with the findings from Kumar *et al.*, our results that were presented in regard to the EMT transactivation and adherent junctions disruption via a switching process from *E-cadherin* to *N-cadherin* together with the elevated expression in *vimentin* levels were resulted in the induction of the invasiveness and metastatic phenotype in RCC (Figure 4.22&4.23.).

Studies showing that expression of TG2 with intact GTP-binding activity was necessary for inducing the cell migration and EMT suggested a possible role for TG2 in the regulation of invasiveness through extensive remodeling of the ECM via MMPs [137, 105-107]. In addition, NF- $\kappa$ B was also shown to be responsible for the activation of MMPs, which are basically responsible for the degradation of ECM in order to get rid of the physical barriers for the cancer cells to facilitate escape from the primary tumor site and hence invasion [166]. Recent evidence showed that the over-expression of TG2 led to an elevation in the expression level of MMPs including *MMP1* [135], *MMP2*, *MMP3* [137] and *MMP9* [167] in epidermoid and breast cancers [168]. Kumar *et al.* investigated which particular function of TG2 was involved in the activation of MMPs in breast cancer

[137]. Their results showed that GTP-binding activity of TG2 enzyme was required in promoting the invasiveness by upregulating the expressions of *MMP2* and *MMP3* while, GTP-binding-deficient form resulted in the decreased expression of the same MMP levels. In this context, our findings also showed that catalytically inactive TG2-W241A cells exhibited a significant increase in the levels of MMP expression when compared to the parental control RenCa cells. Concomitantly, high levels of TG2 expression found in several tumors [23] and considered as a potential negative prognostic marker could also be associated with RCC.

Recent studies indicated that the tumor cells that elevates EMT markers and MMP activation also displayed an enhanced migratory potential [169], MMPs showed to be crucial players in the invasion phase of the primary tumors metastasis by degrading a range of ECM proteins in order to allow cell migration and invasion [82]. In addition, recent study showed that TG2 was involved in the cell migration and invasion processes. The loss of TG2 expression was associated with a reduction in the cell mobility together with the invasiveness in skin cancer cells [170]. Furthermore, Eckert *et al.* investigated which functional activity of TG2 was particularly involved in the induction of cell migration and invasion. Their findings suggested that GTPase related activity of TG2 was required for migration and invasion processes [136]. In this context, in order to understand the role of TG2 functional activities in the cell motility and invasion in RCC, the ability of TG2-expressing mutant RenCa cells to detach from the main colonies and spread to distant vicinity was monitored using scatter and transwell assays. Consistent with the results found by Eckert *et al.*, our findings also indicated that over-expressed TG2 (wt-TG2) and catalytically inactive (TG2-W241A) RenCa cells formed higher number of scattered colonies than the control cells while only, catalytically inactive yet GTP-binding TG2-W241A cells showed an enhanced invasive phenotype when compared to the both control and the other TG2-expressing mutant RenCa cells. These results further supported that GTP-binding activity was essential to induce cell migration and invasion in RCC.

TG2 expression in cancer cells has been linked with the acquisition of drug resistance and metastasis [171]. Therefore several studies reported that the commonly used TG2 enzymatic inhibitors and the knockdown of the TG2 protein might reverse the drug resistance and increased the cancer sensibility to stress and drug-induced apoptosis [59, 63-

65, 68]. Even though the exact molecular mechanism as to how TG2 contributes to the malignant state and drug resistance remains to be determined, it was suggested that the activation of survival pathways and the inhibition of apoptosis could be involved [53, 62, 68, 70, 172]. Boroughs *et al.* showed that TG2 was involved in the activation of canonical PI3K/mTORC1/p70 S6K pathway which was responsible for cancer cells to survive in the face of the apoptotic stimulus such as the treatment with the chemotherapeutic agents [122]. In confirmation with the current knowledge in hand about the role of TG2 in drug resistance, work presented in this thesis indicated that the absence of the GTP-binding activity of TG2 makes the cells more sensitive to the drug treatment. In other words, in the presence of active functional TG2 GTP-binding domain, transamidating inactive cells displayed a more resistant phenotype and exhibited a significant increase in the cell viability when compared to the parental control cells.

In summary, together with the findings presented in this thesis, it was strongly suggested that the GTP-binding activity of TG2 in RCC was essential to acquire CSC ability and to induce NF- $\kappa$ B activation and EMT promoting cell migration, invasiveness and drug resistance. In the context of developing molecularly targeted therapies against RCC, TG2 and its functional site domains are more likely to be a promising target. Development of GTPase specific TG2 inhibitor to intervene with the TG2-GTPase induced metastasis could serve as a novel therapeutic approach for the treatment of advanced RCC.



## 6. CONCLUSION AND FUTURE PERSPECTIVE

Thus far, multifarious studies proved that ectopic expression of TG2 is involved in multiple tumoral process including EMT, migration, invasion, metastasis and drug-resistance. However, this is the first study that mainly focused on the relative contribution of the two well-defined activity of TG2 (transamidating and GTP-binding) in metastatic RCC development.

Hereby, it was shown that the expression of catalytically inactive transaminase-deficient form TG2-W241A cells were able to induce NF- $\kappa$ B-mediated EMT process including cancer stemness, invasiveness and drug-resistance in the mouse RCC cell line RenCa. Whereas, the expression of GTP-binding null form TG2-R580A and transaminase-inactive form with a low GTP-binding affinity TG2-C277S cells muddled to lead these processes. In conclusion, results that were presented in this thesis suggested that GTP-binding function of TG2 was essential and more importantly indispensable when compared to the transamidation activity in RCC in order to induce cancer progression, migration, invasion and drug-resistance. Based on these findings, it can be said that TG2 could be assigned as a novel therapeutic agent in the treatment of mRCC and together with the development of GTP-binding domain specific inhibitors in order to avoid metastatic tumor progression in RCC.

For further studies, it is momentous to reveal the binding partner of the GTP-binding active mutant TG2-W241A while entering through the cell membrane as it might be involved different mechanism or it might be bind to the different proteins in which metastatic potential, invasiveness, drug-resistance or cancer stem cell characteristic would preserved. In such cases one of the possible mediator is thought to be the PDGF and by creating PDGF-related TG2-expressing mutant RenCa cells by transducing the TG2-W241A a detail study could be performed in the aim of enlightening the actual mediated partner of the TG2-W241A through the EMT process. Additionally, in order to further investigate the protein interactions, proteomic analysis could be done.

## REFERENCES

1. Rizzo DC. Urinary Systems. *Fundamentals of Anatomy and Physiology*: Cengage Learning; 2015. p. 433-40.
2. Karl Skorecki GC, Philip Marsden, Maarten Taal, Alan Yu. *Brenner & Receptor's The Kidney*. 10 ed: Elsevier; 2016.
3. Rini BI, Campbell SC, Escudier B. Renal cell carcinoma. *Lancet*. 2009;373(9669):1119-32.
4. Silverthorn DU. Restoring physiology to the undergraduate biology curriculum: a call for action. *Adv Physiol Educ*. 2003;27(1-4):91-6.
5. Sobol Jennifer ZD, Ogilvie Islah. US National Library of Medicine 2015 [Available from: <https://medlineplus.gov/ency/article/003005.html>].
6. Khanna M, Chelladurai B, Gavini A, Li L, Shao M, Courtney D, et al. Targeting ovarian tumor cell adhesion mediated by tissue transglutaminase. *Mol Cancer Ther*. 2011;10(4):626-36.
7. Lopez-Beltran A, Scarpelli M, Montironi R, Kirkali Z. 2004 WHO classification of the renal tumors of the adults. *Eur Urol*. 2006;49(5):798-805.
8. Lopez-Beltran A, Carrasco JC, Cheng L, Scarpelli M, Kirkali Z, Montironi R. 2009 update on the classification of renal epithelial tumors in adults. *Int J Urol*. 2009;16(5):432-43.
9. van Zijl F, Krupitza G, Mikulits W. Initial steps of metastasis: cell invasion and endothelial transmigration. *Mutat Res*. 2011;728(1-2):23-34.
10. Ozturk H. Prognostic features of renal sarcomas (Review). *Oncol Lett*. 2015;9(3):1034-8.

11. Valery JR, Tan W, Cortese C. Renal leiomyosarcoma: a diagnostic challenge. *Case Rep Oncol Med*. 2013;2013:459282.
12. Fujii Y, Ajima J, Oka K, Tosaka A, Takehara Y. Benign renal tumors detected among healthy adults by abdominal ultrasonography. *Eur Urol*. 1995;27(2):124-7.
13. Di Matteo G, Maturo A, Marzullo A, Peparini N, Wedard BM, Zeri KP, et al. Giant abdominopelvic epithelioid angiomyolipoma associated with tuberous sclerosis: report of a case. *Surg Today*. 1999;29(11):1183-8.
14. Licht MR. Renal adenoma and oncocytoma. *Semin Urol Oncol*. 1995;13(4):262-6.
15. Sanchez-Martin, M. F, Millan, Rodriguez, Urdaneta-Pignalosa G, Rubio-Briones J, et al. Small Renal Masses: Incidental Diagnosis, Clinical Symptoms, and Prognostic Factors. *Advances in Urology*. 2008;2008.
16. Jemal A, Siegel R, Xu J, Ward E. Cancer statistics, 2010. *CA Cancer J Clin*. 2010;60(5):277-300.
17. Chae EJ, Kim JK, Kim SH, Bae SJ, Cho KS. Renal cell carcinoma: analysis of postoperative recurrence patterns. *Radiology*. 2005;234(1):189-96.
18. Tun HW, Marlow LA, von Roemeling CA, Cooper SJ, Kreinest P, Wu K, et al. Pathway signature and cellular differentiation in clear cell renal cell carcinoma. *PLoS One*. 2010;5(5):e10696.
19. Motzer RJ, Bander NH, Nanus DM. Renal-cell carcinoma. *N Engl J Med*. 1996;335(12):865-75.
20. Leibovich BC, Blute ML, Chevillie JC, Lohse CM, Frank I, Kwon ED, et al. Prediction of progression after radical nephrectomy for patients with clear cell renal cell carcinoma: a stratification tool for prospective clinical trials. *Cancer*. 2003;97(7):1663-71.

21. Reuter VE, Tickoo SK. Differential diagnosis of renal tumours with clear cell histology. *Pathology*. 2010;42(4):374-83.
22. Gnarr JR, Tory K, Weng Y, Schmidt L, Wei MH, Li H, et al. Mutations of the VHL tumour suppressor gene in renal carcinoma. *Nat Genet*. 1994;7(1):85-90.
23. Huang C, Park CC, Hilsenbeck SG, Ward R, Rimawi MF, Wang Y, et al.  $\beta$ 1 integrin mediates an alternative survival pathway in breast cancer cells resistant to lapatinib. *Breast Cancer Res*. 2011;13(4):R84.
24. Lalwani N, Prasad SR, Vikram R, Katabathina V, Shanbhogue A, Restrepo C. Pediatric and adult primary sarcomas of the kidney: a cross-sectional imaging review. *Acta Radiol*. 2011;52(4):448-57.
25. Kamura T, Sato S, Iwai K, Czyzyk-Krzeska M, Conaway RC, Conaway JW. Activation of HIF1 $\alpha$  ubiquitination by a reconstituted von Hippel-Lindau (VHL) tumor suppressor complex. *Proc Natl Acad Sci U S A*. 2000;97(19):10430-5.
26. Kaelin WG, Jr. The von hippel-lindau tumor suppressor protein: an update. *Methods Enzymol*. 2007;435:371-83.
27. Krause DS, Van Etten RA. Tyrosine kinases as targets for cancer therapy. *N Engl J Med*. 2005;353(2):172-87.
28. Hudson CC, Liu M, Chiang GG, Otterness DM, Loomis DC, Kaper F, et al. Regulation of hypoxia-inducible factor 1 $\alpha$  expression and function by the mammalian target of rapamycin. *Mol Cell Biol*. 2002;22(20):7004-14.
29. Krieg M, Haas R, Brauch H, Acker T, Flamme I, Plate KH. Up-regulation of hypoxia-inducible factors HIF-1 $\alpha$  and HIF-2 $\alpha$  under normoxic conditions in renal carcinoma cells by von Hippel-Lindau tumor suppressor gene loss of function. *Oncogene*. 2000;19(48):5435-43.

30. Yang H, Kaelin WG, Jr. Molecular pathogenesis of the von Hippel-Lindau hereditary cancer syndrome: implications for oxygen sensing. *Cell growth & differentiation : the molecular biology journal of the American Association for Cancer Research*. 2001;12(9):447-55.
31. Di Cristofano A, Pandolfi PP. The multiple roles of PTEN in tumor suppression. *Cell*. 2000;100(4):387-90.
32. Zundel W, Schindler C, Haas-Kogan D, Koong A, Kaper F, Chen E, et al. Loss of PTEN facilitates HIF-1-mediated gene expression. *Genes & development*. 2000;14(4):391-6.
33. Kovacs G. Molecular differential pathology of renal cell tumours. *Histopathology*. 1993;22(1):1-8.
34. Kovacs G. Molecular cytogenetics of renal cell tumors. *Adv Cancer Res*. 1993;62:89-124.
35. Schmidt L, Duh FM, Chen F, Kishida T, Glenn G, Choyke P, et al. Germline and somatic mutations in the tyrosine kinase domain of the MET proto-oncogene in papillary renal carcinomas. *Nat Genet*. 1997;16(1):68-73.
36. Toro JR, Nickerson ML, Wei MH, Warren MB, Glenn GM, Turner ML, et al. Mutations in the fumarate hydratase gene cause hereditary leiomyomatosis and renal cell cancer in families in North America. *American journal of human genetics*. 2003;73(1):95-106.
37. Furge KA, Chen J, Koeman J, Swiatek P, Dykema K, Lucin K, et al. Detection of DNA copy number changes and oncogenic signaling abnormalities from gene expression data reveals MYC activation in high-grade papillary renal cell carcinoma. *Cancer Res*. 2007;67(7):3171-6.

38. Schoenberg M, Cairns P, Brooks JD, Marshall FF, Epstein JI, Isaacs WB, et al. Frequent loss of chromosome arms 8p and 13q in collecting duct carcinoma (CDC) of the kidney. *Genes Chromosomes Cancer*. 1995;12(1):76-80.
39. Martignoni G, Pea M, Gobbo S, Brunelli M, Bonetti F, Segala D, et al. Cathepsin-K immunoreactivity distinguishes MiTF/TFE family renal translocation carcinomas from other renal carcinomas. *Mod Pathol*. 2009;22(8):1016-22.
40. Moch H, Humphrey PA, Ulbright TM, Reuter VE. Chapter 3 Tumours of the prostate. *WHO Classification of Tumours of the urinary system and male genital organs*. Lyon: IARC; 2016.
41. Moch H, Humphrey PA, Ulbright TM, Reuter VE. Chapter 2 Tumours of the urinary tract. *WHO Classification of Tumours of the Urinary system and male genital organs*. Lyon: IARC; 2016.
42. Moch H, Humphrey PA, Ulbright TM, Reuter VE. Chapter 1 Tumours of the kidney. *WHO Classification of Tumours of the urinary system and male genital organs Volume 4th Edition*. Lyon: IARC; 2016.
43. Moch H, Humphrey PA, Ulbright TM, Reuter VE. Chapter 4 Tumours of the testis and paratesticular tissue. *Who Classification of tumours of the urinary system and Male genital organs*. Lyon: IARC; 2016.
44. Moch H, Humphrey PA, Ulbright TM, Reuter VE. Chapter 5 Tumours of the penis. *WHO Classification of tumours of the urinary system and male genital organs*. Lyon: IARC; 2016.
45. Qayyum T, McArdle P, Orange C, Seywright M, Horgan P, Oades G, et al. Reclassification of the Fuhrman grading system in renal cell carcinoma-does it make a difference? *SpringerPlus*. 2013;2:378.

46. Athanazio DA, Trpkov K. What is new in Genitourinary Pathology? Recent developments and highlights of the new 2016 World Health Organization classification of tumors of the urinary system and male genital organs. *Applied Cancer Research*. 2016;36(1):1.
47. Cohen HT, McGovern FJ. Renal-cell carcinoma. *The New England journal of medicine*. 2005;353(23):2477-90.
48. Brugarolas J. Renal-cell carcinoma--molecular pathways and therapies. *N Engl J Med*. 2007;356(2):185-7.
49. Cheng L, Williamson SR, Zhang S, Maclennan GT, Montironi R, Lopez-Beltran A. Understanding the molecular genetics of renal cell neoplasia: implications for diagnosis, prognosis and therapy. *Expert Rev Anticancer Ther*. 2010;10(6):843-64.
50. Eckert RL, Kaartinen MT, Nurminskaya M, Belkin AM, Colak G, Johnson GV, et al. Transglutaminase regulation of cell function. *Physiol Rev*. 2014;94(2):383-417.
51. Sarkar NK, Clarke DD, Waelsch H. An enzymically catalyzed incorporation of amines into proteins. *Biochimica et biophysica acta*. 1957;25(2):451-2.
52. Satchwell TJ, Shoemark DK, Sessions RB, Toye AM. Protein 4.2: a complex linker. *Blood cells, molecules & diseases*. 2009;42(3):201-10.
53. Mangala LS, Fok JY, Zorrilla-Calancha IR, Verma A, Mehta K. Tissue transglutaminase expression promotes cell attachment, invasion and survival in breast cancer cells. *Oncogene*. 2006;26(17):2459-70.
54. Kang SK, Lee JY, Chung TW, Kim CH. Overexpression of transglutaminase 2 accelerates the erythroid differentiation of human chronic myelogenous leukemia K562 cell line through PI3K/Akt signaling pathway. *FEBS letters*. 2004;577(3):361-6.

55. Chen SH, Lin CY, Lee LT, Chang GD, Lee PP, Hung CC, et al. Up-regulation of fibronectin and tissue transglutaminase promotes cell invasion involving increased association with integrin and MMP expression in A431 cells. *Anticancer research*. 2010;30(10):4177-86.
56. Lorand L, Graham RM. Transglutaminases: crosslinking enzymes with pleiotropic functions. *Nat Rev Mol Cell Biol*. 2003;4(2):140-56.
57. Mehta K. Mammalian transglutaminases: a family portrait. *Prog Exp Tumor Res*. 2005;38:1-18.
58. Thiery JP. Epithelial-mesenchymal transitions in tumour progression. *Nat Rev Cancer*. 2002;2(6):442-54.
59. Liu S, Cerione RA, Clardy J. Structural basis for the guanine nucleotide-binding activity of tissue transglutaminase and its regulation of transamidation activity. *Proceedings of the National Academy of Sciences of the United States of America*. 2002;99(5):2743-7.
60. Pinkas DM, Strop P, Brunger AT, Khosla C. Transglutaminase 2 undergoes a large conformational change upon activation. *PLoS biology*. 2007;5(12):e327.
61. Bergamini CM. Effects of ligands on the stability of tissue transglutaminase: studies in vitro suggest possible modulation by ligands of protein turn-over in vivo. *Amino acids*. 2007;33(3):415-21.
62. Mehta K. Prognostic Significance of Tissue Transglutaminase in Drug Resistant and Metastatic Breast Cancer. *Clin Cancer Res*. 2004;10:8068-76.
63. Sarang Z, Toth B, Balajthy Z, Koroskenyi K, Garabuczi E, Fesus L, et al. Some lessons from the tissue transglutaminase knockout mouse. *Amino acids*. 2009;36(4):625-31.



64. Huang L, Xu AM, Liu W. Transglutaminase 2 in cancer. *Am J Cancer Res.* 2015;5(9):2756-76.
65. Huang JC, Basu SK, Zhao X, Chien S, Fang M, Oehler VG, et al. Mesenchymal stromal cells derived from acute myeloid leukemia bone marrow exhibit aberrant cytogenetics and cytokine elaboration. *Blood Cancer J.* 2015;5:e302.
66. Jang GY, Jeon JH, Cho SY, Shin DM, Kim CW, Jeong EM, et al. Transglutaminase 2 suppresses apoptosis by modulating caspase 3 and NF-kappaB activity in hypoxic tumor cells. *Oncogene.* 2010;29(3):356-67.
67. Mangala LS, Fok JY, Zorrilla-Calancha IR, Verma A, Mehta K. Tissue transglutaminase expression promotes cell attachment, invasion and survival in breast cancer cells. *Oncogene.* 2007;26(17):2459-70.
68. Verma A, Mehta K. Tissue transglutaminase-mediated chemoresistance in cancer cells. *Elsevier* 2007;10(4-5):144-51.
69. Nurminskaya MV, Belkin AM. Cellular functions of tissue transglutaminase. *Int Rev Cell Mol Biol* 2012;294:1-97.
70. Ai L, Kim WJ, Demircan B, Dyer LM, Bray KJ, Skehan RR, et al. The transglutaminase 2 gene (TGM2), a potential molecular marker for chemotherapeutic drug sensitivity, is epigenetically silenced in breast cancer. *Carcinogenesis.* 2008;29(3):510-8.
71. Antonyak MA, Li B, Regan AD, Feng Q, Dusaban SS, Cerione RA. Tissue transglutaminase is an essential participant in the epidermal growth factor-stimulated signaling pathway leading to cancer cell migration and invasion. *J Biol Chem.* 2009;284(27):17914-25.
72. Antonyak MA, Li B, Boroughs LK, Johnson JL, Druso JE, Bryant KL, et al. Cancer cell-derived microvesicles induce transformation by transferring tissue transglutaminase and fibronectin to recipient cells. *Proc Natl Acad Sci U S A.* 2011;108(12):4852-7.

73. Choi CM, Jang SJ, Park SY, Choi YB, Jeong JH, Kim DS, et al. Transglutaminase 2 as an independent prognostic marker for survival of patients with non-adenocarcinoma subtype of non-small cell lung cancer. *Mol Cancer*. 2011;10:119.
74. Agnihotri N, Kumar S, Mehta K. Tissue transglutaminase as a central mediator in inflammation-induced progression of breast cancer. *Breast Cancer Res*. 2013;15(1):202.
75. Caffarel MM, Chattopadhyay A, Araujo AM, Bauer J, Scarpini CG, Coleman N. Tissue transglutaminase mediates the pro-malignant effects of oncostatin M receptor over-expression in cervical squamous cell carcinoma. *J Pathol*. 2013;231(2):168-79.
76. Singer CF, Hudelist G, Walter I, Rueckliniger E, Czerwenka K, Kubista E, et al. Tissue array-based expression of transglutaminase-2 in human breast and ovarian cancer. *Clin Exp Metastasis*. 2006;23(1):33-9.
77. Mehta K. Biological and therapeutic significance of tissue transglutaminase in pancreatic cancer. *Amino Acids*. 2009;36(4):709-16.
78. Miyoshi N, Ishii H, Mimori K, Tanaka F, Hitora T, Tei M, et al. TGM2 is a novel marker for prognosis and therapeutic target in colorectal cancer. *Ann Surg Oncol*. 2010;17(4):967-72.
79. Damiano JS. Integrins as novel drug targets for overcoming innate drug resistance. *Curr Cancer Drug Targets*. 2002;2(1):37-43.
80. Cheng Q, Lee HH, Li Y, Parks TP, Cheng G. Upregulation of Bcl-x and Bfl-1 as a potential mechanism of chemoresistance, which can be overcome by NF-kappaB inhibition. *Oncogene*. 2000;19(42):4936-40.
81. Fok JY, Ekmekcioglu S, Mehta K. Implications of tissue transglutaminase expression in malignant melanoma. *Mol Cancer Ther*. 2006;5(6):1493-503.

82. Jacob K, Webber M, Benayahu D, Kleinman HK. Osteonectin promotes prostate cancer cell migration and invasion: a possible mechanism for metastasis to bone. *Cancer research*. 1999;59(17):4453-7.
83. Verderio E, Nicholas B, Gross S, Griffin M. Regulated expression of tissue transglutaminase in Swiss 3T3 fibroblasts: effects on the processing of fibronectin, cell attachment, and cell death. *Exp Cell Res*. 1998;239:119-38.
84. Gross SR, Balklava Z, Griffin M. Importance of tissue transglutaminase in repair of extracellular matrices and cell death of dermal fibroblasts after exposure to a solarium ultraviolet A source. *J Invest Dermatol*. 2003;121(2):412-23.
85. Wang Z, Collighan RJ, Gross SR, Danen EH, Orend G, Telci D, et al. RGD-independent cell adhesion via a tissue transglutaminase-fibronectin matrix promotes fibronectin fibril deposition and requires syndecan-4/2 alpha5beta1 integrin co-signaling. *J Biol Chem*. 2010;285(51):40212-29.
86. Damiano JS, Cress AE, Hazlehurst LA, Shtil AA, Dalton WS. Cell adhesion mediated drug resistance (CAM-DR): role of integrins and resistance to apoptosis in human myeloma cell lines. *Blood*. 1999;93(5):1658-67.
87. Akimov SS, Krylov D, Fleischman LF, Belkin AM. Tissue transglutaminase is an integrin-binding adhesion coreceptor for fibronectin. *J Cell Biol*. 2000;148(4):825-38.
88. Belkin AM, Tsurupa G, Zemskov E, Veklich Y, Weisel JW, Medved L. Transglutaminase-mediated oligomerization of the fibrin(ogen) alphaC domains promotes integrin-dependent cell adhesion and signaling. *Blood*. 2005;105:3561-8.
89. Herman JF, Mangala LS, Mehta K. Implications of increased tissue transglutaminase (TG2) expression in drug-resistant breast cancer (MCF-7) cells. *Oncogene*. 2006;25(21):3049-58.

90. Janiak A, Zemskov EA, Belkin AM. Cell surface transglutaminase promotes RhoA activation via integrin clustering and suppression of the Src-p190RhoGAP signaling pathway. *Mol Biol Cell*. 2006;17(4):1606-19.
91. Yao ES, Zhang H, Chen YY, Lee B, Chew K, Moore D. Increased beta1 integrin is associated with decreased survival in invasive breast cancer. *Cancer Res*. 2007;67.
92. Verderio EA, Telci D, Okoye A, Melino G, Griffin M. A novel RGD-independent cell adhesion pathway mediated by fibronectin-bound tissue transglutaminase rescues cells from anoikis. *J Biol Chem*. 2003;278(43):42604-14.
93. Telci D, Wang Z, Li X, Verderio EA, Humphries MJ, Baccarini M, et al. Fibronectin-tissue transglutaminase matrix rescues RGD-impaired cell adhesion through syndecan-4 and beta1 integrin co-signaling. *J Biol Chem*. 2008;283(30):20937-47.
94. MacDonald IC, Groom AC, Chambers AF. Cancer spread and micrometastasis development: quantitative approaches for in vivo models. *Bioessays*. 2002;24(10):885-93.
95. Hay ED. The mesenchymal cell, its role in the embryo, and the remarkable signaling mechanisms that create it. *Developmental dynamics : an official publication of the American Association of Anatomists*. 2005;233(3):706-20.
96. Kim DS, Park SS, Nam BH, Kim IH, Kim SY. Reversal of drug resistance in breast cancer cells by transglutaminase 2 inhibition and nuclear factor-kappaB inactivation. *Cancer Res*. 2006;66(22):10936-43.
97. Mann AP, Verma A, Sethi G, Manavathi B, Wang H, Fok JY, et al. Overexpression of tissue transglutaminase leads to constitutive activation of nuclear factor-kappaB in cancer cells: delineation of a novel pathway. *Cancer Res*. 2006;66(17):8788-95.
98. Nagafuchi A, Shirayoshi Y, Okazaki K, Yasuda K, Takeichi M. Transformation of cell adhesion properties by exogenously introduced E-cadherin cDNA. *Nature*. 1987;329(6137):341-3.

99. Batlle E, Sancho E, Franci C, Dominguez D, Monfar M, Baulida J, et al. The transcription factor snail is a repressor of E-cadherin gene expression in epithelial tumour cells. *Nature cell biology*. 2000;2(2):84-9.
100. Christiansen JJ, Rajasekaran AK. Reassessing epithelial to mesenchymal transition as a prerequisite for carcinoma invasion and metastasis. *Cancer research*. 2006;66(17):8319-26.
101. Son H, Moon A. Epithelial-mesenchymal Transition and Cell Invasion. *Toxicological Research*. 2010;26(4):245-52.
102. Huang L, Xu AM, Liu W. Transglutaminase 2 in cancer. *American Journal of Cancer Research*. 2015;5(9):2756-76.
103. Odii BO, Coussons P. Biological Functionalities of Transglutaminase 2 and the Possibility of Its Compensation by Other Members of the Transglutaminase Family. *The Scientific World Journal*. 2014;2014:714561.
104. Kumar S, Mehta K. Tissue transglutaminase, inflammation, and cancer: how intimate is the relationship? *Amino Acids*. 2013;44(1):81-8.
105. Verma A, Guha S, Diagaradjane P, Kunnumakkara AB, Sanguino AM, Lopez-Berestein G, et al. Therapeutic significance of elevated tissue transglutaminase expression in pancreatic cancer. *Clin Cancer Res* 2008;14(8):2476-83.
106. Wang Z, Li Y, Kong D, Banerjee S, Ahmad A, Azmi AS, et al. Acquisition of epithelial-mesenchymal transition phenotype of gemcitabine-resistant pancreatic cancer cells is linked with activation of the notch signaling pathway. *Cancer research*. 2009;69(6):2400-7.
107. Ghosh S, May MJ, Kopp EB. NF-kappa B and Rel proteins: evolutionarily conserved mediators of immune responses. *Annu Rev Immunol*. 1998;16:225-60.

108. Shih VF, Tsui R, Caldwell A, Hoffmann A. A single NF-kappaB system for both canonical and non-canonical signaling. *Cell research*. 2011;21(1):86-102.
109. Lawrence T. The Nuclear Factor NF-kB Pathway in Inflammation. *Cold Spring Harbor Perspectives in Biology*. 2009;1(6):a001651.
110. Scheidereit C. IkappaB kinase complexes: gateways to NF-kappaB activation and transcription. *Oncogene*. 2006;25(51):6685-705.
111. Baeuerle PA, Baltimore D. I kappa B: a specific inhibitor of the NF-kappa B transcription factor. *Science*. 1988;242(4878):540-6.
112. Cho BR, Kim MK, Suh DH, Hahn JH, Lee BG, Choi YC, et al. Increased tissue transglutaminase expression in human atherosclerotic coronary arteries. *Coronary artery disease*. 2008;19(7):459-68.
113. Kumar S, Mehta K. Tissue Transglutaminase Constitutively Activates HIF-1 $\alpha$  Promoter and Nuclear Factor-kB via a Non-Canonical Pathway. *PLoS One*. 2012;7(11):49321-32.
114. Yakubov B, Chelladurai B, Schmitt J, Emerson R, Turchi JJ, Matei D. Extracellular tissue transglutaminase activates noncanonical NF-kB signaling and promotes metastasis in ovarian cancer. *Neoplasia*. 2013;15(6):609-19.
115. Devarajan E, Chen J, Multani AS, Pathak S, Sahin AA, Mehta K. Human breast cancer MCF-7 cell line contains inherently drug-resistant subclones with distinct genotypic and phenotypic features. *International journal of oncology*. 2002;20(5):913-20.
116. Han JA, Park SC. Reduction of transglutaminase 2 expression is associated with an induction of drug sensitivity in the PC-14 human lung cancer cell line. *Journal of cancer research and clinical oncology*. 1999;125(2):89-95.

117. Chen JS, Agarwal N, Mehta K. Multidrug-resistant MCF-7 breast cancer cells contain deficient intracellular calcium pools. *Breast cancer research and treatment*. 2002;71(3):237-47.
118. Antonyak MA, Miller AM, Jansen JM, Boehm JE, Balkman CE, Wakshlag JJ, et al. Augmentation of tissue transglutaminase expression and activation by epidermal growth factor inhibit doxorubicin-induced apoptosis in human breast cancer cells. *The Journal of biological chemistry*. 2004;279(40):41461-7.
119. Yuan L, Choi K, Khosla C, Zheng X, Higashikubo R, Chicoine MR, et al. Tissue transglutaminase 2 inhibition promotes cell death and chemosensitivity in glioblastomas. *Molecular Cancer Therapeutics*. 2005;4(9):1293-302.
120. Choi K, Siegel M, Piper JL, Yuan L, Cho E, Strnad P, et al. Chemistry and biology of dihydroisoxazole derivatives: selective inhibitors of human transglutaminase 2. *Chemistry & biology*. 2005;12(4):469-75.
121. Cao L, Petrusca DN, Satpathy M, Nakshatri H, Petrache I, Matei D. Tissue transglutaminase protects epithelial ovarian cancer cells from cisplatin-induced apoptosis by promoting cell survival signaling. *Carcinogenesis*. 2008;29(10):1893-900.
122. Boroughs LK, Antonyak MA, Cerione RA. A novel mechanism by which tissue transglutaminase activates signaling events that promote cell survival. *J Biol Chem*. 2014;289(14):10115-25.
123. Karin M, Cao Y, Greten FR, Li ZW. NF-kappaB in cancer: from innocent bystander to major culprit. *Nat Rev Cancer*. 2002;2(4):301-10.
124. Nakanishi C, Toi M. Nuclear factor-kappaB inhibitors as sensitizers to anticancer drugs. *Nat Rev Cancer*. 2005;5(4):297-309.
125. Aggarwal BB. Nuclear factor-kappaB: the enemy within. *Cancer cell*. 2004;6(3):203-8.

126. Bharti AC, Aggarwal BB. Nuclear factor-kappa B and cancer: its role in prevention and therapy. *Biochemical pharmacology*. 2002;64(5-6):883-8.
127. Han JA, Park SC. Hydrogen peroxide mediates doxorubicin-induced transglutaminase 2 expression in PC-14 human lung cancer cell line. *Experimental & molecular medicine*. 1999;31(2):83-8.
128. Li Z, Xu X, Bai L, Chen W, Lin Y. Epidermal growth factor receptor-mediated tissue transglutaminase overexpression couples acquired tumor necrosis factor-related apoptosis-inducing ligand resistance and migration through c-FLIP and MMP-9 proteins in lung cancer cells. *J Biol Chem*. 2011;286(24):21164-72.
129. Erdem M, Erdem S, Sanli O, Sak H, Kilicaslan I, Sahin F, et al. Up-regulation of TGM2 with ITGB1 and SDC4 is important in the development and metastasis of renal cell carcinoma. *Urol Oncol*. 2014;32(1):25 e13-20.
130. Erdem S, Yegen G, Telci D, Yildiz I, Tefik T, Issever H, et al. The increased transglutaminase 2 expression levels during initial tumorigenesis predict increased risk of metastasis and decreased disease-free and cancer-specific survivals in renal cell carcinoma. *World J Urol*. 2015;33(10):1553-60.
131. Park MJ, Baek HW, Rhee YY, Lee C, Park JW, Kim HW, et al. Transglutaminase 2 expression and its prognostic significance in clear cell renal cell carcinoma. *Journal of pathology and translational medicine*. 2015;49(1):37-43.
132. Min Jee Park HWB, Ye-Young Rhee, Cheol Lee, Jeong Whan Park, Hwal Woong Kim, Kyung Chul Moon. Transglutaminase 2 Expression and Its Prognostic Significance in Clear Cell Renal Cell Carcinoma. *J Pathol Transl Med*. 2015;49(1): 37–43.
133. Wykoff CC, Pugh CW, Maxwell PH, Harris AL, Ratcliffe PJ. Identification of novel hypoxia dependent and independent target genes of the von Hippel-Lindau (VHL) tumour suppressor by mRNA differential expression profiling. *Oncogene*. 2000;19(54):6297-305.



134. Hidaka H, Seki N, Yoshino H, Yamasaki T, Yamada Y, Nohata N, et al. Tumor suppressive microRNA-1285 regulates novel molecular targets: aberrant expression and functional significance in renal cell carcinoma. *Oncotarget*. 2012;3(1):44-57.
135. Belkin AM. Extracellular TG2: emerging functions and regulation. *Febs j*. 2011;278(24):4704-16.
136. Eckert RL, Fisher ML, Grun D, Adhikary G, Xu W, Kerr C. Transglutaminase is a tumor cell and cancer stem cell survival factor. *Mol Carcinog* 2015;54(10):947-58.
137. Kumar A, Xu J, Sung B, Kumar S, Yu D, Aggarwal BB, et al. Evidence that GTP-binding domain but not catalytic domain of transglutaminase 2 is essential for epithelial-to-mesenchymal transition in mammary epithelial cells. *Breast Cancer Res*. 2012;14(1):R4.
138. Choueiri TK, Motzer RJ. Systemic Therapy for Metastatic Renal-Cell Carcinoma. *New England Journal of Medicine*. 2017;376(4):354-66.
139. Gupta K, Miller JD, Li JZ, Russell MW, Charbonneau C. Epidemiologic and socioeconomic burden of metastatic renal cell carcinoma (mRCC): a literature review. *Cancer Treat Rev*. 2008;34(3):193-205.
140. Begg GE, Carrington L, Stokes PH, Matthews JM, Wouters MA, Husain A, et al. Mechanism of allosteric regulation of transglutaminase 2 by GTP. *Proc Natl Acad Sci U S A*. 2006;103(52):19683-8.
141. Begg GE, Holman SR, Stokes PH, Matthews JM, Graham RM, Iismaa SE. Mutation of a critical arginine in the GTP-binding site of transglutaminase 2 disinhibits intracellular cross-linking activity. *J Biol Chem*. 2006;281(18):12603-9.
142. Mehta K, Fok J, Miller FR, Koul D, Sahin AA. Prognostic significance of tissue transglutaminase expression in drug-resistant and metastatic breast cancer. *Clin Cancer Res*. 2004;10:8068-76.

143. Kang J, Lee J, Hong D, Lee S, Kim N, Lee W, et al. Renal cell carcinoma escapes death by p53 depletion through transglutaminase 2-chaperoned autophagy. *Cell Death Dis.* 2016;7(3):e2163.
144. Ku BM, Lee CH, Lee SH, Kim SY. Increased expression of transglutaminase 2 drives glycolytic metabolism in renal carcinoma cells. *Amino acids.* 2014;46(6):1527-36.
145. Mi Ku B, Kim S-J, Kim N, Hong D, Choi Y-B, Lee S-H, et al. Transglutaminase 2 inhibitor abrogates renal cell carcinoma in xenograft models2014.
146. Kumar A, Xu J, Brady S, Gao H, Yu D, Reuben J, et al. Tissue Transglutaminase Promotes Drug Resistance and Invasion by Inducing Mesenchymal Transition in Mammary Epithelial Cells. *PLoS One.* 2010;5(10).
147. Nam JM, Ahmed KM, Costes S, Zhang H, Onodera Y, Olshen AB. beta1-Integrin via NF-kappaB signaling is essential for acquisition of invasiveness in a model of radiation treated in situ breast cancer. *Breast Cancer Res.* 2013;15.
148. Kryczka J, Stasiak M, Dziki L, Mik M, Dziki A, Cierniewski CS. Matrix Metalloproteinase-2 Cleavage of the  $\beta$ 1 Integrin Ectodomain Facilitates Colon Cancer Cell Motility. *The Journal of Biological Chemistry.* 2012;287(43):36556-66.
149. Verma A, Wang H, Manavathi B, Fok JY, Mann AP, Kumar R, et al. Increased expression of tissue transglutaminase in pancreatic ductal adenocarcinoma and its implications in drug resistance and metastasis. *Cancer Res.* 2006;66(21):10525-33.
150. Kanda R, Kawahara A, Watari K, Murakami Y, Sonoda K, Maeda M, et al. Erlotinib Resistance in Lung Cancer Cells Mediated by Integrin  $\beta$ 1/Src/Akt-Driven Bypass Signaling. *Cancer Research.* 2013;73(20):6243-53.
151. Matysiak M, Kapka-Skrzypczak L, Jodlowska-Jedrych B, Kruszewski M. EMT promoting transcription factors as prognostic markers in human breast cancer. *Archives of gynecology and obstetrics.* 2017;295(4):817-25.

152. Pardali K, Moustakas A. Actions of TGF-beta as tumor suppressor and pro-metastatic factor in human cancer. *Biochimica et biophysica acta*. 2007;1775(1):21-62.
153. Wu Y, Zhou BP. Snail: More than EMT. *Cell adhesion & migration*. 2010;4(2):199-203.
154. Wu Y, Zhou BP. TNF-alpha/NF-kappaB/Snail pathway in cancer cell migration and invasion. *British journal of cancer*. 2010;102(4):639-44.
155. Barrallo-Gimeno A, Nieto MA. The Snail genes as inducers of cell movement and survival: implications in development and cancer. *Development (Cambridge, England)*. 2005;132(14):3151-61.
156. Shao M, Cao L, Shen C, Satpathy M, Chelladurai B, Bigsby RM, et al. Epithelial-to-mesenchymal transition and ovarian tumor progression induced by tissue transglutaminase. *Cancer research*. 2009;69(24):9192-201.
157. Kundu SD, Kim IY, Zelner D, Janulis L, Goodwin S, Engel JD, et al. Absence of expression of transforming growth factor-beta type II receptor is associated with an aggressive growth pattern in a murine renal carcinoma cell line, Renca. *The Journal of urology*. 1998;160(5):1883-8.
158. Zhang Q, Rubenstein JN, Liu VC, Park I, Jang T, Lee C. Restoration of expression of transforming growth factor-beta type II receptor in murine renal cell carcinoma (renca) cells by 5-Aza-2'-deoxycytidine. *Life sciences*. 2005;76(10):1159-66.
159. Cao L, Shao M, Schilder J, Guise T, Mohammad KS, Matei D. Tissue transglutaminase links TGF-beta, epithelial to mesenchymal transition and a stem cell phenotype in ovarian cancer. *Oncogene*. 2012;31(20):2521-34.
160. Karicheva O, Rodriguez-Vargas JM, Wadier N, Martin-Hernandez K, Vauchelles R, Magroun N, et al. PARP3 controls TGFbeta and ROS driven epithelial-to-mesenchymal

transition and stemness by stimulating a TG2-Snail-E-cadherin axis. *Oncotarget*. 2016;7(39):64109-23.

161. Dave N, Guaita-Esteruelas S, Gutarra S, Frias A, Beltran M, Peiro S, et al. Functional cooperation between Snail1 and twist in the regulation of ZEB1 expression during epithelial to mesenchymal transition. *The Journal of biological chemistry*. 2011;286(14):12024-32.

162. Chua HL, Bhat-Nakshatri P, Clare SE, Morimiya A, Badve S, Nakshatri H. NF-kappaB represses E-cadherin expression and enhances epithelial to mesenchymal transition of mammary epithelial cells: potential involvement of ZEB-1 and ZEB-2. *Oncogene*. 2007;26(5):711-24.

163. Pires BR, Mencialha AL, Ferreira GM, de Souza WF, Morgado-Diaz JA, Maia AM, et al. NF-kappaB Is Involved in the Regulation of EMT Genes in Breast Cancer Cells. *PLoS one*. 2017;12(1):e0169622.

164. Huber MA, Azoitei N, Baumann B, Grünert S, Sommer A, Pehamberger H, et al. NF- $\kappa$ B is essential for epithelial-mesenchymal transition and metastasis in a model of breast cancer progression. *Journal of Clinical Investigation*. 2004;114(4):569-81.

165. Shtutman M, Levina E, Ohouo P, Baig M, Roninson IB. Cell adhesion molecule L1 disrupts E-cadherin-containing adherens junctions and increases scattering and motility of MCF7 breast carcinoma cells. *Cancer research*. 2006;66(23):11370-80.

166. Himelstein BP, Canete-Soler R, Bernhard EJ, Dilks DW, Muschel RJ. Metalloproteinases in tumor progression: the contribution of MMP-9. *Invasion & metastasis*. 1994;14(1-6):246-58.

167. Lin C-Y, Tsai P-H, Kandaswami CC, Chang G-D, Cheng C-H, Huang C-J, et al. Role of tissue transglutaminase 2 in the acquisition of a mesenchymal-like phenotype in highly invasive A431 tumor cells. *Molecular Cancer*. 2011;10(1):87.

168. Chen S-H, Lin C-Y, Lee L-T, Chang G-D, Lee P-P, Hung C-C, et al. Up-regulation of Fibronectin and Tissue Transglutaminase Promotes Cell Invasion Involving Increased Association with Integrin and MMP Expression in A431 Cells. *Anticancer Research*. 2010;30(10):4177-86.
169. Muller PA, Trinidad AG, Timpson P, Morton JP, Zanivan S, van den Berghe PV, et al. Mutant p53 enhances MET trafficking and signalling to drive cell scattering and invasion. *Oncogene*. 2013;32(10):1252-65.
170. Fisher ML, Keillor JW, Xu W, Eckert RL, Kerr C. Transglutaminase is required for epidermal squamous cell carcinoma stem cell survival. *Mol Cancer Res*. 2015;13(7):1083-94.
171. Chhabra A, Verma A, Mehta K. Tissue transglutaminase promotes or suppresses tumors depending on cell context. *Anticancer Res*. 2009;29(6):1909-19.
172. Satpathy M, Cao L, Pincheira R, Emerson R, Bigsby R, Nakshatri H, et al. Enhanced peritoneal ovarian tumor dissemination by tissue transglutaminase. *Cancer Res*. 2007;67(15):7194-202.